Improving inhibitor and glycerol tolerance of *Cupriavidus necator* H16 via adaptive laboratory evolution (ALE)

By:

Sepwin Nosten Sitompul

A thesis submitted for the degree of Doctor of Philosophy

The University of Sheffield

Faculty of Engineering

Department of Chemical and Biological Engineering

May 2024

DECLARATION

***I**, Sepwin Nosten Sitompul, confirm that the Thesis is my own work. I am aware of the University's Guidance on the Use of Unfair Means (www.sheffield.ac.uk/ssid/unfair-means). This work has not been previously been presented for an award at this, or any other, university. Parts of this work will be presented elsewhere in the form of scientific publications.*

List of Figure

List of Tables

List of Abbreviations

A	Adenine
AA	Ammonium acetate
AckA	Acetate kinase gene
ACS	Acetyl-CoA synthetase gene
ALE	Adaptive laboratory evolution
ATP	Adenosine Triphosphate
B. subtilis	*Bacillus subtilis*
BA	Benzoic acid
bp	base pairs
C	Cytosine
Ca^{2+}	Calcium ion
CaCl2	Calcium chloride
CBB	Calvin-Benson-Bassham
CCU	Carbon capture utilisation
Co^{2+}	Cobalt ion
CO_2	Carbon dioxide
CoA	Coenzyme A
CNVs	Copy number variations
DNA	Deoxyribonucleic acid
DO	Dissolved oxygen
dNTPs	deoxynucleotide triphosphate
EMS	Ethyl methanesulfonate
ED	Entner-Duodoroff
G	Guanine
g	gramme
Gen^r	Gentamicin resistance gene
GlpD	Glycerol-3-phophate dehydrogenase gene
GlpK	Glycerol kinase gene
H_2O	Water
HMF	Hydroxymethylfurfural
Indels	Insertions and deletions
M	Molar
MB	Megabase
mcl-HA	medium-chain length HA
Mg^{2+}	Magnesium ion
MgCl2	Magnesium chloride
mL	milli-Liter
mM	milli-Molar
mg	milli-gramme
MMC	Microbial microdroplet culture
Mn^{2+}	Manganese ion
MSM	Mineral salts medium
NA	Not available
NADH	Nicotinamide Adenine Dinucleotide
NADPH	Nicotinamide Adenine Dinucleotide Phosphate
NB	Nutrient Broth
Ni^{2+}	Nickel ion
NTG	N-methyl-N'-nitro-N-nitrosoguanidine
nm	nano-meter
OD	Optical density
pH	Potential of hydrogen
PHA	Polyhydroxyalcanoate
PHB	Poly[(R)-3-hydroxybutyrate]
pta	Phosphotransacetylase gene
R	Round
rpm	revolution per minute
RuBisCO	Ribulose-1,5-bisphosphate carboxylase/oxygenase

SAM	S-adenosyl-L-methionine
scl-HA	short-chain length HA
SNP	Single nucleotide polymorphism
T	Thymine
UV	Ultraviolet
v/v	volume per volume
WGS	Whole genome sequencing
WT	Wild-type
Zn^{2+}	Zinc ion
w/v	weight per volume
ºC	degree Celsius
α	alpha
β	beta
µg	microgram
µL	microliter
µm	micrometer
µM	micromolar

Acknowledgement

Many helped me along the way on this PhD journey. I want to take a moment to thank them.

First, I would like to express my gratitude to my lead supervisor, Professor Tuck Seng Wong, without whom I would have been unable to produce this work. Over these years, his encouragement and feedback have been invaluable. For this, I am extremely grateful. I would also like to thank my co-supervisor, Dr. Kang Lan Tee, for her insight throughout the development of this study. Her insightful reasoning and advantageous observations made significant contributions to this journey.

I want to thank Wuttichai for the significant assistance with the sequencing results and Youssef Ghoneim for his substantial contribution to aspects of this work.

I sincerely thank my fellow lab/office mates Nur Azizah, Amy (Aonn), Ming Chen Laura, Ming Long, Rashid, Melvin, Robert, Fang yi, Abdul, Daniel, Abdul, Ivona, and colleagues for their invaluable contributions throughout the past four years. Also, I wish to thank my international and Indonesian friends in Sheffield, who have been among the most fruitful of my life. On multiple occasions, their presence was sufficient to inspire a thought or, at the very least, to brighten the day. Furthermore, I am grateful to my sponsor, the Ministry of Education, Culture, Research, and Technology of The Republic of Indonesia, for supporting my doctoral studies financially.

Lastly, I thank my parents, L. Sitompul and N. Nadapdap, and my siblings (Kak Yulien and her partner + adorable nephews, Kak Monika and Noem) for their unwavering encouragement throughout my academic career.

Abstract

In the realm of biotechnology, adaptive laboratory evolution (ALE) stands out as a critical method for enhancing the desired traits of microbial strains. This study showcases the efficacy of ALE in evolving *Cupriavidus necator* H16 to bolster its tolerance against two prevalent inhibitors found in lignocellulosic hydrolysates: benzoic acid and ammonium acetate. Through ALE, we produced a novel variant of *C. necator* H16 capable of thriving in the presence of 5 mM benzoic acid at 37°C, a feat unattainable by the parental strain. Additionally, our research yielded variants capable of withstanding ammonium acetate concentrations of up to 50 mM, surpassing the limitations of the parental strain. Notably, ALE showcased its superiority over alternative techniques by obviating the need for genetically modified strains or specific genetic tools. Furthermore, we innovatively employed chemical-assisted ALE to bolster *C. necator* H16 against elevated glycerol concentrations. The approach intentionally boosts gene diversity by regulating exposure to metal ions ($MnCl_2$, $ZnCl_2$, and $CoCl_2$), facilitating the rapid discovery of improved variants. Importantly, two rounds of $MnCl_2$-assisted ALE produced a variant that exhibited a nine-fold increase in OD growth when cultivated in the presence of 15% glycerol compared to the parental strain. The incorporation of $MnCl_2$ in the ALE approach demonstrated notable efficacy, accelerating the identification of improved variants compared to previous methods. Moreover, we propose an alternative method for augmenting genetic diversity, leveraging divalent metal ions as mutagens. This approach not only promises increased efficiency but also ensures safety and cost-effectiveness. In summary, the methodologies employed in our study hold significant promise for advancing microbial strain engineering and optimising bioprocesses, heralding a new era of innovation in biotechnology.

Introduction

ALE has been developed into a robust method, facilitating the improvement of numerous microbial properties essential for biomanufacturing. These properties range from maximising carbon use to improving microbial growth and tolerance against inhibitors. ALE is notable for its uncomplicated technical execution and versatility in handling various microbial strains. By employing a top-down approach, this method eliminates the requirement for a complex understanding of the microbe's metabolic network as well as an advanced genetic toolkit.

ALE has proven highly effective in enhancing the traits of *C. necator* H16. Its potential applications are incredibly diverse, spanning from enhancing substrate utilisation [1], to improving tolerance to carbon monoxide [2], and acetic acid [3]. These examples underscore the versatility of ALE in reshaping the physiological and metabolic profile of *C. necator* H16 to address a wide array of industrial needs.

Chapter 1 examined the existing strategies and employed in ALE experiments to generate improved variants and novel approaches to accelerate the completion of ALE studies. Additionally, it delved into the exploration of *C. necator* H16's potential as a versatile cell factory for utilising cost-effective compounds derived from lignocellulosic biomass.

This study aimed to enhance the substrate utilisation range of *C. necator* H16 by including lignocellulose, which stands as the most abundant organic material on Earth. Employing the ALE technique, our objective is to pinpoint *C. necator* H16 variants with enhanced tolerance to two common inhibitory compounds found in lignocellulosic hydrolysate: benzoic acid (**Chapter 2**) and ammonium acetate (**Chapter 3**). Our projects are focused on two primary objectives. Our first aim is to utilize the ALE methodology to discover variants of *C. necator* H16 that exhibit enhanced tolerance to benzoic acid and ammonium acetate, notable inhibitory compounds in lignocellulose hydrolysate. Furthermore, our primary objective is to investigate the benzoic acid and ammonium metabolism of *C. necator* H16 to attain a solid understanding via evolutionary exploration. While proposed pathways have been suggested based on genomic insights and existing literature [4] [5], our grasp of benzoic acid and ammonium acetate metabolisms remains somewhat constrained. This study aimed to unveil

pivotal insights that can enrich the broader comprehension of the intricate metabolic pathways of this microbe.

Despite being simple, the ALE technique can be time-consuming because of the need for serial or continuous cultivation under selective conditions. To speed up evolution, increasing genetic diversity by creating a larger and more intricate pool of variants for future selection is essential. This approach is often accomplished using physical agents such as UV light [6] and chemical agents such as DNA alkylating chemicals [7]. Metal ions, such as Mn^{2+}, are commonly used in random mutagenesis for protein evolution [8]. However, their use in ALE has not been investigated. **Chapter 4** aimed to create a novel, faster ALE procedure by incorporating divalent metal ions. This technique represents the initial use of metal ions in ALE, signifying a notable progression in the area.

CHAPTER 1

Literature Review:

Adaptive laboratory evolution (ALE) technologies & tools and *Cupriavidus necator* H16: A chosen strain for phenotype improvement

Chapter 1 – Adaptive laboratory evolution (ALE) technologies & tools and *Cupriavidus necator* H16: a chosen strain for phenotype improvement

Introduction

Microbial cell factories are of particular significance for biotechnological applications, and bacteria have been used for a wide range of biotechnological activities, from biofuel production [9] to industrial [10] and biopharmaceutical chemicals [11]. In addition, biological catalysis offers several advantages over chemical synthesis, such as producing stereoselective chemical compounds [12]. Synthetic biology is a newly emerging discipline, and systems metabolic engineering has proved highly effective for designing, modifying, and implementing biotechnological production processes [13]. To create all of these modifications, however, it is necessary to have information about the pathways/enzymes that participate in the reactions, the metabolic pathway that includes these reactions, and the organism in which the modifications will be made; this makes metabolic engineering challenging.

Based on Darwinian survival of the fittest, the ALE approach is a potent tool for improving the characteristics of microbial cell factories without prior biological knowledge. The ALE of microorganisms can serve as a simple model system to help us comprehend the evolutionary process of natural selection, how genetic diversity is preserved, and gain insight into more specific evolutionary phenomena. Most importantly, the ALE approach improves microbial cell properties essential in industrial applications [14], such as (1) optimisation of growth rate [15, 16], (2) improvement of the environment tolerance [17], (3) enhancement of substrate utilisation [18], (4) improvement of targeted metabolites production [19-21], and (5) general discovery of evolutionary phenomena [22-24].

C. necator H16, a gram-negative bacterium, thrives in freshwater and soil environments, making it a ubiquitous presence in nature. Recently, there has been a surge of interest in harnessing the potential of *C. necator* H16 as a versatile platform for producing valuable compounds. To fully leverage its capabilities, enhancing the bacterium's characteristics is imperative. Polyhydroxyalkanoates (PHAs) stand out as one of the valuable products

synthesised by various species, including *C. necator* H16. These biopolymers, which are similar to naturally occurring polyesters, have great potential for a wide range of applications. Significantly, we can produce PHAs by utilising lignocellulosic hydrolysates as a substrate. This approach is both sustainable and environmentally beneficial while also being commercially feasible as a source of carbon. However, it's essential to address a prevalent challenge: the presence of toxic compounds like benzoic acid and ammonium acetate in lignocellulosic hydrolysates. These toxic compounds, originating from the hydrolysis process of plant biomass, pose hurdles to efficient PHA production. Despite their harmful nature, *C. necator* H16 exhibits remarkable adaptability, capable of utilising low concentrations of benzoic acid and ammonium acetate and converting them into PHA. This unique ability underscores the bacterium's potential as a robust candidate for PHA synthesis, even in the face of challenging substrates.

Chapter 1.1 provided an in-depth analysis of the primary approaches and methodologies used in ALE experiments with the goal of generating superior variants. Moreover, it provided insight into the expanding range of methodologies designed to expedite the duration of ALE experiments, thereby accelerating the pace of evolutionary engineering. Meanwhile, **Chapter 1.2** served as a focal point for a comprehensive examination of *C. necator* H16's potential as a formidable cell factory for synthesising economically viable chemicals (PHAs) derived from lignocellulosic biomass. This investigation underscores the bacterium's prowess in leveraging renewable resources to produce a diverse range of cost-effective compounds with promising industrial applications. **Chapter 1.3** provided the aims of this thesis.

1.1 Adaptive laboratory evolution (ALE)

ALE experiments are a potent method for studying the factors that shape the characteristics, efficiency, and stability of strains and obtaining desired strains [25, 26]. William Dallinger performed ALE a century ago [27], in the last quarter-century, it has been used to build microbial cell factories. Technically, ALE includes prolonged cell cultivation under generally harmful growth conditions to isolate a strain with advantageous mutations that perform better than the parental strain. The evolutionary process can take days, weeks, or even years.

As reviewed by Sanberg *et al.,* 2019 [26], the key to the success of ALE experiments is the fitness advantage conferred by adaptive mutations, which allows mutant strains to outcompete their parental strain and dominate the population. During ALE, cells acquire advantageous mutations to adapt to conditions created in the laboratory; as a result, changes in cellular physiological features, including the transcription process, translation process, metabolite synthesis, and metabolic fluxes, are generated. Genome resequencing of the adapted strains from the population is undertaken to discover beneficial mutations responsible for enhanced fitness to comprehend cell adaptation processes in ALE [28].

The ALE experiment is effective in microbes over animals due to the ease of maintaining large populations of rapidly dividing cells. Moreover, their relatively small genomes ease the study and comprehension of adaptation mechanisms. ALE provides genetic diversity from which advantageous mutants naturally enrich [29]. In addition, the accessibility of high-throughput DNA sequencing facilitates the identification of mutations during the ALE process (**Figure 1.1**).

The primary advantages of ALE involve its simplicity of implementation and the fact that no prior knowledge of genotype-phenotype relationships is required. ALE provides useful applications in industrial settings [14], including (1) optimisation of growth rate [15, 16], (2) improvement of the environment tolerance [17], (3) enhancement of substrate utilisation [18], (4) optimisation of targeted metabolites production [19-21], and (5) general discovery of evolutionary phenomena [22-24]. The recent studies associated with the ALE experiment discovered the adaptive response of microbes to environmental stress caused by different conditions such as temperature [30], pressure [31], ionising radiation [32], and ultraviolet (UV) radiation [33]. ALE is more reliable than other approaches for identifying the gene responsible for stress regulators [14]. ALE also plays an important role in system biology, including the metabolic engineering [34] and *in silico* experimental evolution [35]. ALE has uncovered the basic genetics of microorganisms on a genome-scale [36]. Serial transfers in stirring flasks, also known as "serial batch cultivations," and continuous cultivation (chemostat) are currently the most common methods for conducting an ALE experiment.

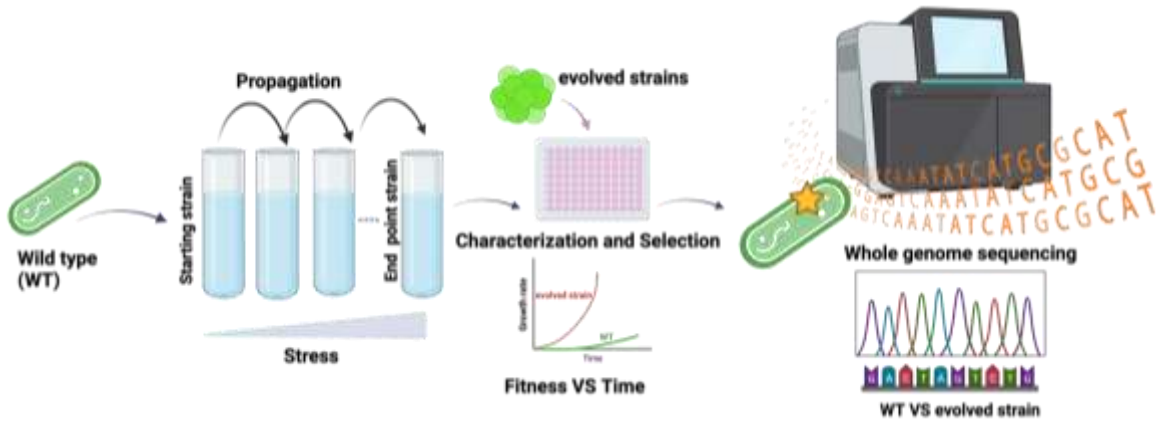

Figure 1.1 Adaptive laboratory evolution (ALE) workflow (Adapted from Sanberg et al., 2019 [15]). Wild-type microbes are cultivated in a desired growth environment for a prolonged period, allowing natural selection to enrich mutant strains with enhanced fitness. ALE experiment is carried out through a serial transfer of batch culture. Evolved strains are characterised by phenotypic enhancements compared to the parent strain, using the "fitness" metric (growth rate). The DNA of evolved strains is sequenced to reveal the adaptive mutations that allow for phenotypic improvement.

1.1.2 Traditional methods for ALE experiment

1.1.2.1 Serial batch culture

Serial batch culture is arguably the most rudimentary and well-known technique for running ALE experiments. Richard Lenski and his crew pioneered the batch culture for ALE [37] [38]. This method propagates microbial cells by serial transfer in a single vessel without maintaining constant conditions (**Figure 1.2**) [29, 39]. Batch culture consists of several essential elements:

(1) The cell culture is incubated in a designated medium containing a carbon source, such as glucose, under selective pressure.
(2) Generally, 1% of the starting population is transferred to a fresh medium at regular intervals with or without an increase in selective pressure. This strategy permits a new cycle of population growth.
(3) The cell populations must be stored frozen to track the evolution [29, 40].

In most ALE experiments, batch culture depends on the growth phase [14]. During the ALE experiment, a population with greater fitness will be created, which will triumph over the least fit population. One of the most important aspects of serial batch culture is avoiding the stationary phase and maintaining the exponential phase [41]. As reviewed by Sanberg *et al*.,

2019 [26], if exponential-phase growth is not constantly maintained, fitness expands to include factors other than growth rate alone, such as survival in stationary or reduced lag phases. However, the abrupt shifts during the growth phase in batch culture make maintenance difficult. But maybe this issue could be resolved by raising the passage volume; however, this becomes more difficult to achieve without automation [14]. As Lenski [37] worked with *Escherichia coli*, employing a fixed volume with a defined daily interval may be less demanding in batch culture without automation.

Difficulties with batch culture that often enhance the likelihood of failure, including (1) measuring the exponential phase growth rate in batch cultures with a daily sample is less precise and more susceptible to human error [42]; (2) As reviewed in Fernandes *et al.,* 2023 [39], variations in population density, growth rates, and food supplementation, as well as environmental variables, make batch cultures more susceptible to random drift than continuous cultures.

1.1.2.2 Continuous culture

The continuous culture approach is the second preferred culture method for ALE experiments. Continuous culture can be achieved using a chemostat or turbidostat. Those two methods exert a constant and consistent selective pressure [29].

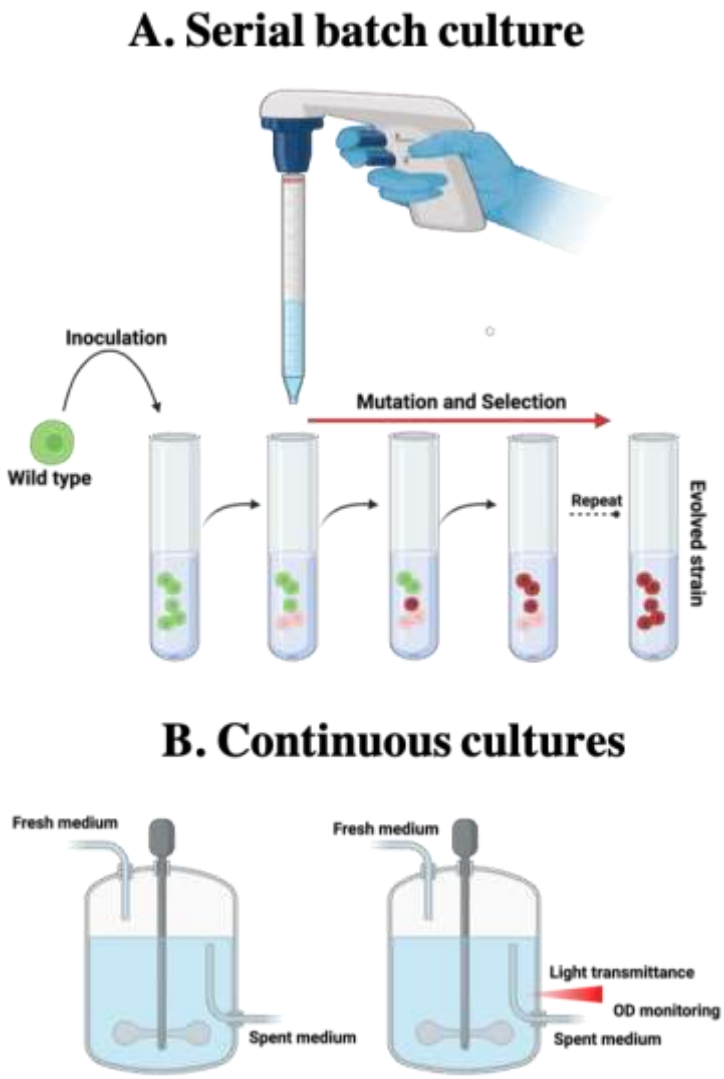

Figure 1.2 Traditional Adaptive Laboratory Evolution (ALE) experiments. (A) Serial batch transfer. Serial transfers are carried out by subculturing the cell on a particular condition for an extended period. Aliquots of the cells' population are repeatedly transferred into a new culture medium. The serial transfer allows selection to produce evolved strains (altered colouration) with enhanced fitness. (B) Continuous culture. Typically, continuous cultures are performed in a chemostat or turbidostat. The chemostat is comprised of a bioreactor that can maintain a constant growth rate, cell density, and selection pressure. Fresh medium is added constantly, and the spent medium is removed. Instead of establishing medium at a constant rate, a turbidostat maintains a constant cell density. This is accomplished through a feedback mechanism that adjusts the nutrient addition rate in response to changes in density, which are typically measured by light transmission.

1.1.2.2.1 Chemostat

Chemostat has been implemented as one of the principal strategies for the ALE experiment [43]. This technique has been utilised in numerous adaptive evolution research [18, 43-47]. In contrast to batch culture, the chemostat allows constant environmental conditions in which the

fresh medium is continually fed to the culture (open system) and the used medium is removed at a constant rate [48]. The chemostat comprises a bioreactor, which permits accurate control of environmental parameters such as pH and oxygen availability [39]. Cell dilution is employed to achieve a constant growth rate of cell culture in a bioreactor.

The principle of a chemostat is that the number of cells equals the dilution rate of a diluted culture (steady-state) [43]. The key feature of a chemostat is that the cell culture occurs in a well-defined medium, and the final cell density relies on the limiting substrate and the presence of growth inhibitors [29, 39]. In both batch culture and chemostat, the early growth phase is unaffected by the availability of nutrients. According to David Gresham and Jungeui Hong [29], the number of cells and the growth-limiting nutrients are crucial variables in a chemostat. Due to cell division, the concentration of cells will increase, while dilution will gradually decrease the cell concentration. With time, the concentration of the growth-limiting nutrient increases due to adding fresh media and falls due to dilution and cell culture consumption. It is important to note that the concentration of the growth-limiting nutrient is low, which contributes to the selection of the cell (the crucial factor in experimental evolution) [6, 30].

Compared to batch culture, the chemostat facilitates significant aspects when a constant state is required. However, the chemostat can be constrained by the formation of wall growth within a culture chamber [49]. Even while the wall growth can be prevented by replacing the chamber, it is still inconvenient. In addition, the high operating cost requires a considerable initial investment in equipment.

1.1.2.2.2 Turbidostat

As reviewed in Gresham & Dunham, 2014 [29], similar to a chemostat, a turbidostat continuously dilutes a culture by adding fresh medium to achieve a constant density. This is accomplished by a feedback mechanism that allows the nutrient addition rate to be adjusted in response to changes in density, which are typically measured by light transmittance [50]. Contrary to a chemostat, the objective of a turbidostat is to prevent cells from ever experiencing limited nutrients.

In the case of a turbidostat, all nutrients are available in abundance, and the dilution rate is adjusted to be near the cells' maximal growth rate. The growth rate of cells in a turbidostat is affected by the cell's intrinsic properties. As the turbidostat environment is always nutrient-rich, the growth potential of cells is not constrained by nutrient excess. Instead, the limits of growth are determined by the inherent properties of the cell, which assess its replication rate. The rate of nutrient assimilation, the rate of macromolecular and organelle biogenesis, and the rate of complex molecular processes (DNA replication, transcription, and translation) are likely factors that limit the rate at which a cell can replicate when resources are abundant.

1.1.3 Automation for ALE methods

In the early stages of the bacterial cultivation method of adaptive evolution, difficult processes such as manual handling, lengthy procedures, and massive independent cultivation led to the experiment's failure. Although the simple experimental setup of serial batch culture and the well-defined selection pressure in a chemostat have been recognised as strengths of both approaches, automation could improve the investigation of adaptive evolution. Automation will boost production and enable multiple independent replicates of the same test to be performed simultaneously. In addition, automation enables experimental approaches involving a complex culturing operation to be executed faster than other methods. In approximately eight months, the Blaby group finished their adaptation study with automated equipment (eVolugator). In contrast, the Rudolph group required two years to get nearly comparable results utilising traditional batch culture series [51, 52]. Furthermore, the automated ALE exhibited a level of fitness that was ten times higher than that seen in the traditional ALE experiment conducted by the Lenski group [53]. The parameters, such as temperature, pH, DO, and agitation, can be monitored and regulated. Using the conventional method, this outcome is ludicrous. This type of automation has considerably boosted production and reduced the number of procedural steps and risks of contamination.

In an ALE study, selection pressures must be considered for toxic tolerance. This is because too strong selection pressure eliminates the beneficial mutations, while insufficient selection pressure slows evolution. Researchers can only attain such exact control over ALE conditions with low throughput. Thus, automation devices (**Table 1.1**) have a strong affinity with ALE to address the constraints of the manual method. In addition to enhancing throughput, automation can eliminate human mistakes and monitor the status quickly or in real time, regardless of the researcher's schedule.

Table 1.1 Current Types of ALE Methods.

ALE method	Key features	Advantages	Disadvantages	Applications
Serial batch culture	Constant condition is not necessary.	Simple installation and operation	Susceptible to abrupt changes in cell growth phase during cultivation; requires extensive manual labour; high risk of contamination during cell transfer; high risk of human error; limited control over growth conditions.	- **Substrate utilization and growth rate optimization:** Improve galactose utilization of *Saccharomyces cerevisiae* [54]; increase glycerol utilization of *C. necator* H16 [1]; increase growth rate of *Corynebacterium glutamicum* on glucose minimal medium; - **Improve product titre:** Increase production of L-ornithine by *C. glutamicum* [55]; enhanced production of dihydroxyacetone by *Gluconobacter oxydans* [56]; - **Increase tolerance:** increased tolerance to various acidic conditions [17]; tolerance to hydroxypropionic [57]; adaptation of *S. cerevisiae* to NaCl [58]
Continuous culture	Constant condition is required.	It is capable of sustaining environmental control; selective; population density; nutrient availability	High cost of operating as it requires a considerable initial investment in equipment; wall growth formation within the chemostat chamber	- **Substrate utilization and growth rate optimization:** Sugar synthesis from CO_2 by *E. coli* [59] - **Improve product titre:** improved ethanol yield by incorporating chemostat-ALE, engineering topology and kinetics of sucrose metabolism of *S. cerevisiae* [60]; enhancement of carotenoid biosynthesis in *Dunaliella salina* [20] - **Increase tolerance:** enhance tolerance to inhibitors from spruce biomass [61]; adaptation to high concentration of ethanol [62]
Automated cultivation	It can be employed in both serial batch culture and continuous culture.	Reduce human error and increase the ALE experiment's productivity	Expensiveness of the instruments; Some of automated ALE devices require knowledge of software and basic programming	- **Substrate utilization and growth rate optimization:** glycerol uptake optimization [63] - **Increase tolerance:** automated Morbidostat for studying bacterial resistance [64]; increase tolerance to higher temperature [51]

1.1.4 Evaluation of automated technologies for ALE experiment

Automated ALE devices are becoming recognised as crucial equipment in evolutionary studies. Numerous automated ALE devices are available, including bioreactors and do-it-yourself (DIY) systems (**Table 1.2**). It is necessary to ascertain the most suitable instrument for the intended ALE experiment. Below is a discussion of essential considerations that must be considered for a device to fulfil all of its requirements, including real-time monitoring, minimal human intervention, and autonomous data storage.

1.1.4.1 Automated real-time monitoring of ALE experiment

Automation enables the completion of the ALE experiment through the real-time monitoring of growth response to environmental factors [65]. A study conducted by Toprak *et al.* (2013) [64] showed that automation can effectively regulate chemical concentrations by implementing real-time monitoring of growth response to environmental parameters. For instance, this approach may be used to maintain cultures in a growth-inhibiting but non-lethal antibiotic environment, therefore facilitating the investigation of processes underlying the development of antibiotic resistance. In addition, a function that monitors growth makes the data collecting more reliable and allows for the elimination of substantial errors. With automatic monitoring, all the data during a running experiment is recorded without the users' supervision or concern over losing certain key trajectories, while the productivity between runs is increased. Hence, several users have utilised automated devices to facilitate the creation of an adaptive laboratory, while others have created their own automated devices.

Under more intense selective pressure in the ALE experiment, sudden death of cell culture is inevitable. Due to this event, the scientist must restart the evolution experiment from a glycerol stock. The scientist may immediately reduce the selection pressure experienced by such an event with real-time growth monitoring, allowing the cells to recover and adaptive mutations to appear without restarting the culture. The Blaby group [51] claimed that they only destroyed the culture twice over eight months, but they recovered the culture after selective pressure increases and avoided wasting time.

The Biolector microbioreactor and the Personal Bioreactor (Biosan) allow monitoring in real-time. These devices simultaneously enable cultivation in multiple conditions and tracks crucial parameters, including OD and temperature. In addition, the Biolector is capable of measuring biomass, pH, DO, humidity, and carbon dioxide [66]. Since 2019, some studies have employed Biolector for high-throughput fermentation. Using scattered light supervision and accurate measurements, the Biolector allows for the continuous monitoring of *Yarrowia lipolytica* in real-time, facilitating the investigation of growth optimisation and lipid accumulation [67].

Meanwhile, a few groups could develop a low-cost, straightforward device that achieved the accurate measurement requirements of the ALE investigation. Harrison and the Oxford University team present automatic monitoring and analysis of bench-scale data, Chi.Bio [68] (**Figure 1.3**). This device's capacity to customise experimental settings using a simple-to-assemble technology is a major feature. The Chi.Bio, which offers automated monitoring and measurement of Optical Density (OD), fluorescent protein, optogenetics, and growth rate, has a bigger working volume than the Biolector.

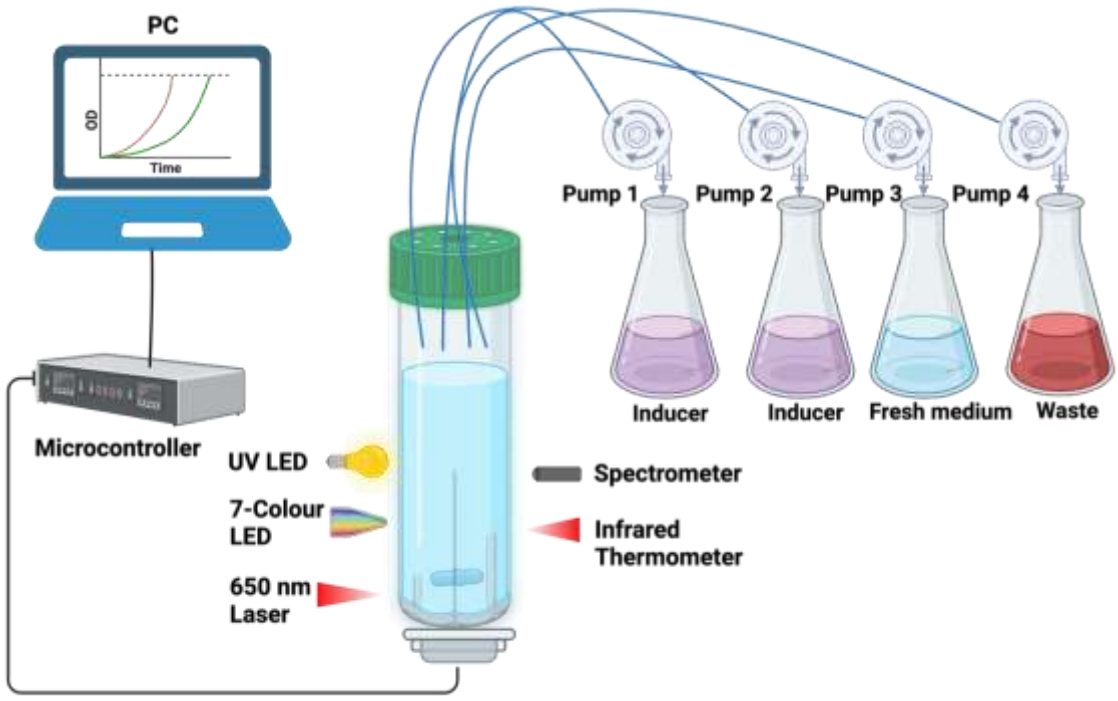

Figure 1.3 The scheme of Chi.Bio with sub-systems and interconnections (adapted from Steel et al. (2019) [68]). The computer connects to the microcontroller, which runs the operating system and can connect up to eight reactor/pump pairs parallelly. Every reactor comes with measurement and actuation tools, including a UV LED, a 650 nm laser, a seven-coloured LED, and a spectrometer. A heat plate and thermometer are used for temperature regulation. Magnetic stirring is used for shaking. The reactor has a modular pump.

Both eVolver [69] and Chi.Bio [68] share comparable functionality. An eVolver is a scalable DIY framework that regulates and monitors the growth of a culture. This framework enables continuous control and monitoring of hundreds of individual cultures by collecting, measuring, and recording experimental data in real time. The setting can be found online at *https://www.fynchbio.com*. This device could detect temporal adaptations, such as bet-hedging and transcriptional variations [70]; the monitoring systems enable the detection of minute phenotypic changes [69, 71]. Both eVolver and Chi.Bio have the enormous benefit of being cost-effective and easily reconfigurable for any high-throughput ALE study.

1.1.4.2 Minimising human intervention requirements

Manual labour of ALE experiments presents many difficulties and inconveniences, such as sampling and passage, vessel loading and unloading, feeding the culture, etc. In the majority of ALE studies, regular human intervention is necessary. However, human intervention may result in concerns such as (a) higher work costs and longer working hours for scientists, (b) a limited number of samples runs, (c) human error, and (d) a less flexible practice due to the availability of human resources.

A typical ALE experiment involves pre-cultivation, preparing the culture vessel, inoculation, a period of cultivation, and then collecting the culture for analysis. This procedure requires up to ten hours of manual labour per attempt. In the culture phase of ALE, monitoring pH, shaking conditions, and temperature in real time are advantageous to get accurate data. Collecting data often requires users to gather and assess the sample manually. Researchers can add or feed cultures manually in chemostat/turbidostat operations. The chemostat/turbidostat operations may be executed in an automated and remote manner using an automatic chemostat positioned upon a bioreactor. The ALE automated culture system incorporates a range of technologies necessary for the execution of a comprehensive automated ALE experiment. With the unique combination of a culture system and measuring system, cells can be maintained in a consistent environment through a rapid serial transfer [72]. In the typical ALE experiment, for instance, the operation can take hours, not to mention the time between processes. One cycle of automated cell culture can be completed in a maximum of seven minutes. The purpose of this technology is to avoid dynamic conditions in laboratory evolution

by maintaining a low cell concentration [73]. As the low concentration of the cell is maintained, the stationary phase will be maintained, which is essential for the growth advantage in ALE experiments [40].

The third version of the Biolector series, Robolector, runs a Biolector system integrated with a robotic system for liquid handling, allowing for fully automated functions requiring minimal human intervention. This technology will create media compositions automatically from experimental designs (DoE). Furthermore, the Robolector enables the control of nutrient feeding, fermentation inducers, and pH adjustment, enabling fed-batch mode. This device and a liquid handling system enable high-throughput sample collection by generating significant kinetics data [74]. When combined with a cooling carrier, microtiter plate shaker, and vacuum filtration, the Robolector has permitted the screening of up to 46 mutant strains of *E. coli* for cellulase production [75].

An automated ALE that maintains a constant level of growth inhibition (morbidostat) was created by Toprak *et al.* [64] to study bacterial drug resistance. This device can conduct up to fifteen distinct cultures simultaneously. In addition, Toprak's device can monitor how bacteria react to a drug and adjust the drug's concentration to maintain bacterial growth inhibition. The morbidostat provides the advantage of enabling ALE studies in a dynamic environment compared to other methods. The concentration of the desired drug must be manually supplemented daily by measuring the resistance of the evolving population, despite the morbidostat being automated throughout the cultivation period of the device [64]. The Liu group [76] developed a low-cost, customisable morbidostat to investigate the adaptive evolution of bacteria. The automated morbidostat is available online and can be assembled by biologists with some electronic understanding. Notably, the above devices are suitable for examining drug resistance.

1.1.4.3 Working volume

An automated microbial microdroplet culture system (MMC) allows for continuous cultivations in ALE experiments with a small working volume (2 mL) and up to 200 replicates per run. *E. coli* strain MeSV2.2 was successfully evolved using MMC. The wide linear range

of optical density (OD of 600 nm) measurement of the MMC eliminates the need for manual sample dilution before conducting UV-Vis spectrophotometry measurements [77]. An automated chemostat has been applied in many studies with working volumes ranging from 16 nL [78] to a larger working volume of 20 mL [68, 79]. The new ambr® 250 devices from Sartorius is an improved bioreactor that provides precise measurements of microbial fermentation at greater volumes (100-250 mL) (www.sartorius-steam-tap.com). The previous work used the ambr® 250 devices in a mammalian cell for biological therapy [60]. However, it is visible that this device can also be utilised for microbial fermentation.

1.1.4.4 Data retrieving and recording

Automated bioreactors have emerged as a compelling platform for facilitating high-throughput ALE. Research on ALE is often conducted continuously, including both day and night, necessitating the comprehensive documentation of a substantial amount of information. The ability to store and export data is quite advantageous. Additionally, it enhances the capability to monitor real-time data. It mitigates human errors, such as data loss or failure to record the data collection time accurately. An advanced bioreactor, such as the Biolector and Personal Bioreactor RST-1 (Biosan), can generate automated data recordings. Sadly, the cost of these high-end bioreactors makes them the most important limitation. The Chi.Bio [68] has a user-friendly interface that measures, controls, and records all culture parameters. Additionally, it is offered at an affordable price. The process of retrieving data in Chi.Bio [68] is a straightforward procedure facilitated by Filezilla to record all relevant parameters throughout the experiment. Even with no previous Linux experience, the user may quickly pick up the operating system. The practicality aspect is significant since users can easily reach the assembly guide and software installation instructions via internet platforms.

1.1.4.5 Price

The cost of a bioreactor is a critical factor that may be considered when selecting a suitable one. Biolector and ambr® 250 demonstrate a fully automated, computer-controlled, sterile workstation with extensive metabolite measurement capabilities. Undoubtedly, a fully

automated framework reduces the need for human intervention, but it is extremely costly. Chi.Bio is a cost-effective solution for automatic liquid control and monitoring. The device is open-source and can be constructed from a printed circuit board (PCB); all the components are available to order and can be assembled by the user for approximately $300 per unit. This self-assembly feature is also available on the eVolver platform, where all components required to assemble the device are accessible online [69]. Despite the accessibility of information on the design and construction of those devices, users still need the skills necessary to construct one. The completely completed Chi.Bio platform can be acquired from LABMAKER for approximately 580 USD; hence, it will save a great deal of assembly time and expedite the experiment.

Table 1.2 Author's choice of various automated devices for ale experiments and tested strains.

Name	Supplier	Volume	Observed strains	Application	References
Automated Morbidostat	Self-assembled device	Up to 20 mL	*E. Coli* MG1655, *Bacillus Subtilis*	OD measurement, growth measurement, drug resistance study.	[64]
Biolector (Biolector II, Biolector Pro, Robolector)	M2P-labs	800-2400 µl	*E. Coli, Pichia Pastoris, Bacillus subtilis Candida sp., Clostridium diolis, Clostridium acetobutylicum, C. glutamicum, Hansenula polymorpha, Lactobchacillus* sp.*, Paracoccus* sp.*, Penicillium* sp.*, Photorhabtus luminescens, Saccharomyces cerevisiae, Schizosaccharomyces pombe, Streptomyces* sp.*, Tetrahymena sp., Vibrio natregiens* sp.*, Yarrowia lipolytica, Zymomonas* sp.	Cell line and strain screening, media optimization and screening, fermentation optimization, anaerobic and microaerophilic fermentation, fed-batch, protein kinetics and expression, genomics, proteomic, toxicity test, quality control, statistical design of experiment (doe), growth characterization, pH profiling ALE study combined with MPP	[80] M2P.lab [81]
Chi.Bio	Labmaker (*open source technology*)	12-25 mL	*E. Coli* strain MG1655, BL21(DE3), BW29655	Optical density regulation, fluorescent protein measurement, optogenetics, online feedback control, growth rate measurement, growth curves.	[68]
eVolver	Self-assembled device	Up to 40 mL	*Saccharomyces cerevisiae* ATCC 28383, *S. cerevisiae* W303 strain matα haploid, *S. cerevisiae* W303 strain matα haploid, *E. coli* K-12, *E. Coli* K-12 ATCC 47076, *Serratia marcescens* ATCC 13880	Long-term bacterial growth, evolution experiment, growth selection, media mixing for sugar sensing, automated passaging for prevention of biofilm, yeast evolution and mating, chemostat and turbidostat purpose.	[69]
Evolugator	Evolugator	10 mL	*E. coli, Acinetobacter baylyi, Metarhizium anisopliaae*	OD measurement, Growth, adaptive evolution, chemostat, and turbidostat	[51], [82], [83]
Personal Bioreactor RST-1	Biosan	Up to 20 mL	*C. necator* H16	OD measurement and Growth rate,	[84]
Microbial microdroplet culture system (MMC)	Self-assembled device	2 µl	*E. Coli* MG1655, *Lactobacillus plantarum* subsp. *Plantarum* CICC 20418, *C. glutamicum* ATCC 13032, *S. cerevisiae* BY4741, *Pichia pastoris* Ppink– HC S–1, *Methylobacterium extroquens* AM1	Optical density measurements, antibiotic drug resistance study, adaptive evolution experiment	[77]

The automated culture system for laboratory evolution	Self-assembled device	40-280 μl (*typical working volume of 96 well microplates*)	*E. Coli* strain MDS42	Optical density measurements, growth measurement, batch culture, and laboratory-evolution experiment.	[73]

1.1.5 Current tools to enable accelerated ALE experiments

Traditional ALE techniques have proven their capacity to generate strains with superior characteristics. However, when a quick solution is required, the duration of these methods frequently outweighs their potential benefits. In addition, the course of an ALE experiment is determined by the mutation rates that can generate genetic diversity through random mutational processes. Consequently, several techniques have been developed to expedite the ALE process, including combining ALE with mutagenesis tools such as chemical mutagens [85], physical mutagenesis [85], genome shuffling, modification of polymerase (*dnaQ* [86] & mutaEco [87]), modification of DNA mismatch repair (MMR) [88], modification of restriction-modification system [88], multiplex automated genome engineering (MAGE) [89] and CRISPR-enabled trackable genome engineering (CREATE) [90] (**Table 1.3**).

Table 1.3 Current mutagenesis tools and strategies to accelerate ALE experiment.

Type	**Strategy**	**Reference**
Chemical mutagenesis	Incorporating ALE with ethyl methanesulfonate to the improvement of bioethanol production in *S. cerevisiae*	[7]
Physical mutagenesis	UV mutagenesis technique to generate citric acid-overproducing *Aspergillus niger* mutants	[91]
Genome shuffling	Mutants of *Streptomyces* sp. U121 were generated by a combination of nitrosoguanidine and three rounds of genome shuffling to enable fivefold hydroxycitric acid production	[92]
Modification of polymerase	Generating a mutant with mutaEco in *E. coli* to improve microbial stress tolerance	[87]
Modification of polymerase	Generating a mutant library of *dnaQ* in *E. coli* to improve microbial tolerance	[93]
Modification of DNA mismatch repair (MMR) (*mutS*)	Constructing *Lactobacillus casei* mutants in ALE experiment by deleting *mutS* to increase lactic acid resistance at low PH	**[94]**
Modification of restriction-modification (RM) system	Utilising RM to expedite bacterial ALE *in vivo* in the population-cultivation procedure in *E. coli* MG16	[95]
CREATE	Incorporating CREATE with ALE to produce *E. coli* mutants with improved furfural tolerance	[96]

1.1.6 Chemical-assisted ALE experiments

Traditional ALE depends on random genetic mutations occurring naturally in the genome when transferring microbial cells repeatedly, which may sometimes be a lengthy procedure. Incorporating chemical mutagens in ALE experiments is beneficial for accelerating natural evolution by increasing the mutation rate. The advantage of applying chemical mutagens is that there is no requirement for a complicated recombinant [97]. Chemical mutagens are a common technique for mutagenesis within the entire genome of an organism and may result in a high frequency of base-pair substitution. Alkylating compounds, base analogues, and genotoxic antibiotics are frequently used in chemical mutagenesis (**Table 1.4**) [98].

Alkylating mutagens can react with various DNA active regions [99]. For example, Alkyl groups will react with the phosphate backbone, causing frameshift mutations [97]. In recent years, Ethyl methanesulfonate (EMS) and N-methyl-N'-nitro-N-nitrosoguanidine (NTG) have been the most widely used chemical mutagens. EMS is an alkylating agent with mutagenic, teratogenic, and carcinogenic effects on organisms [100]. EMS and other alkylating agents alkylate cytosine and adenine, resulting in GC transformations to AT [99, 100]. The high mutagenic activity of EMS has been demonstrated in a wide variety of bacterial strains, including *E. coli*, *Salmonella typhimurium*, *Proteus mirabilis, Haemophilus influenzae, Staphylococcus aureus*, and more [100]. EMS has been utilised in numerous studies, such as optimising industrial enzyme production of laccase [85], protease [101], and various enzyme secretions [102].

Extensive research has focused on the interactions between DNA and chemical mutagens due to the significant role of DNA as a prime target for chemical mutation. DNA polymerases facilitate precise DNA synthesis throughout DNA replication and repair [103]. However, modifying DNA replication or repairing genes to enhance mutation rates is possible. All DNA polymerases use the nucleotidyl transfer process. The nucleotidyl transfer process requires the presence of triphosphates (dNTPs), DNA substrates, and metal ions [103]. Metal ions, namely Mg^{2+}, are necessary for elongating and removing incorrectly inserted dNTPs via the intrinsic 3′→5′ exonuclease activity of DNA polymerase 1. The 3′→5′ exonuclease proofreading activity is associated with different DNA polymerases [104]. Substituting Mg^{2+} with other divalent metal ions is technically possible. However, doing so may compromise the precision

of DNA synthesis [8, 105, 106] and lead to DNA polymerase damage [107]. The precision of DNA replication is a key factor in maintaining the stability of the genome and the insertion of nucleotides [104]. Vashishtha *et al.* (2016) [105] conducted a review which found that metal ions capable of substituting Mg^{2+} have various effects on DNA polymerases. These effects include (a) influencing the ability of incoming dNTPs to bind to polymerase binary complexes, (b) decreasing the accuracy of base selection by promoting incorrect incorporation during primer extension, (c) slowing down the process of base excision, and (d) causing incorrect matching of the primer-template terminus due to alterations in primer extension.

Several metal ions, such as Mn^{2+} [8, 106-110], Zn^{2+} [8, 108], CO^{2+} [8, 108], and Ni^{2+} [8, 108, 111] have been demonstrated to be potential mutagens in *in vitro* studies. Compounds containing metal ions can potentially be used as mutagens to accelerate ALE experiments.

Table 1.4 Common chemical agents and newly identified chemical agents for mutagenesis.

Chemical	**Application in various strains**	**Reference**
Ethyl methanesulfonate (EMS)	• Improvement of bioethanol production in *S. cerevisiae* • Citric acid overproduction in *Aspergillus niger* • Enhancement of extracellular glucose oxidase production in *Aspergillus niger* • Resistance to antifungal in *S. cerevisiae*	[7, 91, 112, 113]
Nitrosoguanidine (NTG)	• Expression of penicillin G acylase and β-lactamase in *E. coli* • Creating Mutant libraries of avermectin producer *Streptomyces avermitilis* • Induction of T5-R mutation in *E. coli* • Study of glucose to L-lysine in an industrial L-lysine producer of *C. glutamicum*	[114-117]
Acridine orange	• Citric acid overproduction in *Aspergillus niger*	[91]
N-methyl-N′-nitro-N-nitrosoguanidine (MNNG)	• Mutagenesis in *E. coli* K12 • High penicillin acylase activity of *E. coli* • The study of resistance with Daptomycin in *Staphylococcus aureus*	[118-120]
Acriflavine	• Control of methicillin resistance and toxin production in *S. aureus*	[121, 122]
Diethyl sulfate	• Biosynthesis of lysine in *S. aureus*	[123]
L-glutamic acid γ-hydrazide (GAH)	• The mutagenic activity of GAH in *E.coli*	[124]

1.1.7 Mutation in ALE

Mutations promote genetic shifts and the selection of enhanced phenotypes in nature and the laboratory. Microbial species undergo around 10^{-10} mutations per base pair per replication despite the remarkable accuracy of DNA replication [12, 125]. The mutations discovered in ALE experiments have shown their advantageous use for biological study and applied biotechnology. A population's mutation is typically beneficial, neutral, deleterious, or lethal. The majority of newly occurring mutations are considered to be neutral in the majority of environments, whereas detrimental mutations tend to arise at a quicker rate than beneficial mutations. During ALE studies, deleterious mutations are removed by selection, whereas beneficial mutations play a crucial role in shaping the genetic changes in new populations [25]. ALE offers new opportunities for metabolic engineering by pinpointing advantageous mutations linked to particular selection pressures.

In recent ALE experiments, a variety of mutations were identified, including single-nucleotide polymorphisms (SNPs), insertions and deletions (indels), transposable element movements and amplifications, deletions of larger genomic regions, and copy number variations (CNVs) (**Figure 1.4**) [12, 126]. Collectively, these genomic alterations contribute to the evolution of traits in the laboratory. For instance, the ALE experiment produced an insertion of a nucleotide into the start codon of the *glf* gene, which codes for glucose-facilitated diffusion protein and is native to *Zymomonas mobilis*. In addition, in *Z. mobilis,* SNPs were found in the genes *amtB*, *gcrA*, *gyrB2*, and *kdsB*, which code for an ammonium transporter, cell cycle, DNA gyrase subunit B, and 3-deoxy-manno-octulosonate cytidylyltransferase, respectively. Compared to the parental strain, these mutations in evolved *Z. mobilis* strains increased the rate of xylose utilisation, ethanol production and enhanced the ability to co-ferment xylose and glucose [127].

After identifying the desirable phenotype of evolved microbial cells, these cells can be used directly for biological production. However, it should be noted that tolerance to one stress frequently comes with compromises in a different growth environment, depending on the particular adaptive mutations acquired. For instance, strains that evolved to succeed at high temperatures typically lose fitness at low temperatures.

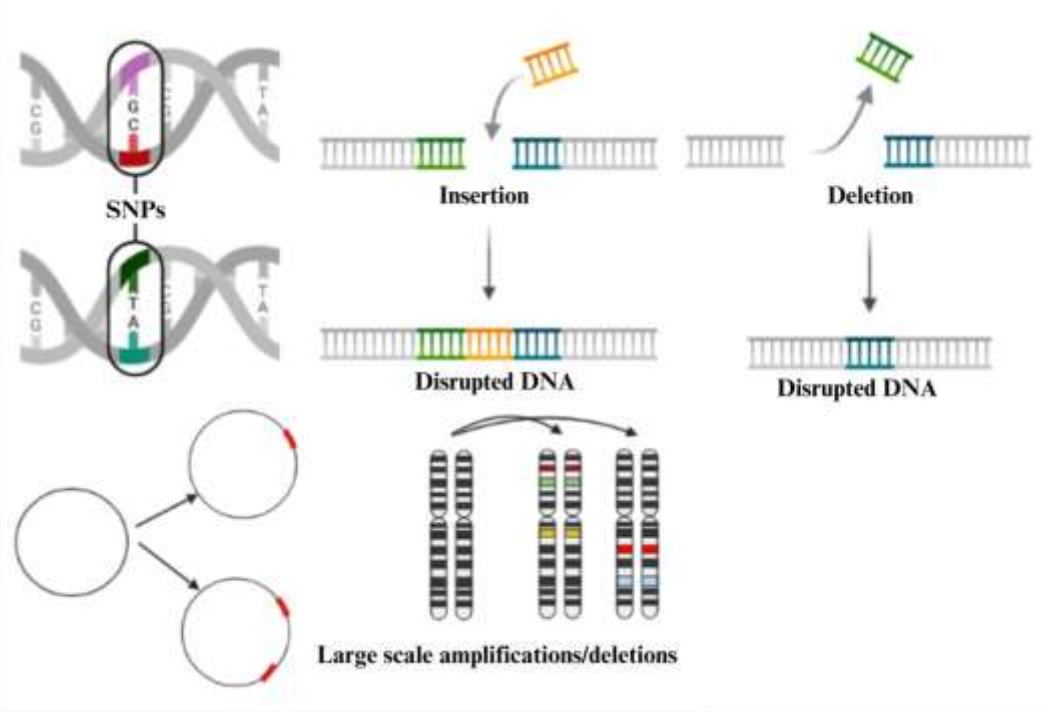

Figure 1.4 Mutations that are usually found in ALE experiments. During the selection for improved phenotypes, single nucleotide polymorphisms (SNPs), smaller insertions and deletions (indels), and larger insertions and deletions contribute to genetic and gene regulatory changes and fitness changes (Adapted from Dragosits & Mattanovich, 2013[12]).

1.1.8 ALE applications

ALE has become an indispensable tool in recombinant engineering for strain development and optimisation by efficiently facilitating fitness improvements of microorganisms. In biotechnology, parameters such as growth rate, survival rates in toxic compounds, and biomass yield are suitable fitness criteria. Based on a review by Sanberg *et al*. (2019), the various applications of ALE can be classified into four categories applicable to industrial biotechnology, including growth rate improvement [15, 16], tolerance improvement [17], substrate utilisation [18], and desired product yield improvement [19-21]. Notably, these application categories are not mutually exclusive, and ALE experiments frequently improve multiple strain traits [26]. Each category will be discussed separately in the sections below.

1.1.8.1 Growth rate improvement

ALE has been used to effectively enhance the growth capabilities of numerous species, most notably *E. coli*. For example, after 1300 generations, Kim *et al.* (2022) obtained the evolved strain of *E. coli* CY02. Its growth rate increased by nearly 40%, from 0.67 h^{-1} to 0.94 h^{-1} [128].

The short generation time of microbes is a key factor in their application in biotechnology and scientific research, and ALE enables the rapid improvement of this desirable characteristic. ALE has been used to optimise the growth rate of several industrially significant microbial species. For example, *C. glutamicum*, one of the essential industrial platform organisms, has been used to produce 3.1 million tons of L-glutamate annually. Pfeifer *et al.* (2017) conducted a comparative ALE experiment to increase the growth of *C. glutamicum* on a minimal glucose medium. ALE generated evolved *C. glutamicum* (UBw and UBm) with a 26% enhanced growth rate on a minimal glucose medium [16].

ALE used for improving growth revealed mutations that contributed to increased fitness. *E. coli* can evolve various modes of lacZ expression depending on the presence of lactose, glucose, or carbon sources in its environment. Most mutations that result in altered expression patterns have accumulated in the *lacI* and *lacO1* regions of the lac operon. These mutations contributed to a decreased lag phase and increased maximal growth rates in the lactose growth medium [12].

1.1.8.2 Tolerance improvement

The most common use of ALE experiments is to increase an organism's resistance to toxic environments. Stress caused by a toxic environment can rapidly inhibit growth potential; when microbial cells are exposed to high-stress levels, cellular resources are perturbated [129], resulting in reduced growth, which is undesirable for industrial production. Due to the toxicity, many bio-renewable feedstocks have a detrimental effect on microorganisms' production viability. For instance, a cheap feedstock such as lignocellulosic hydrolysate contains many fermentable sugars, usually contaminated with toxic compounds [130]. Most wild-type (WT) strains and production chassis are not exposed to high concentrations of certain chemicals in

their native environments; consequently, enhanced tolerance mechanisms are always advantageous to designing a successful strain.

ALE has been utilised to mitigate the detrimental effects of different stress, including temperature [131], pH [17], osmotic pressure [31], solvents [132], and various inhibitors [30]. ALE is frequently more effective than rational engineering methods for enhancing stress tolerance. Due to the complexity of an organism's stress response, the precise tolerance mechanisms are often unknown, and attempts to use rational engineering fail [26]. ALE effectively addresses prominent industrial stressors, including hydrolysate inhibitors, acid, salt, and temperature.

1.1.8.2.1 Hydrolysate inhibitor tolerance

Numerous hydrolysate substances inhibit microorganisms [133], including aliphatic acids and aromatic compounds. These inhibitors derive from cellulose, hemicellulose, and lignin, the three principal components of the lignocellulosic biomass [134]. Menegon *et al.* utilised ALE to generate a strain of *Saccharomyces cerevisiae* capable of withstanding inhibitors in the lignocellulosic hydrolysate [135].

1.1.8.2.2 Acid tolerance

Due to their toxicity, compounds with potential biotechnological value cannot be effectively metabolised or produced in microorganisms. For instance, numerous carboxylic acids are promising biorenewables but induce membrane damage, and attempts to engineer a greater membrane strength rationally have failed to enhance carboxylic acid production. Royce *et al.* (2015) [136] addressed this issue with an ALE experiment of *E. coli* onto octanoic acid, wherein strains were obtained with enhanced tolerance to octanoic acid and several other carboxylic acids and butanol isomers. Furthermore, the ALE method was employed to investigate the mechanism by which *S. cerevisiae* developed tolerance to inhibitory concentrations of three dicarboxylic acids: pimelic, glutaric, and adipic acid [137].

1.1.8.2.3 Temperature

The inability of a microorganism to thrive at optimal production temperatures hinders the effectiveness of numerous industrial processes. A significant effort was made to improve the thermotolerance of a microorganism using ALE to increase the efficacy of a process and, consequently, the economic potential of multiple processes [26].

Caspeta *et al.* (2014) [131] provided a successful example of ALE results identifying the molecular mechanisms of adaptation; yeast was evolved for enhanced thermotolerance, resulting in strains that grew more than 50% faster at 40°C. Mutational convergence in independently evolved duplicates revealed that a gene inactivation altered the sterol composition of the cells from ergosterol to fecosterol, thereby optimising membrane fluidity at elevated growth temperatures.

1.1.8.3 Substrate utilisation

In most industrial applications, efficient substrate utilisation is required to produce metabolites and other products of interest. Adaptive evolution is frequently utilised to enhance fitness in a novel substrate. For example, ALE has generated large fitness improvements of microorganisms for many different substrates and even established growth on non-native substrates like 1,2-propanediol [138]. Such initiatives are an effective method for expanding the substrate repertoire and bioprocessing efficiency of chassis strains.

ALE has been utilised to overcome obstacles such as the toxic compound acetate in using lignocellulosic biomass as a source of nutrients. This was investigated by Rajaraman *et al.* (2016) using an ALE on various *E. coli* strains with acetate as the sole carbon source. A single amino acid substitution in the RNA polymerase subunit RpoA resulted in a 25% increase in the specific growth rate of evolved strains and a significant change in gene expression for several genes [18].

1.1.8.4 Desired product yield improvement

Maximising the bioproduction of desired metabolites is challenging, and rational approaches to strain design are often insufficient to achieve the desired productivity. The ALE approach has been successfully used to increase the production of various desired metabolites using microbial factories, such as carboxylic acid [136], L-ornithine [55], L-valine [139], isobutanol [140], lipid production [141], carotenoid production [142], glutamate production [143], lysine production [144], and many more.

ALE approach can also be combined with *in silico* work to increase the production rate of the desired product. For instance, the Fong group used a combination of in silico design and adaptive evolution to increase the lactate yield of three *E. coli* strains. Results indicated that lactate secretion was directly linked to growth. This study demonstrated the potential of growth coupling to boost productivity [145].

1.2. *Cupriavidus necator* H16: A chosen strain for phenotype improvement

C. necator (formerly known as *Ralstonia eutropha*) is a gram-negative, chemolithoautotrophic, facultative bacterium. This organism thrives in soil and freshwater environments and was initially isolated from a German spring [146, 147]. *C. necator* uses oxygen as the primary electron acceptor under aerobic conditions but can utilise nitrate and nitrite under anaerobic conditions [148]. It can grow without heterotrophic conditions by utilising H_2 and CO_2 as primary energy sources [149]. Friedrich *et al.* (1982) in Volodina *et al.* (2016) [147] reported that *C. necator* could also mixotrophic growth, using both inorganic and organic substrates as energy sources. Depending on the availability of carbon sources, *C. necator* H16 can switch between autotrophic, heterotrophic, and mixotrophic growth [150]..

C. necator utilises the enzyme RuBisCo to assimilate CO_2 into its system via the Calvin-Benson-Bassham cycle (CBB) (**Figure 1.5**) [151]. CBB gene expression and CO_2 assimilation studies have focused on this strain [152]. Carbon dioxide capture and utilisation (CCU) has garnered significant attention owing to its environmentally conscious and sustainable approach. *C. necator* has undergone genetic modification to synthesise formate from carbon dioxide [150] and enhanced CO_2 conversion into terpene α-humulene [153]. *C. necator* H16 was used to synthesise several industrial chemicals such as alcohols, alkenes [1], dicarboxylic acids, diamines [154], and polyhydroxybutyrates.

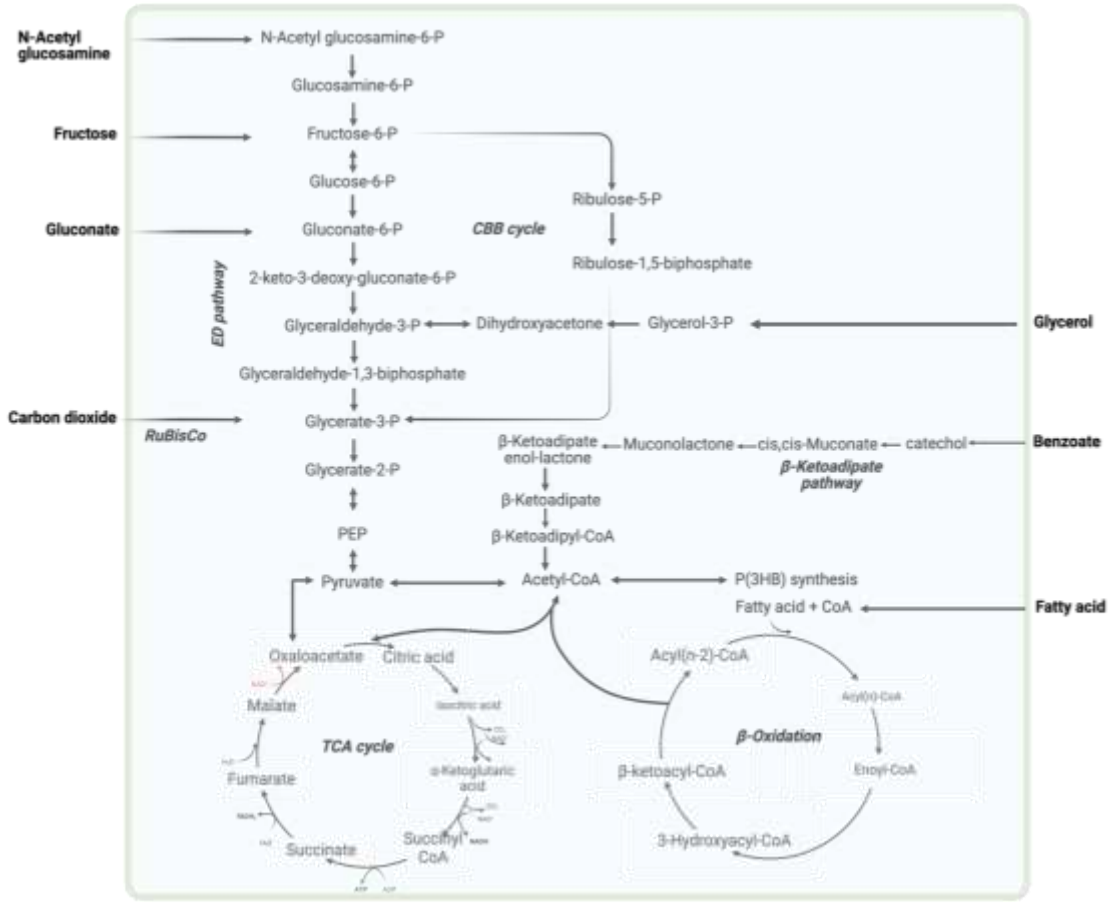

Figure 1.5 Primary metabolic pathways in heterotrophic and autotrophic C. necator. Ribulose-1,5-bisphosphate carboxylase/oxygenase (RuBisCo) converts Ribulose-1,5-bisphosphate to Glycerol-3-P, which then enters the Entner-Duodoroff (ED) pathway for pyruvate accumulation. N-acetylglucosamine, fructose, and gluconate are also converted to pyruvate via the same metabolic pathway. Pyruvate is catabolised by pyruvate dehydrogenase, which converts pyruvate into acetyl-CoA, which can either be converted into poly[(R)-3-hydroxybutyrate] (PHB) or enters the tricarboxylic acid cycle (TCA). Fatty acids and certain organic acids are metabolised via β-oxidation, producing acetyl-CoA. C. necator converts glycerol to glycerol-3-phosphate and later enters the ED pathway. C. necator degrades BA via the catechol branch in the β-ketoadipate pathway (Adapted from Volodina et al. (2016) [147], Pantoja et al. (2008) [155]).

Due to its ability to naturally accumulate biodegradable bioplastic PHA, *C. necator* has been a major research focus, especially in biomanufacturing. This β-proteobacterium can store poly-3-hydroxybutyrate (P(3HB)), a typical type of PHA, up to 90% of its dry cell weight in intracellular granule (**Figure 1.6**) [147]. *C. necator* requires the essential enzymatic steps of β-ketothiolase (*phaA*), aceto-acetyl reductase (*phaB*), and PHA synthase (*phaC*) to produce PHA [156]. PHA accumulation is only possible if the carbon source is abundant and one essential nutrient, such as nitrogen, oxygen, magnesium, potassium, or phosphorus, is insufficient [147]. Short-chain length hydroxyalkanoate (scl-HA with the monomer of 3 to 5 carbons) and medium-chain length hydroxyalkanoate (mcl-HA with the monomer of 6 to 14 carbons) are the two types of PHA. Scl-PHA possesses thermoplastic properties comparable to polyethene

[157] and can replace chemical plastic in specific applications, such as cosmetic containers and bottle packaging. Although PHAs have been used in the industry for over ten years, manufacturing costs are still high. Production of PHA-based bioplastic is primarily restricted by its high cost. A high-value carbohydrate is the source of current bioplastic manufacture. The use of this costly feedstock is debatable as it may compete with food sources; as a result, there is a great need for an inexpensive feedstock.

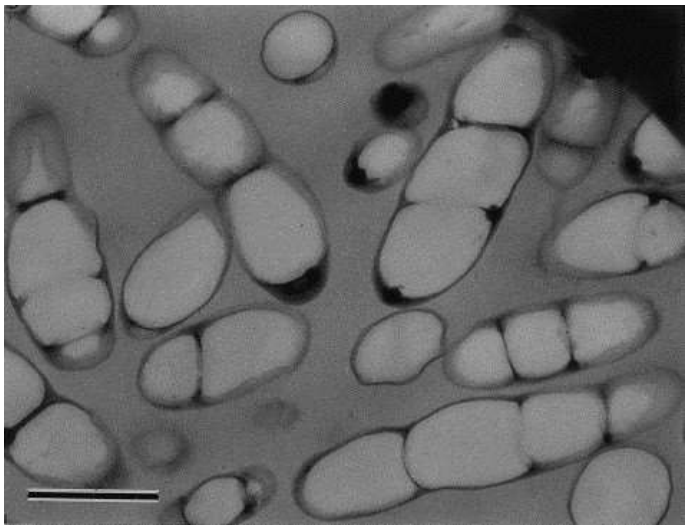

Figure 1.6 A transmission electron micrograph (TEM) image of PHA inclusion bodies within C. necator (Sudesh et al., 2000 [158]).

Additionally, *C. necator* is desirable due to its diverse carbon utilisation. Studies have investigated the ability of *C. necator* to effectively use a diverse range of carbon sources, ranging from fructose to abundant lignocellulosic waste [159]. Moreover, the phenotypic aspects of *C. necator* have been significantly enhanced, enabling it to efficiently use substrates that are considered less favourable, such as glycerol [1].

To expand the range of carbon substrate utilisation, a wild-type *C. necator,* incapable of naturally using glucose, was genetically modified to enable glucose utilisation [160]. Relevant to the ALE approach (**Table 1.5**), mutants of *C. necator* have been generated to utilise various carbon sources. These characteristics and the fact that this species is considered a harmless organism make it an interesting subject for study.

Table 1.5 ALE studies in *C. necator.*

No	Description	Reference
1	The utilization of ALE to enhance the utilization of glycerol	[1]
2	The growth improvement of *C. necator* on formate using ALE-informed engineering	[161]
3	Improving the tolerance of *C. necator* to carbon monoxide using ALE	[2]

1.2.1 Genome

C. necator strain H16 genome has been completely sequenced, making it less complicated to study. The complete genome of *C. necator* comprises three replicons: chromosome 1 (4.1 Mb), chromosome 2 (2.9 Mb), together encode 6,116 putative genes [149], and megaplasmid pHG1 (452,156 bp), which carries 429 potential genes [162].

According to distribution analysis, chromosome 1 is responsible for DNA replication, transcription, translation, and ribosomal proteins. Chromosome 1 encodes genes for DNA replication, which is essential for aerobic and organic acid metabolism and Poly[(R)-3-hydroxybutyrate] (PHB) synthesis. The genes on chromosome 2 are responsible for the central steps of 2-keto-3-deoxy-6-phosphogluconate (*KDPG*), sugar acid metabolism, aromatic compound decomposition, and alternative nitrogen sources [151]. Meanwhile, megaplasmid pHG1 contains anaerobic growth-related genes [162].

1.2.2 Lignocellulosic hydrolysates as a potential feedstock for bioplastic production

Lignocellulosic biomass is a dry plant material that makes up a significant portion of the terrestrial biomass on the Earth's surface. Common classifications for lignocellulosic biomass include virgin biomass, energy crops, and waste biomass [163]. The main parts of lignocellulose biomass are cellulose, hemicellulose, and lignin. These polymers are closely linked to each other, make up the complex covalent bond, and are difficult for microbes to digest [164]. Cellulose is a high-molecular-weight homopolysaccharide made up of D-glucopyranosyl units. The structure is rigid, and pretreatment is required to break it down. Hemicelluloses are linear and branched heteropolysaccharides of L-arabinose, D-galactose, D-glucose, D-mannose, and D-xylose that may also have acetyl groups. The hemicellulose structure is not crystalline, so it is easy to break it down. Lignin is the third-most important

part. It is made up of phenylpropane units linked by ether bonds, which are the most common type of bond between units. There are three phenylpropionic alcohol molecules in lignin. They are p-coumaryl alcohol, coniferyl alcohol, and sinapyl alcohol. Due to its molecular structure, lignin is highly resistant to chemical and enzymatic breakdown [133, 165, 166].
About 75% of lignocellulose biomass consists of polysaccharides, which may be converted to monosaccharides for fermentation [167]. However, the sugar in lignocellulosic biomass remains encased in the complex and recalcitrant lignocellulosic plant cell wall, making its extraction difficult and costly. To convert this biomass to a liquid fermentation medium, pretreatment and hydrolysis are required to remove the biomass structure and produce monomer sugars such as glucose and xylose [168].

There are numerous pretreatment techniques available for obtaining fermentable sugars from lignocellulosic biomass. These include using steam, alkaline and chemicals such as dilute-acid [169]. During pretreatment, coproducts, also known as hydrolysates, are accumulated. Hydrolysates are comprised of pentose sugars, sugar acids, aliphatic acids (acetic acid, formic acid, and levulinic acid), and furan aldehydes [130]. In addition, depending on the severity of pretreatment conditions, short-chain organic acids are produced as the major hydrolytic by-products [170].

Many hydrolysate substances, including aliphatic acids and aromatic compounds, inhibit microorganisms [171]. These inhibitors are derived from cellulose, hemicellulose, and lignin, the three primary constituents of lignocellulosic biomass [134]. More than 100 compounds have been investigated as lignocellulosic hydrolysates inhibitors [172].

1.2.3 Inhibitory effects of lignocellulosic hydrolysates

Lignocellulosic hydrolysates may be produced by processing hardwood or softwood, agricultural waste such as corn stover and various types of straw (including wheat and rice straw), or solid municipal waste. The composition of the many lignocellulosic materials, including the inhibiting compounds, can vary considerably depending on the raw material source, the prehydrolysis, the hydrolysis procedures, and the recirculation [173]. In general,

there are three categories of inhibitors: weak acids, furan derivatives, and phenolic compounds. Each category has different inhibitory mechanisms against microorganisms.

First, substances released during prehydrolysis and hydrolysis include weak acids such as acetic acid (released when the hemicellulose structure is degraded) and other extractives (**Figure 1.7**). The extractives are comprised of terpenes, alcohols, and aromatic compounds like tannins[166]. The hydrophobicity and pK values correlate with weak acids' inhibitory effect. Although the inhibition mechanism of weak acids has yet to be thoroughly investigated, it is known that the mechanism of inhibition is associated with the dissociated and undissociated forms of weak acids [172]. According to Palmqvist *et al*. (2000) [174], the undissociated form of weak acids can diffuse through the plasma membrane into the cytosol, inhibiting cell proliferation. Furthermore, accumulating weak acids within a cell can harm ATP synthesis in mitochondria, glycolysis, cell growth, and fermentation [172].

During the process of pre-hydrolysis and hydrolysis, a variety of inhibitors, such as furan derivates (furfural and 5-hydroxymethyl-2-furaldehyde (HMF)), clavulanic acid, and formic acid, accumulate as a result of the breakdown of sugars. Research has been conducted on the furan derivatives to assess their capacity to hinder the growth of microbes. Furan build-up impacts glycolysis and enzymes in the central metabolic route, including pyruvate dehydrogenase, acetaldehyde dehydrogenase, alcohol dehydrogenase, and glyceraldehyde-3-phosphate dehydrogenase. Furan derivatives have been shown to reduce growth rate, cell mass, and fermentation yield [172]. For instance, according to a review by Palmqvist *et al.* (2000) [174], these furan derivatives limit the growth of *Scheffersomyces stipitis*. In a previous study, the inhibitory effects of several hydrolysis by-products, such as acetic acid, furfural, levulinic acid, and vanillin, were investigated on the production of PHA in the culture [175].

Thirdly, the oxidative cleavage of lignin results in the accumulation of phenolic and aromatic groups [172]. Catechol, 4-hydroxybenzoic acid, and vanillin were the primary constituents of the hydrolysates [174]. Wang discovered eleven toxic compounds in corn stover slurry, including ammonium acetate and benzoic acid [4]. The clear inhibitory mechanism of these compounds has yet to be thoroughly elucidated; however, the inhibition may be due to the interaction with the cell membrane [172]. Cell growth is inhibited by hydroxybenzoic acid via its effect on membrane fluidity [169]. A comparatively low concentration of benzoic acid (1 g/L) has been reported to inhibit bacterial growth [176]. Wang *et al*. (2014) investigated the

inhibitor sensitivity of *C. necator* and found that benzoic acid in lignin degradation products was the most toxic compound [4].

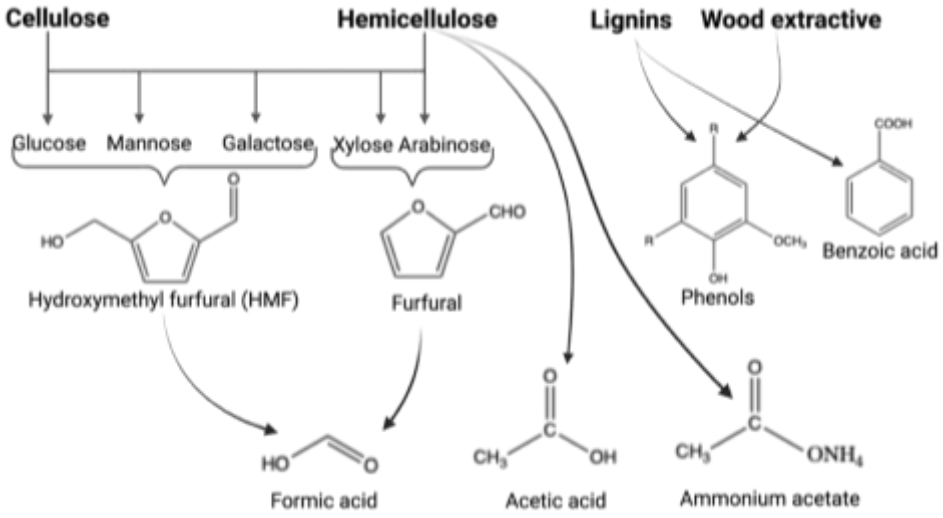

Figure 1.7 Schematic illustrating the principal inhibitor formation pathways. Typically, the pretreatment degrades the hemicellulose, resulting in the formation of pentose and hexose sugars, sugar acids, aliphatic acids (principally acetic acid, formic acid, and levulinic acid), and furan aldehydes (5-hydroxymethylfurfural (HMF) and furfural). Lignocellulose hydrolysates contain aliphatic acids, including acetic acid, formic acid, and levulinic acid. Lignin is the primary source of phenolic compounds. The formation of ammonium acetate by hydrolysis of acetyl groups of hemicellulose and formic acid by acid-catalysed thermochemical degradation of polysaccharides (Adapted from Jonsson et al. (2013) [133]).

1.2.4 Benzoic Acid (BA)

Benzoic acid and hydroxybenzoic acid are common lignin monomer intermediates detected in high concentrations in lignocellulosic waste slurry [4]. Hydroxybenzoic acid is a major component of the total phenol [4]. Many microorganisms are significantly inhibited by benzoic acid and hydroxybenzoic acid. These two acids can eliminate energy generation in the cell by depleting the proton motive force in the cytoplasm. Liposoluble p-hydroxybenzoic acid can diffuse into the cytoplasm, dissociating the acid and decreasing the cytoplasmic pH [177]. Even though ATPase can neutralise the pH by hydrolysing ATP and pumping the proton out of the cell, this process requires additional ATP. The ATP compensation can reduce the growth rate and biomass production. Krebs *et al*. (1983) [129] discovered that benzoic acid inhibits the growth of *S. cerevisiae* by lowering intracellular pH, which inhibits phosphofructokinase in glycolysis.

According to Warth [178], an increase in the concentration of benzoic acid led to a greater restriction in the glycolysis pathway, namely at the reaction steps involving phosphoglycerate kinase and pyruvate kinase. Conversely, the enzymatic steps of phosphofructokinase and hexokinase become less severe. For instance, in a glucose-limited medium supplemented with 10 mM benzoate, the biomass production of *Saccharomyces cerevisiae* CBS 8066 decreased from 0.51 g/g (biomass/glucose) to 0.15 g/g [179]. The ATP depletion caused by benzoic acid also occurred in *Zygosaccharomyces bailii* [178]. Several investigations have demonstrated the effect of hydroxybenzoic and benzoic acids on microorganisms **(Table 1.6)**.

Table 1.6 Effect of hydroxybenzoic acid and benzoic acid on bacterial growth.

Microorganism	**Concentration**	**Effect on Growth**	**Reference**
Thermoanaerobacter mathranii.	10 mM of hydroxybenzoic acid	Growth is inhibited	[180]
E. coli LY01	3 mM of hydroxybenzoic acid	Inhibiting 50% of growth	[181]
Klebsiella pneumoniae	1.5 mM of hydroxybenzoic acid	Inhibiting 50% of growth	[182]
S. cerevisiae	3.8 mM hydroxybenzoic acid	Inhibiting 30% of growth	[183]
S. cerevisiae	10 mM of benzoic acid	Full inhibition	[178]
Adapted *C. necator* DSM 545	9.6 mM of benzoic acid	2.5 g/L was found to be toxic at initial concentration	[184]
Pseudomonas stutzeri A1501	8 mM benzoic acid	No growth was found	[185]
Halomonas sp. KHS3	0.7 mM benzoic acid	No growth	[186]

1.2.4.1 The catabolic pathway for benzoic acid in *C. necator* and its potential as a carbon source for bioplastic production

As stated in a study conducted by Pantoja *et al.* (2008) [155], *C. necator* JMP134 can use benzoate or benzoic acid and 4-hydroxybenzoate as its primary carbon sources. These compounds are among the 140 aromatic compounds investigated as potential substrates for value-added chemical production.

Certain indigenous soil bacteria can break down benzoate and 4-hydroxybenzoate through the β-ketoadipate pathway [187]. This pathway is exclusive to soil bacteria, namely *Pseudomonas strains, Acinetobacter calcoaceticus, Rhodococcus erythropolis*, and *Agrobacterium tumefaciens* [187]. The β-ketoadipate pathway has been analysed at the genome level in many organisms, including *C. necator* JMP134 [155], *Cupriavidus balensis* B-8[188], *C. basilensis* B-8 [188], *C. basilensis* OR16 [189], and *C. necator* NH9.

In their study, Pantoja *et al.* (2008) [155] investigated the degradation of aromatic compounds and the metabolic reconstruction process in *C. necator* JMP134. The research used benzoic acid and 4-hydroxybenzoate as substrate models to represent the aromatic catabolic pathway. *C. necator* JMP134 metabolises benzoic acid via the catechol branch and 4-hydroxybenzoate through the protocatechuate branch in the β-ketoadipate pathway (**Figure 1.8**). The *ben/cat* operon and *the pob/pca* operon metabolise benzoic acid and 4-hydroxybenzoate into β-ketoadipate, respectively. Both branches converge at the same enzymatic step during the conversion of β-ketoadipate to acetyl-CoA. The analysis of the amino acid sequence data demonstrated that the ketoadipate pathway is remarkably conserved in creatures that possess it [188].

Prior research demonstrated that benzoate was favoured as a carbon source when grown on substrates containing benzoic acid and 4-hydroxybenzoate in *P. putida* PRS2000 [190]. Brzostowicz *et al.* (2003) studied the preferences of *Acinetobacter* sp. strain ADP for benzoic acid over 4-hydroxybenzoate consumption. The study found that BenM and CatM inhibited *pobA* from being expressed when benzoic acid was present. These regulators inhibit the PcaK-mediated uptake of 4-hydroxybenzoate [191]. Based on these data, benzoic acid may be used as a supplemental carbon source for chemical production, particularly to enhance bioplastic production. Wang *et al.* (2014) [4] reported that when the concentration of the benzoic acid is low, catechol can be further converted into cis,cis-muconate or 2-hydroxymuconate-6-semialdehyde through two different metabolic pathways leading to the accumulation of the key intermediate of acetyl-CoA for PHB production.

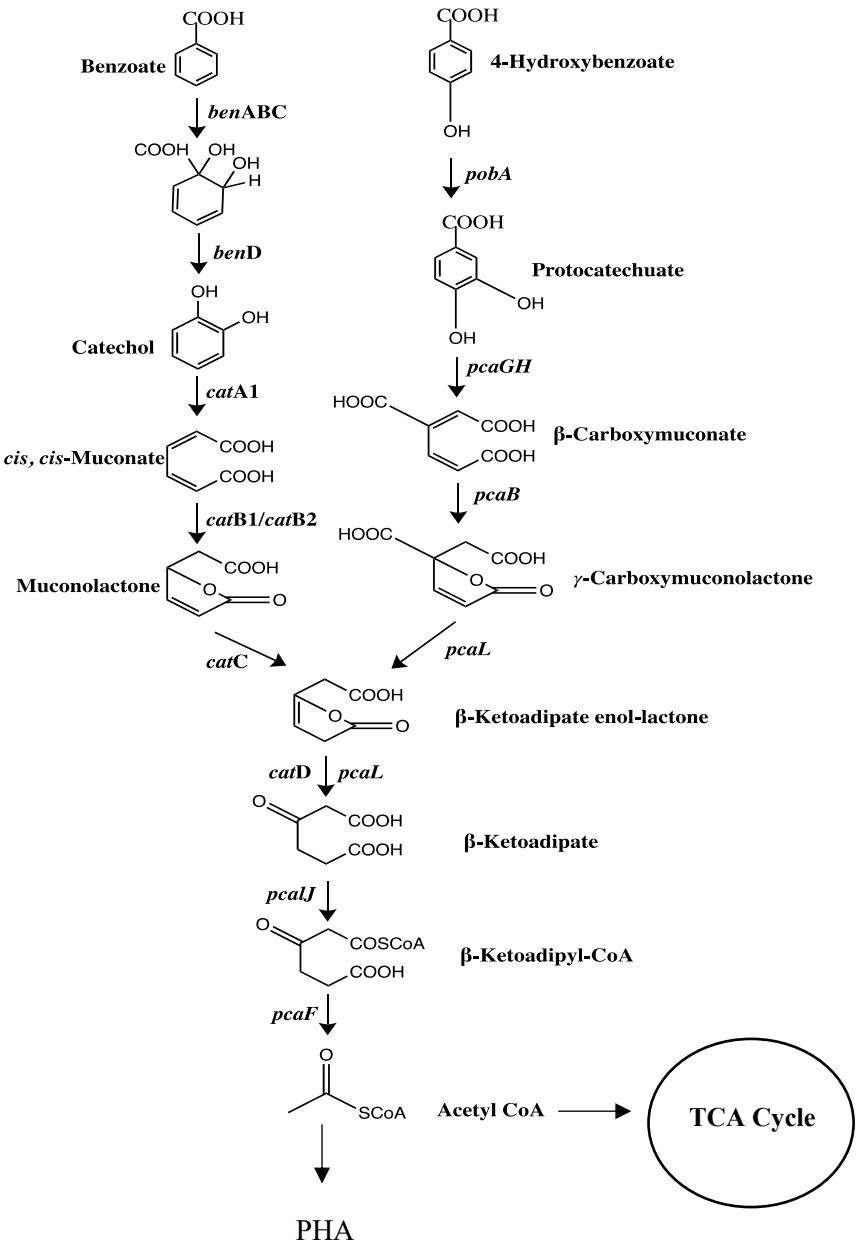

Figure 1.8 The β-ketoadipate pathway in C. necator (Adapted from Pantoja et al. (2008) [155]). The conversion of Benzoate and 4-Hydroxybenzoate to acetyl CoA & PHA via catechol and protocatechuate branches in C. necator JMP134. The depicted pathway includes genes; benA (Benzoate-1,2-dioxygenase α subunit), benB (Benzoate-1,2- dioxygenase β subunit), benC (Benzoate-1,2-dioxygenase electron transfer component), benD (Benzoate cis-diol dehydrogenase), catA1 (Catechol-1,2-dioxygenase), catB1 (Muconate cycloisomerase), catB2 (Muconate cycloisomerase), catC (Muconolactone d-isomerase), catD (3-Oxoadipate enol-lactone hydrolase), pcalJ (β-Ketoadipate succinyl-CoA transferase), pcaF (b-Ketoadipyl-CoA-thiolase), pobA (4-Hydroxybenzoate-3-monooxygenase), pcaG (Protocatechuate-3,4-dioxygenase α chain), pcaH (Protocatechuate-3,4-dioxygenase β subunit), pcaB (3-Carboxy-cis,cis-muconate cycloisomerase), and pcaL (4-carboxymuconolactone decarboxylase) (Adapted from Pantoja et al. (2008).

1.2.4.2 The *ben* and *cat* operons of benzoic acid degradation pathway

The *ben* and *cat* operons are required for catechol degradation of -ketoadipate in *C. necator* JMP134. The amino acid sequences of the proteins encoded by these operons are highly similar to those of aromatic compound decomposers such as *Pseudomonas, Burkholderia*, and *Acinetobacter*. The gene encoding CatA1, which initiates the catechol branch of the β-ketoadipate pathway, clusters with the *benABCD* genes, which direct benzoate into this pathway. The *catB1* gene encodes muconate cycloisomerase and is located near the *ben* and *catA1* genes but is not part of the putative operon. In *C. necator* JMP134, the *catR* genes encoding a putative LysR-type transcriptional regulator controls the *ben* and *cat* gene operons [155, 192].

Pantoja *et al*. (2008) state that β-ketoadipate pathway operons vary between strains that contain this pathway. The *catB1* gene is near the *catA1* and *ben* genes but not part of the operon. The *catC* gene is in the second operon. The enzyme encoded by this specific gene catalyses the conversion of muconate to β-ketoadipate. In *C. necator* JMP134, the catechol and protocatechuate branches of the β-ketoadipate pathway converge at the β-ketoadipate stage. In contrast, in *P. putida* KT2440, they converge at the β-ketoadipate enol lactone stage [193]. The β-ketoadipate-CoA transferase and thiolase enzymatic steps are not encoded within *ben/cat* operons in *Acinetobacter*.

Investigations have been conducted on the operons of the β-ketoadipate pathway (**Table 1.7**) after discovering their essential role in breaking down aromatic chemicals. To bridge the gap between sequence analysis and function for aromatic degradation genes, it is necessary to ascertain the evolutionary process of the aromatic catabolic pathway in a soil bacterium.

Table 1.7 The current studies of genes encoding β-ketoadipate pathway.

No	Strain	Description	Reference
1	*Sinorhizobium meliloti*	• Designing a plasmid, namely pSymB expressing *pcaDCHGB* operon and *pcaIJF* (β-ketoadipate succinyl-CoA transferase). *(β-ketoadipate enol- lactone hydrolase (*pcaD*), protocatechuate 3,4-dioxygenase alpha-subunit (*pcaG*), β-carboxymuconolactone decarboxylase (*pcaC*), protocatechuate 3,4-dioxygenase β-subunit (*pcaH*), and β-carboxy-*cis*, *cis*-muconate cycloisomerase (*pcaB*). • β-ketoadipate accumulated from protocatechuate (carbon source).	[194]

2	*Rhodococcus* species AN-22	• Expression of *catABC* genes in the aniline-assimilating.	[195]
3	*Rhodococcus erythropolis*	• Expressing gene *catR-catABC* (β-ketoadipate pathway) along with *pheA2A1-pheR* from *R. erythropolis* CCM2595 to degrade phenol.	[196]
4	*P. putida mt-2*	• Study of TOL Pathway for the degradation of toluene/m-xylene through the production of intermediate compounds benzoate/3-methylbenzoate.	[197]
5	*P. putida*	• The effect of *benR* transcriptional regulator and Crc on the expression of *benABCD* genes.	[198]
6	*Halomonas organivorans*	• Cloning, characterization and analysis of *cat* and *ben* genes from the Phenol Degrading Halophilic Bacterium *Halomonas organivorans.*	[199]
7	*P. putida* KT2440	• Genomic analysis of aromatic catabolic pathway in *P. putida* KT2440 including the protocatechuate (*pca* genes) and catechol (*cat* genes) branches of the β-ketoadipate pathway.	[193]
8	*C. glutamicum*	• Engineered *Corynebacterium glutamicum* for the production of muconic acid (MA) from lignin by deleting *catB* gene (muconate cycloisomeraase) in the β-ketoadipate pathway. • Optimization of MA production by constitutive overexpression of *catA* catechol 1,2-dioxygenase.	[200]
9	*P. stutzeri* A1501	• Genome analysis of the benzoate and 4-hydroxy benzoate catabolic pathway • The benzoate degradation was subject to CCR induced by glucose and acetate.	[185]
10	*Klebsiella pneumoniae*	• Metabolic engineering of *K. pneumoniae* to produce MA. • Overexpression of *catA* to increase the accumulation of catechol to cis,cis-muconate. • Deletion of *catB*	[201]
11	*Chromohalobacter sp.* strain HS-2	• Expression of *benABC* and *pobA*	[202]

2.4.3 The connection between the benzoic acid degradation pathway and *C. necator* growth

Wang's research team has shown a clear relationship between the presence of catechol and the initial amount of benzoic acid in cell growth. The research demonstrated that *C. necator* cannot metabolise catechol to cis, cis-muconate or 2-hydroxymuconate-6-semialdehyde when exposed to high benzoate concentrations. The elevated level of benzoic acid promotes the buildup of catechol, resulting in the creation of 1,2 benzoquinone. This chemical has a very detrimental effect on cellular growth. Catechol may be detected using a colourimetric test, where the culture media changes to a dark brown [4, 203]. Berezina *et al.* (2015) [184] observed that the medium exhibited a dark green-brown couloration when benzoic acid was present. This

research proposed that the concurrent existence of cis-1,2-dihydroxy-cyclohexa-3,5-diene-1-carboxylate and catechol primary metabolites altered the medium's colour.

1.2.5 Ammonium acetate (AA)

Acetate is a very abundant organic acid in by-products obtained from lignocellulosic sources. Acetate is a common inhibitor in hydrolysates at high concentrations [204]. Acetate, one of the eleven chemicals in the lignocellulosic waste, exhibits toxicity towards *C. necator.* Ammonium is often used to counterbalance the effects of pre-treated corn stover by neutralising two commonly occurring anions: acetate (derived from hemicellulose hydrolysis) and sulphate (resulting from sulfuric acid pretreatment). Ammonium acetate exhibited higher toxicity compared to ammonium sulphate [4].

Acetate may be naturally excreted throughout the process of growing. During aerobic growth, *E. coli* produces acetate, a by-product of glycolysis, when glucose is the only carbon source [5]. Nevertheless, its build-up in the medium hinders cell growth. When acetate is protonated, it may readily diffuse across the cell membrane. Due to the significant difference between the pKa and the intracellular pH, the compound dissociates inside the cell, forming an acetate anion and a proton. To maintain the membrane potential, surplus protons must be removed from the cell, requiring energy and limiting cell growth [5, 205]. Moreover, acetate anions within the cell elevate the internal osmotic pressure.

The inhibitory effect of acetate on growth is also attributed to reducing the intracellular pool of methionine and the accumulation of the toxic intermediary homocysteine. This amplifies the significance of the drop in cytoplasmic pH. Acetate may hinder the function of an enzyme in the latter stage of the methionine formation process (**Figure 1.9**), leading to the build-up of homocysteine [202]. Roe *et al.* (2002) [206] found that exposure to an inhibitory concentration of acetate leads to a decrease in intracellular levels of other anions, particularly glutamate, to regulate osmotic pressure. The resulting disruption of anion pools may influence metabolic function and growth.

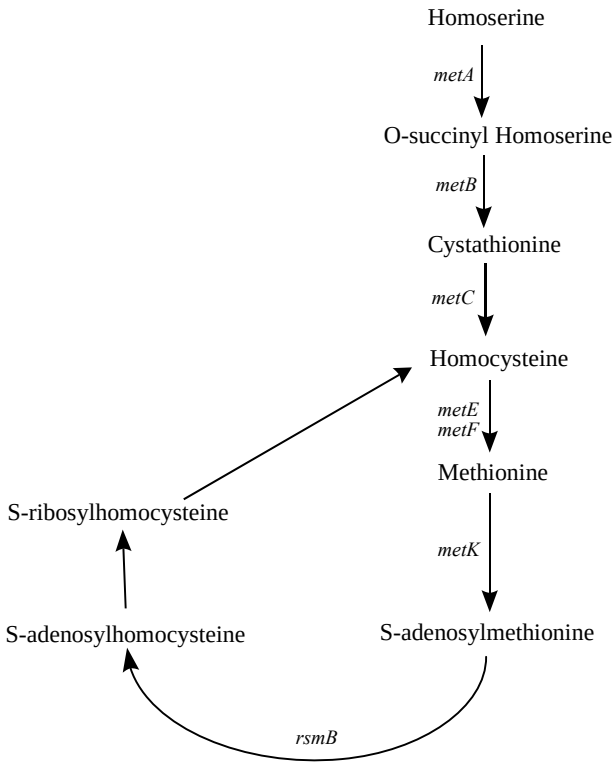

Figure 1.9 A schematic representation of E. coli's methionine biosynthesis pathway. The gene names are italicised (Adapted from Roe et al. (2002) [206].

Regarding the effect of ammonium on the growth of *C. necator*, it has been reported that ammonium concentrations above 2 g/L are detrimental to its growth [207] (**Table 1.8**). A number of the proposed mechanisms for ammonium inhibition are alterations in intracellular pH, an increase in energy consumption for maintenance, and the inhibition of specific enzymatic reactions. Specifically, Prasada-Reddy and Venkitasubramanian observed an inhibitory effect of ammonium on the activity of citric acid cycle enzymes in multiple strains [208].

Table 1.8 Effect of acetate on bacterial growth.

Microorganism	**Concentration of acetate**	**Effect on Growth**	**Reference**
E. Coli	Above 60 mM	Growth is inhibited	[209]
E. Coli BW25113	100 mM	Lower 50 % of growth rate	[5]
C. necator H16	100 mM	decreased the growth rate to 20.5%.	This work

1.2.5.1 The catabolic pathway for ammonium acetate

Although toxic to *C. necator* at high concentrations, *C. necator* could utilise AA to grow. The first pathway in acetate metabolism involves the enzymes acetate kinase (AckA), phosphotranacetylase (Pta), and acetyl-CoA synthetase (Acs) (**Figure 1.10.B**). AckA and Pta are responsible for acetyl-CoA synthesis in higher acetate concentrations (>30 mM acetate). The ATP-dependent acetate CoA ligase (or acetyl-CoA synthetase) is required for the second pathway of acetate activation. When the acetate concentration in the condition is low (>10 mM acetate), ACS is needed [170, 210].

In the presence of acetate, *C. necator* upregulated a fatty acid-CoA synthetase. Adding acetate and levulinic acid to the growth medium increased the expression of fatty acid-CoA synthetase. CoA is ligated to a free fatty acid by fatty acid-CoA synthetases. Additionally, this pathway requires ATP, magnesium, and CoASH. Therefore, the short organic acid may induce fatty acid biosynthesis in *C. necator* [170].

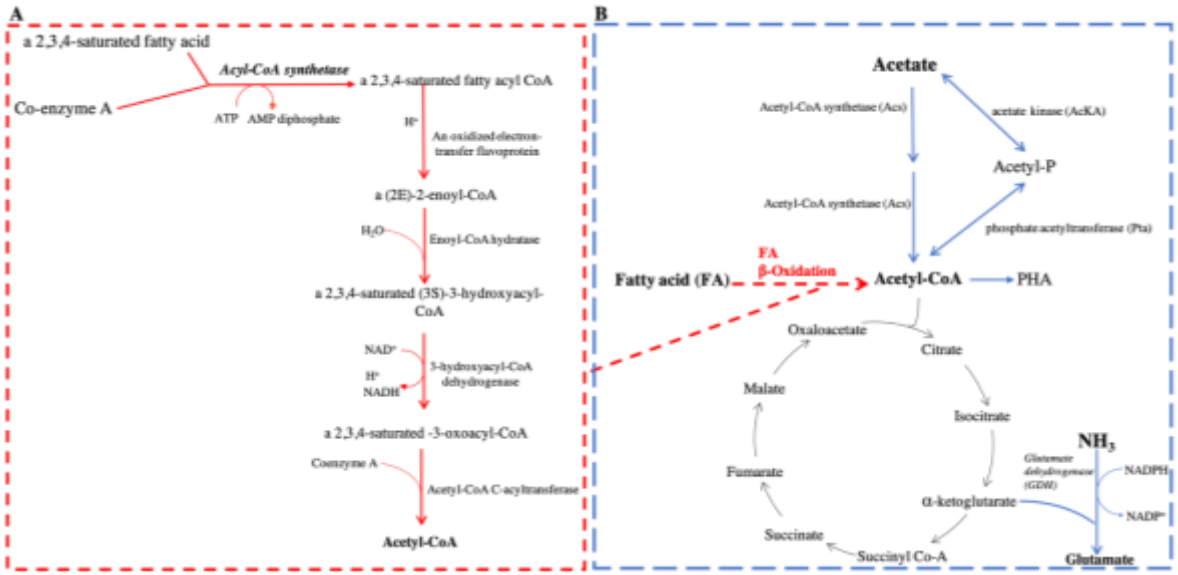

Figure 1.10. A Conversion of fatty acid to acetyl-CoA. B. Acetate metabolic pathway in E. coli. The enzyme acetyl-CoA synthetase, ACS, efficiently converts intracellular acetate into acetyl-CoA. Acetate is also involved in several metabolic pathways. For example, the biosynthesis of methionine is inhibited by acetate. Excess intracellular acetate perturbs the anion balance in the cell and thus could inhibit other metabolic reactions (20). The pool of the major intracellular anion, glutamate, is strongly reduced when the intracellular acetate concentration is high.

C. necator cells grown in acetate-treated media increased glutathione biosynthesis by upregulating S-adenosylmethionine (SAM) synthetase, responsible for SAM formation from

methionine (**Figure 1.9**) and ATP. SAM is an essential donor of methyl for transmethylation and polyamine biosynthesis. SAM is also a necessary substrate of glutathione-regenerating methylases. In response to acetic acid exposure, acetate-treated cells may utilise SAM as a crucial substrate for glutathione production [170]. The relevant genes/proteins associated with acetate tolerance are listed in the table below (**Table 1.9**).

Table 1.9 The relevant genes/proteins for acetate tolerance in various microorganisms.

No	Genes/Protein	Function	Reference
1	cAMP-receptor protein (CRP)	Transcription factor that regulates transcription initiation, regulatory networks, and metabolic processes.	[209]
2	Homoserine o-Succinyltransferase (*metA)*	Catalyses the initial step in the biosynthesis of methionine	[211]
3	Phosphotranacetylase (*pta*)	Involved in acetate metabolism; catalyses the reversible interconversion of acetyl-CoA and acetyl phosphate.	[5, 212, 213]
4	Acetyl-CoA synthetase (*acs*)	Catalyses the conversion of acetate, CoA, and ATP into acetyl-CoA.	[5]
5	Acetate kinase (*ackA*)	Catalyses the conversion of acetate and ATP into acetyl phosphate. Also catalyses the opposite reaction	[5, 213]
6	Pyruvate dehydrogenase (*poxB*)	This enzyme catalyses the oxidative decarboxylation of pyruvate to produce acetate and carbon dioxide.	[5]
7	S-adenosylmethionine (SAM) synthetase (*metK*)	Catalyses the conversion of methionine and ATP into S-adenosylmethionine (AdoMet).	[170]

The main intracellular nitrogen donors, glutamate and glutamine, are the primary products of ammonia assimilation. Nitrogen is supplied by glutamine to purines, pyrimidines, asparagine, tryptophan, histidine, glucosamine, p-aminobenzoate, and arginine. Glutamate provides nitrogen to many bacterial transaminases [214]. Ammonia can be metabolised via glutamate dehydrogenase (GDH) or the glutamine synthetase/glutamate synthase cycle (GS/GOGAT) [215]. GDH converts α-ketoglutarate, ammonia, and reducing power (NADPH) into glutamate in a direct way. The GDH reaction consumes no ATP.

- α-ketoglutarate + NH_3 + NADPH → glutamate + $NADP^+$ (GDH*)*
- glutamate + ATP + NH_3 → glutamine + ADP+$PO4^{-2}$ (GS)
- glutamine + α-ketoglutarate + NADPH → 2 glutamate + NADP+ (GOGAT) [214]

C. necator JMP134 possesses NAD glutamate dehydrogenase (NAD-GDH) encoded in its chromosome 1. The NAD-GDH protein shares 55% and 57% of its amino acid sequence

identity with the NAD-GDH proteins of *Azoarcus* sp. and *Pseudomonas aeruginosa*, respectively [216].

1.2.5.2 Acetate as a co-substrate for bioplastic production

Aside from the toxicity of acetic acid, acetate from activated acetic acid is also a known co-substrate for synthesising PHB [217, 218]. It was reported that 0.38 grams of PHB was produced per gramme of acetic acid-based substrate [219]. According to the metabolic model developed by Dias *et al*. (2008) when acetate is consumed by the cell, it can be utilised for growth and, most importantly, PHA production [220]. The synthesis of PHA is dependent on the type of available substrate. In their study, Lemos *et al.* (2006) found that when sludge was fed with acetate, PHA synthesis produced a homopolymer of hydroxybutyrate (HB). On the other hand, when sludge was fed with propionate, a copolymer of hydroxybutyrate (HB) and hydroxyvalerate (HV) was generated [221].

Acetyl-CoA is essential to the production of PHA and is generated directly from the acetate [221]. When the cell utilises active transport to uptake acetate, it undergoes a process to generate acetyl-Pi, generating acetyl-CoA. The acetyl-Pi will be transformed into acetyl-CoA by the use of 1 ATP. For every two moles of acetyl-CoA, one mole of β-hydroxybutyrate is created. Hydroxybutyrate will undergo conversion into PHB in an ATP-independent manner [222].

The proposed reaction for acetate metabolism is shown below (**Figure 1.11**). Higuchi-Takeuchi *et al*. (2019) postulated that the acetate-dependent pathway is crucial for PHA synthesis [223]. Acetate is not only a by-product of glycolysis but also a potential co-substrate. A previous study demonstrated that glucose and acetate can serve as co-substrates for *E. coli* if acetate is present in the medium at sufficient concentrations. When 32 mM acetate was added to the medium, acetate and glycolytic substrates were utilised simultaneously. In addition to being a by-product of glycolytic nutrients, acetate can also be their co-substrate, dependent solely on its extracellular concentration [213].

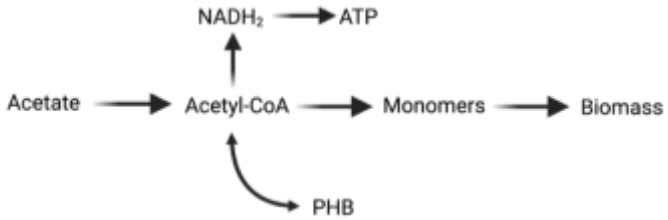

Figure 1.11 Schematic representation of an organism's metabolism capable of producing and consuming bioplastic (PHB) from acetate in Paracoccus pantotrophus [222].

1.2.6 Engineering strategies for phenotype improvement in *C. necator* H16

To produce value-added chemicals that effectively utilise specific carbon sources in *C. necator* H16, such as economical and sustainable biological feedstock, engineering the cell's native metabolic pathways is essential. Strategies such as rational design engineering—leveraging metabolic engineering supported by bioinformatics studies and recombinant strain engineering to regulate protein expression—and evolutionary engineering employing directed and adaptive evolution tools play crucial roles in strain engineering. For instance, Salinas *et al.* (2022) [224] used rational design engineering to construct a strain of *C. necator* capable of heterotrophic and autotrophic production of 3-hydroxypropionic acid. In addition, metabolic engineering was also used to enhance tolerance to formate in *C. necator* [225].

Unlike metabolic engineering, ALE doesn't require delving into the complex, interconnected metabolic networks of the cell. Instead, it focuses solely on designing selection pressures aligned with the desired phenotype. This approach offers broad applicability across microbial species and practicality, facilitating the discovery of novel mechanisms and phenotypic optimization with relative ease [12]. Recent research has identified genetic targets for rational metabolic engineering using evolved isolates [161].

1.3 Projects Aim

This PhD research endeavours to employ the ALE technique to bolster the tolerance of *C. necator* H16 against prevalent inhibitors found in lignocellulosic hydrolysates, such as benzoic acid and ammonium acetate. Furthermore, it seeks to innovate by devising a method that expedites the conventional ALE approach.

The work in this thesis is divided into three parts.

1.3.1 Adaptive laboratory evolution (ALE) to improve the tolerance of a bioplastic producer *Cupriavidus necator* H16 to benzoic acid (BA) found in lignocellulosic hydrolysates

The ALE technique will enhance the tolerance of *C. necator* H16 WT to BA present in lignocellulosic hydrolysates. Phenotypic characterisation will be performed on the adapted variants, and the whole genomes will be sequenced to identify causal mutations responsible for driving adaptation.

The main focus of this study will be to enhance the industrial characteristics of *C. necator* H16. Additionally, it will facilitate the investigation of the evolutionary processes that lead to adaptability under selection pressure.

1.3.2. Adaptive laboratory evolution (ALE) to improve the tolerance of a bioplastic producer *Cupriavidus necator* H16 to ammonium acetate (AA) found in lignocellulosic hydrolysates

The ALE strategy will be used to enhance the tolerance of the wild-type strain of *C. necator* H16 to the presence of organic acids, such as AA, often present in lignocellulosic hydrolysates. The adapted variants will undergo phenotypic characterisation, and the process of microbial whole-genome sequencing will be conducted to identify the causative mutations responsible for driving adaptation.

This part of study mainly focuses on enhancing the industrial characteristics of *C. necator* H16 using ALE investigations. Additionally, it will uncover the evolutionary processes that propel adaptability in response to selection pressure.

1.3.3 Chemical-assisted adaptive laboratory evolution (ALE) of a bioplastic producer *Cupriavidus necator* H16

While traditional ALE has shown previous effectiveness in generating improved variants, this traditional method frequently requires substantial time and effort. To accelerate the traditional ALE process, we have developed a novel mutagenesis approach to expedite the adaptive evolution of *C. necator* H16. This study used the chemical ALE to increase tolerance to high glycerol concentrations by *C. necator* H16.

This study mainly focuses on using several ALE strategies to enhance the industrial characteristics of *C. necator* H16. Additionally, it will facilitate the investigation of the evolutionary processes that contribute to adaptability. Furthermore, this study will investigate if various methods of ALE provide comparable levels of genetic diversity.

CHAPTER 2

Adaptive laboratory evolution (ALE) to improve the tolerance of a bioplastic producer *Cupriavidus necator* H16 to benzoic acid found in lignocellulosic hydrolysates

Chapter 2 – Adaptive laboratory evolution (ALE) to improve tolerance of a bioplastic producer *Cupriavidus necator* H16 to benzoic acid found in lignocellulosic hydrolysates.

Introduction

Lignocellulosic biomass stands as a crucial and sustainable carbon source for biomanufacturing endeavours. However, the conversion of biomass into valuable bioproducts often encounters obstacles posed by the presence of phenolics, aromatic compounds, and aliphatic acids. These compounds emerge during the pretreatment and hydrolysis stages of lignocellulose processing [133]. Regrettably, these compounds act as growth inhibitors for biomanufacturing hosts, thereby diminishing their production capacity. Among the common inhibitors found in pretreated lignocellulosic biomass are benzoic acid and ammonium acetate, both recognised for their toxicity to *C. necator* H16 [4]. This bacterium is commonly used as a representative model organism in bioplastic production. Consequently, mitigating the inhibitory effects of these compounds is essential for unlocking the full potential of lignocellulosic biomass as a sustainable feedstock for biomanufacturing processes.

Notably, although benzoic acid exhibit toxicity towards *C. necator* H16 at higher concentrations, their presence at lower concentrations promotes growth [4]. As a soil bacterium, *C. necator* evolved within an environment characterised by fluctuating and transient carbon and energy sources. Based on its evolutionary background, its genome is likely that of a strong generalist, with a diverse chemolithotrophic metabolism that can easily thrive on a wide range of substrates. Previously, ALE has been utilised on *C. necator*, resulting in a significant improvement in its capacity to utilise formate, a challenging carbon substrate for the unmodified wildtype strain [161]. This occurrence suggests that the bacterium may develop greater tolerance to benzoic acid. This adaptability is a crucial foundation for carrying out ALE experiments. *C. necator* H16 exhibits an inherent capability or biological mechanism essential for converting these potentially harmful compounds.

C**hapter 2** aimed to increase *C. necator* H16's tolerance to benzoic acid. To accomplish this objective, we implemented an ALE technique that involved serial batch transfers. This

approach aimed to select mutations that naturally facilitated faster cell growth. Afterwards, we subjected the adapted variants to a thorough study using whole-genome sequencing to identify the genetic changes that caused the observed improvement.

2.1 Aim

The aim of **Chapter 2** is to adapt *C. necator* H16 to a lignocellulosic hydrolysate inhibitor (benzoic acid (BA)) and to determine the tolerance mechanism of adapted variants by employing whole genome sequencing to examine gene mutations.

2.2 Bacterial strain and chemical

C. necator H16 (DSM 428) was cultivated in mineral salts medium (MSM) based on Schlegel *et al.* (1961) [226] including modified trace element solution SL7 [227] (4.4758 g/L $Na_2HPO_4.2H_2O$, 1.5 g/L KH_2PO_4, 0.5 g/L, NH_4Cl, 0.2 g/L $MgSO_4.7H_2O$, 20 mg/L $CaCl_2.2H_20$, 1,2 mg Fe(III)NH_4-Citrate, 100 µL/L, 1 mL SL7 solution (40 µL $ZnSO_4.7H_2O$, 12 µL $MnCl_2.4H_2O$, 30 mg/L H_3BO_3, 80 µL $CoCL_2.6H_2O$, 4 µL $CuCl_2.2H_2O$, 8 µL $NiCl_2.6H_2O$, 12 µL $Na_2MoO_2.2H_2O$, all solutions were from 0.25 g/mL stock, except H_3BO_3), 10 g/L sodium gluconate, pH 7.0) (SL7 solution was prepared separately and sterilised by 0.2 µm filter, was added to MSM after it has been autoclaved)) or nutrient broth (NB) (5 g/L peptone, 1 g/L beef extract, 2 g/L yeast extract, 5 g/L sodium chloride), supplemented with 10 µg/mL at 30°C or 37°C. Chemicals were purchased from FORMEDIUM (Norfolk, UK) or Sigma-Aldrich (Dorset, UK) (unless otherwise stated).

2.3 Cultivation of *C. necator* H16 in different concentration of BA

To assess the influence of BA on the microbial growth and determine an appropriate selective condition for ALE, *C. necator* H16 was cultured in Chi.Bio [68]. The procedure was conducted using a sealed 30-mL transparent borosilicate glass container (Thermo Fisher Scientific), containing 15 mL of MSM medium with 1% (w/v) sodium gluconate. The medium was enriched with 10 µg/mL of gentamicin and different concentrations of BA (0 mM, 2.5 mM,

and 5 mM). An overnight culture was used to inoculate a new medium, aiming for an initial OD_{600} of 0.2. The cultivation occurred at either 30°C or 37°C, with constant agitation at a speed of 0.6 utilising a disc-shaped PTFE stir bar (Thermo Fisher Scientific). The experiment involved regular measurement of optical density at 650 nm.

2.4 ALE of *C. necator* H16 for increased tolerance to BA

The ALE experiment was conducted using a series of batch cultivation in MSM medium supplemented with 1% (w/v) gluconate, 10 μg/mL of gentamicin, and 5 mM BA. The cultivation was maintained at a temperature of 30°C. All cultivations were carried out in Chi.Bio, using the same experimental setup as previously mentioned in section **2.3.** For each cultivation round, a new medium was inoculated with the culture from the previous round, aiming for an initial OD_{600} of 0.2. Cell culture continued until the early stationary phase was reached. The serial cultivation process continued until no further noticeable improvements in phenotype were observed. For future analysis, an aliquot of the cell population was stored at -80°C as a glycerol stock at the end of each cultivation round.

2.5 Continuous enrichment of *C. necator* H16 strains with permanent adaptations and isolation of BA-tolerant variants

The cell population obtained from the 12^{th} round was subjected to a series of 5 rounds of cultivation in NB medium, followed by a single round of cultivation in MSM medium with the addition of 1% (w/v) sodium gluconate. Subsequently, there were 1 (Method B) or 2 rounds (Method A) (**Figure 2.1**) of growth on MSM media supplemented with 1% (w/v) sodium gluconate and 5 mM BA. After every 24 hours of growth, ~ 2% (100 μL) of the culture was used to inoculate the subsequent culture (5 mL medium). All of these cultivations, a concentration of 10 μg/mL of gentamicin was included in the medium. The cultivations were performed in 50-mL Falcon tubes, with each tube containing 5 mL of the designated media. The temperature was kept constant at 30°C. The implementation of this cultivation sequence was crucial in order to avoid the isolation of *C. necator* H16 strains that had temporarily adapted, due to changes in their expression profile caused by environmental influences.

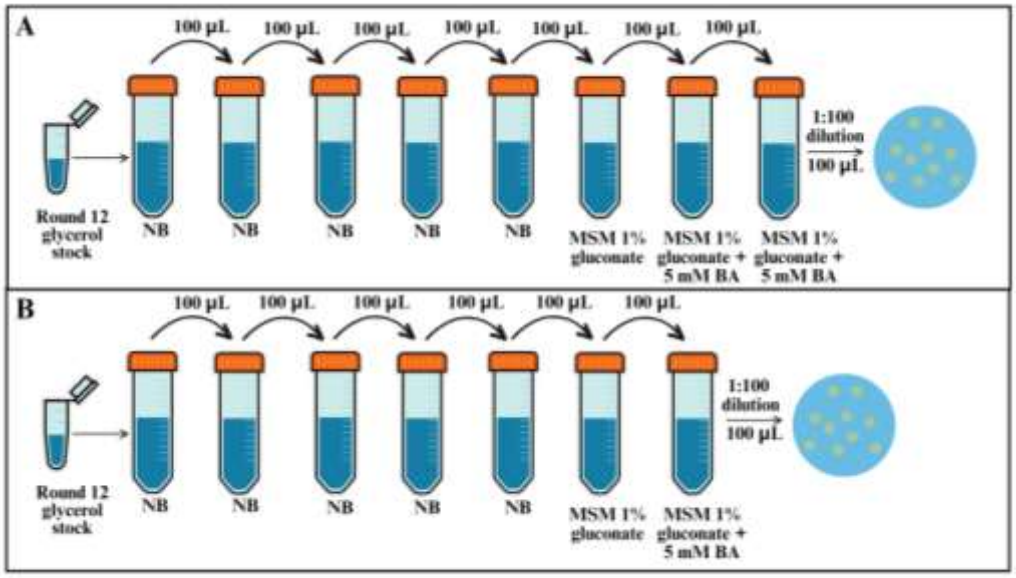

Figure 2.1 A scheme of continuous enrichment of obtained variants with permanent adaptations from round 12 of ALE.

After the last round of cultivation in selective conditions, the culture was diluted with fresh medium and spread onto NB agar plates that contained 10 µg/mL of gentamicin. The agar plates were incubated at a temperature of 30°C for a duration of about 48 hours. More than a hundred colonies were selected from plates A and B and moved onto 96-well microplates, along with the wild-type (WT) strain used as a comparison and control (**Figure 2.2**). These variants were cultivated in microplates containing 150 µL of MSM media supplemented with 1% (w/v) sodium gluconate, 10 µg/mL of gentamicin, and 5 mM benzoic acid. The microplates were positioned on a Titramax 1000 shaker (Heidolph) set at a temperature of 30°C and a speed of 1050 rpm. The optical density was regularly measured at a wavelength of 595 nm using a MultiskanTM FC microplate photometer (Thermo Fisher Scientific).

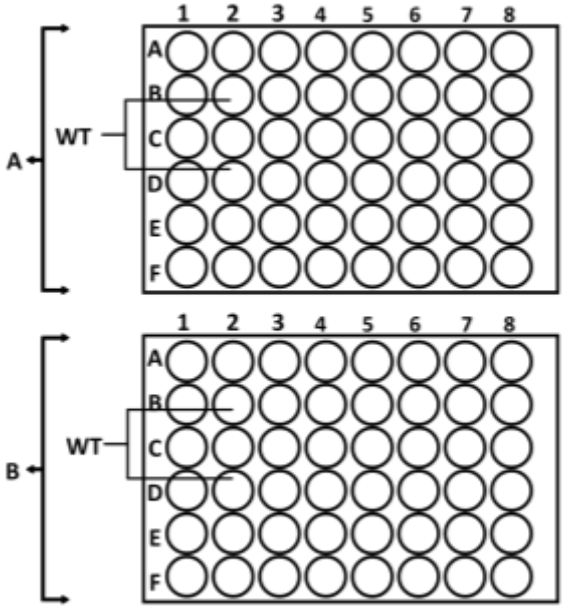

Figure 2.2 A visual summary of the process of isolating BA-tolerant variants. This was done by comparing the growth of the WT and variants from round 12 using 96-well plates.

2.6 Cell growth comparison of BA-tolerant variant and unadapted WT strain

Pre-cultures of selected adapted variants and WT strains were created by overnight incubation in 5 mL of MSM medium, which contained 1% (w/v) sodium gluconate and 10 µg/mL of gentamicin, at a temperature of 30°C. The comparative growth investigation was performed utilising three different growing vessels: a 96-well microplate, a 50-mL TPP® TubeSpin bioreactor tube with a membrane filter, and a standardl 250-mL Erlenmeyer flask.

For the microplate cultivation, 150 µL of MSM medium, containing 10 µg/mL of gentamicin, a range of gluconate concentrations (0 – 1% w/v), and BA concentrations (0 – 12.5 mM), were added to each well of the 96-well microplate. The microplates were stirred on a Titramax 1000 shaker (Heidolph) at either 30°C or 37°C and 1050 rpm. The optical density was measured at 595 nm using a MultiskanTM FC microplate photometer (Thermo Fisher Scientific).

For tube cultivation, the bioreactor tube contained 20 mL of MSM medium, supplemented with 10 µg/mL of gentamicin, 1% (w/v) sodium gluconate, and 5 mM BA. The cultivation process took place in a personal bioreactor RST-1 (Biosan) at a temperature of 37°C. The tube was

rotated at a speed of 2000 rpm and included a reverse spin of 1 s-1. The cultivation process involved the measurement of optical density at a wavelength of 850 nm.

The flask used for growth was filled with 50 mL of MSM medium, which was supplemented with 10 μg/mL of gentamicin, 1% (w/v) sodium gluconate, and 5 mM BA. The cultivation process was carried out at a temperature of 37°C. The optical density was determined at a wavelength of 600 nm using a BioPhotometer Plus UV/Vis photometer (Eppendorf).

2.7 Genome sequencing

The strains (WT and three selected adapted variants) were spread onto an NB agar plate with a concentration of 10 μg/mL of gentamicin and incubated at a temperature of 30°C for a period of 40 to 48 hours. Following the isolation of a single colony, it was suspended in 100 μL of sterile PBS. Subsequently, the cells that were resuspended were streaked onto a new NB agar plate with 10 μg/mL of gentamicin, resulting in the formation of a bacterial lawn that covered roughly one-third of the plate. Afterwards, the plate was incubated at a temperature of 30°C for a duration of 40 to 48 hours. By employing a sterile loop, all the bacteria present on the plate were carefully transferred into the barcoded bead tube provided by MicrobesNG (Birmingham, UK). The next procedures involved genomic DNA extraction and genome sequencing performed by MicrobesNG.

2.8 Results

2.8.1 Selection condition scouting by cultivating *C. necator* H16 WT in different concentrations of benzoic acid (BA).

Before any ALE experiment can commence, the initial selective pressure strength must be determined. For BA tolerance strain to evolve, the concentration of the BA must be high enough to exert selective pressure on the evolving population but not so high that growth is greatly impaired. When grown in a medium with BA, *C. necator* H16 is significantly toxic by above 2.5 g/L of BA [184]. In this study, we used three cultivation conditions: (1) MSM 1% sodium gluconate (w/v) with no inhibitor, (2) MSM 1% sodium gluconate (w/v) with 2.5 mM

BA, and MSM 1% sodium gluconate (w/v) with 5 mM BA. All cultivations were performed at either 30°C or 37°C (**Figure 2.3**). During the ALE process, the growth was monitored, and the concentration of the inhibitor was kept constant.

In 15 hours of incubation, the culture of *C. necator* H16 WT grew to a maximum OD of 650 nm of 4.3 in non-inhibitor conditions. The culture in 2.5 mM BA grew 50% lower than the growth obtained in non-inhibitor cultivation, while in 5 mM BA, the culture showed an extended lag phase time compared with two other conditions, failing to reach an OD greater than 2. Hence, the condition with 5 mM BA was chosen for the ALE experiment as it will provide pressure on the cells without terminating growth completely.

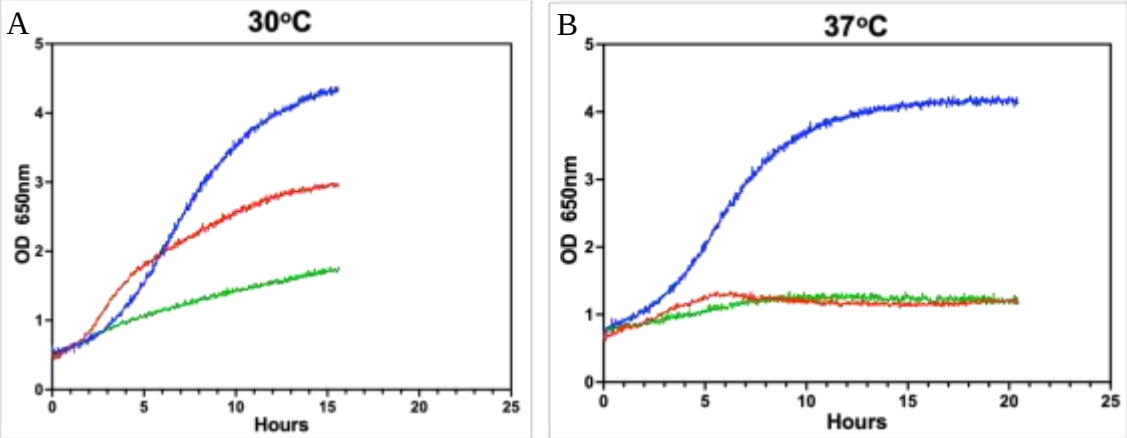

Figure 2.3 Growth profile of C. necator H16 at 30°C (A) and 37°C (B) in 15 mL of MSM 1 % (w/v) sodium gluconate, with no BA (blue line), 2.5 mM (v/v) BA (red line), and 5 mM (v/v) BA (green line).

The cell growth performance of *C. necator* H16 WT in the presence of BA at 37ºC was performed separately. The inhibitory effect of BA increased with the increase in temperature. The culture in 2.5- and 5-mM BA failed to reach an OD greater than 1 in more than 20 hours of incubation (**Figure 2.3.B**).

C. necator H16, a mesophile, was typically grown at 30ºC for bacterial proliferation and PHA accumulation [228]. The results indicated that the cell's growth was greatly inhibited when *C. necator* H16 was exposed to non-optimal growth conditions and a toxic compound.

2.8.2 Growth profile of *C. necator* H16 in the twelve-serial transfer during adaptive laboratory evolution (ALE).

An ALE with serial transfer was chosen to increase the tolerance of *C. necator* H16 against BA. As reviewed by Porcar [229], adaptation is the evolutionary process by which an organism improves its ability to survive in its habitat. An experimental approach based on adaptive has been developed to enhance genetic circuitry. Essentially, the experimental procedure includes sustaining exponential growth by daily transferring cultures into the fresh medium under selection pressure.

This study used serial transfer with 15 mL MSM 1% sodium gluconate (w/v) supplemented with 5 mM BA as a selective pressure. The serial transfer was monitored until 12 rounds of ALE. For each cultivation round, a fresh medium was inoculated with the culture from the previous round, aiming for an initial OD_{600} of 0.2. Cell culture continued until the early stationary phase was reached (**Figure 2.4**). The ALE experiment was continued until there was no further improvement in the cell growth in the presence of BA.

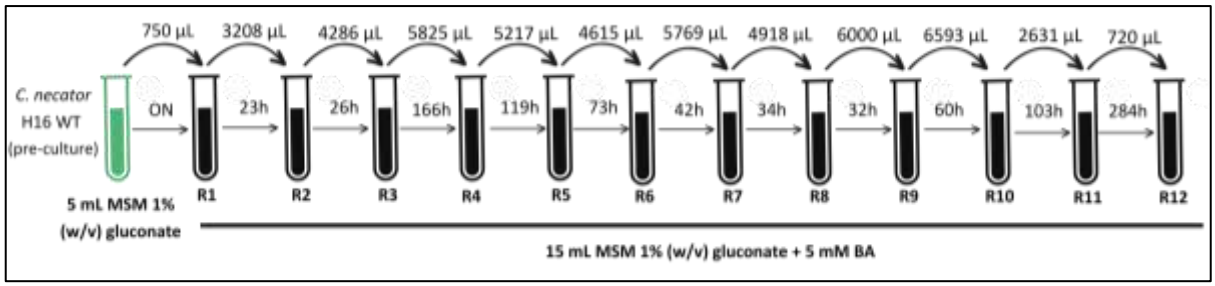

Figure 2.4 A diagram illustrating the ALE process using serial transfers. For each cultivation round, a new medium was inoculated with the previous round's culture, targeting an initial OD_{600} of 0.2. ON: overnight, R: round, h: hour.

As shown in **Figure 2.5**, a significant improvement in cell growth in the presence of BA by the population of *C. necator* H16 was seen from round 10 of ALE onwards. In the third round**,** the cell culture showed an extended lag phase. The following rounds recovered, and the lag phase of the cells decreased gradually, indicating adaptation to BA. A similar pattern was shown in a previous study, where the growth of *G. oxydans* in the presence of various inhibitors at the serial passage (four transfers) was reduced and gradually gained better growth [230]. The maximum OD achieved by rounds 2 to 9 remained the same, although the lag phase in these

rounds showed a different pattern. The cell culture from rounds 10 to 12 surpassed the maximum OD achieved by *C. necator* H16 WT in the initial cultivation of the ALE experiment.

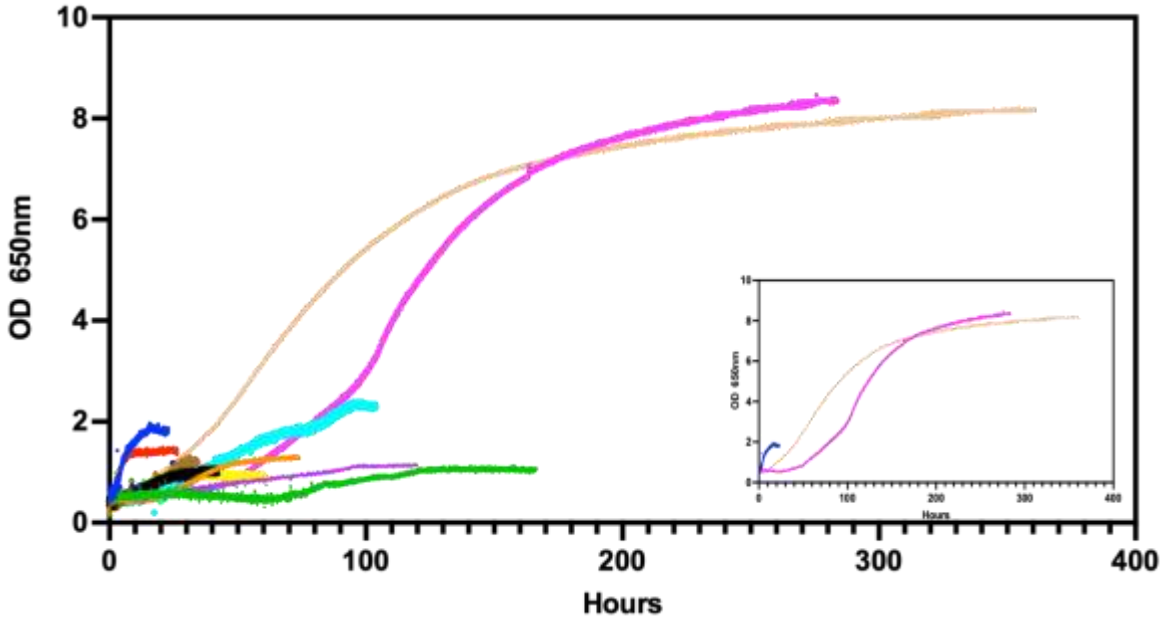

Figure 2.5 Growth profile of C. necator H16 in twelve serial transfers of ALE; round 1 (blue line), round 2 (red line), round 3 (green line), round 4 (purple line), round 5 (orange line), round 6 (black line), round 7 (brown line), round 8 (dark blue), round 9 (yellow line), round 10 (cyan line), round 11 (magenta line), and round 12 (light brown line).

In this study, with the same condition without supplementation of BA, we observed that the maximum OD of 650 nm of *C. necator* H16 WT was 4.3. In contrast, the culture from round 12 reached a maximum OD of 650 nm of 8 after 300 hours of incubation with 5 mM BA supplementation. The significant difference in final OD growth shows the possibility of the population of *C. necator* H16 from round 12 utilising BA as a carbon source for growth.

Based on the growth profile in **Figure 2.5**, the population from rounds 12 and 11 obtained approximately the same maximum OD after ~300 hours of incubation. Round 12 showed better cell growth performance with a shorter lag phase. Hence, the ALE experiment was terminated at round 12. The culture from round 12 was plated to isolate individual colonies for phenotype screening analysis.

2.8.3 Isolation of BA-tolerant variants

To confirm that the improved phenotype of the adaptive strain is not a transient adaptation, the population from round 12 of ALE was subjected to further selection by consecutive rounds of cultivation, as depicted in **Figure 2.1**. These two methods aimed to isolate the variants with a true adaptation**.** After the rounds of cultivation, the subcultures were plated to produce single colonies.

The single colonies were grown in the microtiter plate containing 1% MSM (w/v) of sodium gluconate supplemented with 5 mM BA. Each microtiter plate included a control (*C. necator* H16 WT) and single colonies from round 12. The screening of round 12 of ALE showed that the adapted variants displayed higher growth rates (h^{-1}) and lower doubling times (T) than WT (**Table 2.1**). All the adapted variants reached the maximum OD in 24 hours of cultivation and plateaued afterwards, as depicted in **Figure 2.6**. Both methods produced a similar growth pattern of the single colony of adaptive variants. A variant from method A (R12AD3) displayed the highest growth rate (h^{-1}) and was chosen to be studied further for cell growth studies. This variant was indicated as R12AD3, "R12" for round 12, followed by an "A" corresponding to method A, "letter + number" related to the well of the microtiter plate where the strain was grown (**Figure 2.2**). The variant R12AD3 was confirmed to be a true variant.

Table 2.1 The specific growth rate and doubling time rate of ten selected variants from round 12 and *C. necator H16* WT in MSM 1% (w/v) sodium gluconate + 5 mM BA using methods A and B.

Strain	Method	Growth rate (h^{-1})	Doubling time (T) (h)
WT	A	0.026	26.66
R12AG2	A	0.074	9.37
R12AD3	A	0.077	9.00
R12AC8	A	0.074	9.37
R12AE9	A	0.071	9.76
R12AF9	A	0.074	9.37
R12BF2	B	0.071	9.76
R12BG2	B	0.073	9.50
R12BD3	B	0.070	9.90
R12BC4	B	0.070	9.90

R12BF5	B	0.073	9.50

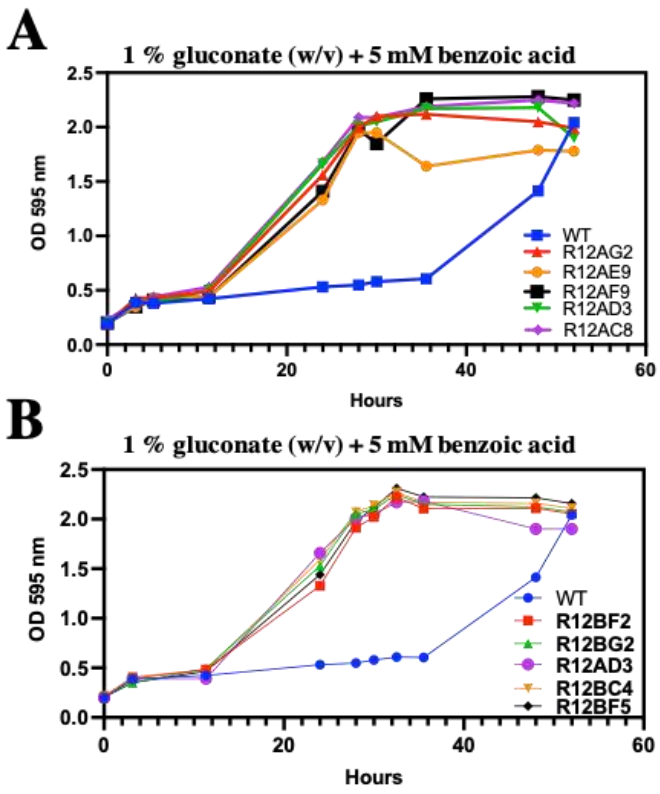

Figure 2.6 The growth of selected five single colonies from round 12 using methods A (A) and B (B), in comparison to the WT.

2.8.4 Cell growth studies of variant R12AD3 in different bioreactors, concentrations of BA and temperature.

A cell growth study of the variant of *C. necator* H16 from round 12 (R12AD3) was used to observe the growth performance at various concentrations of gluconate (0–1% w/v) and benzoic acid (0 – 12.5 mM) (**Figure 2.7**). In this study, the effect of temperature was also performed to observe its effect on the toxicity of BA to the growth of *C. necator* H16. It was observed that the *C. necator* H16 WT grew when cultivated in MSM 1% sodium gluconate (w/v) supplemented with 5 mM BA at 30ºC. When the cultivation temperature was raised to 37ºC, with the same medium, the *C. necator* H16 WT failed to reach an OD greater than 1 in more than 20 hours of incubation (**Figure 2.3.B)**. An additional point regarding the effect of BA's toxicity was that the culture's colour was observed to turn dark brown. Wang *et al.* (2014) [4] reported a similar result in which the colour of the culture medium darkened as the

concentration of benzoic acid increased, and the response changed from growth stimulation to inhibition.

The growth performance of *C. necator* H16 WT and R12AD3 in MSM 1% sodium gluconate (w/v) at 30ºC and 37ºC in the absence of BA was closely identical (**Figure 2.7.H**). When the concentration of BA was increased to 7 mM (**Figure 2.7.H**), the R12AD3 variant remained the highest-performing strain in terms of OD growth compared to the WT. However, neither the *C. necator* H16 WT nor the R12AD3 variant exhibited growth when grown in MSM 1% sodium gluconate (w/v) supplemented with 10- and 12-mM BA.

The effect of the concentrations of gluconate and BA was observed. *C. necator* H16 WT and the R12AD3 variant showed no growth in MSM no gluconate at 30ºC and 37ºC (**Figure 2.7.A-B**). This occurred due to lack of essential carbon sources for growth. Both *C. necator* H16 WT and the R12AD3 variant showed minimal growth in MSM supplemented with 5 mM of BA with no gluconate. The final OD of 595 nm of WT and the R12AD3 variant reached under 1 at 30ºC. This indicated that both strains could utilise BA as a carbon source and energy for growth. Interestingly, at 37ºC, no growth was found in WT in MSM no gluconate with 5 mM of BA, while the variant R12AD3 grew similarly with the same conditions at 30ºC.

C. necator H16 WT and the R12AD3 variant exhibited growth in MSM 0.25% (w/v) sodium gluconate supplemented with 5 mM of BA at 30ºC. However, at 37ºC, wild-type strain of *C. necator* H16 did not exhibit growth in MSM containing 0.25% and 0.5% (w/v) gluconate supplemented with 5 mM of BA, whereas the R12AD3 variant strain grew under these conditions. Cell culture persisted until the early stationary phase was obtained (**Figure 2.7.C-F**). This outcome demonstrated that the R12AD3 variant is superior to WT in tolerating BA. An analytical method such as quantitative gas chromatography (GC) is required to explore the difference in BA and gluconate consumption.

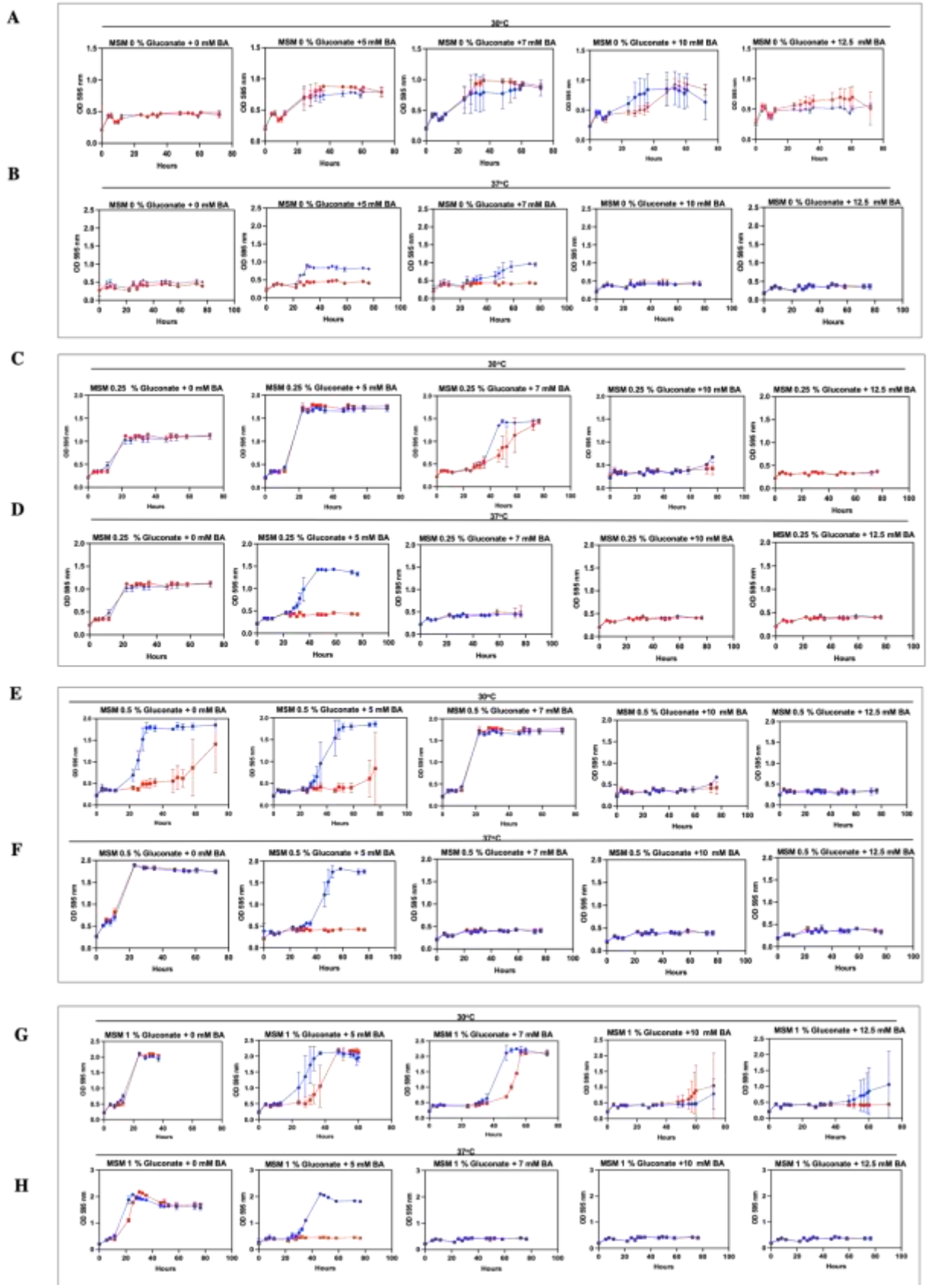

Figure 2.7 Growth profile of C. necator H16 WT (red line) and variant R12AD3 (blue line). Cultivation condition: 150 µL MSM 1% sodium gluconate (w/v) + gentamicin (10 µg/mL), supplemented with various concentrations of gluconate (0–1% w/v) and benzoic acid (0 – 12.5 mM) at 30°C and 37°C using a 96 well-plate. Error bars indicate three biological replicates.

Observations were made regarding the impact of volume and bioreactor varieties. In this investigation, two additional cultivations were conducted in a shaker incubator and a Personal Bioreactor RST-1 (Biosan). Consistent with the prior results in the microtiter plate at 37ºC, WT did not grow in 5 mM in all selected conditions, indicating that the R12AD3 variant outperformed its parental strain (**Figure 2.8**).

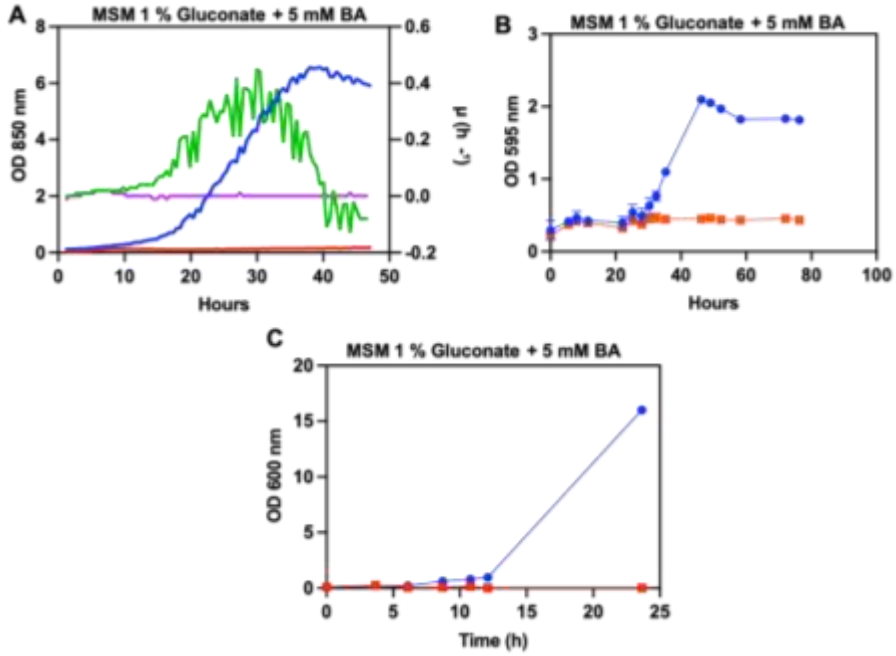

Figure 2.8 OD growth of variant C. necator H16 WT (red line) and variant R12AD3 (blue line) and Growth rate (μ (h^{-1})), C. necator WT (purple line) and variant R12AD3 (green line) in a Personal Bioreactor RST-1 (Biosan) (A). Growth profile of C. necator WT (red line) and variant R12AD3 (blue line) in Chi.Bio (B). OD growth of C. necator WT (red line) and variant R12AD3 (blue line) in a 250 mL-flask (C). All cultivations were conducted at 37ºC.

2.8.5 Reaction medium aspect at different cultivation conditions.

As discussed in **Chapter 1**, *C. necator* contains homologous genes encoding the enzymes BenA,B,C,D, which convert benzoate to catechol [155]. Further investigation of the metabolic pathways of BA transformation revealed that BA was first converted to cis-1,2-dihydroxybenzoate and then to catechol (**Figure 1.8**). The catechol 1,2-dioxygenase catalyses the subsequent transformation of catechol into cis, cismuconate. The accumulation of catechol can lead to its conversion into 1,2-benzoquinone, which causes the culture medium to turn dark and inhibits cellular growth because benzoquinone is a toxic agent against microorganisms. In this study, the colour of the culture medium also darkened when *C. necator* H16 WT was

inoculated in MSM medium supplemented with 5 mM BA, similar to what was observed in previously published research [4, 155, 184] and in addition, it did not exhibit growth at all. The R12AD3 variant exhibited no change in the colour of the culture medium when cultivated in BA, indicating its ability to adapt to BA by converting catechol into essential intermediates necessary for growth (**Figure 2.9**). The change of the colour medium was only observed when cells were cultivated at 37ºC, a similar result as Wang *et al.* (2014) reported [4].

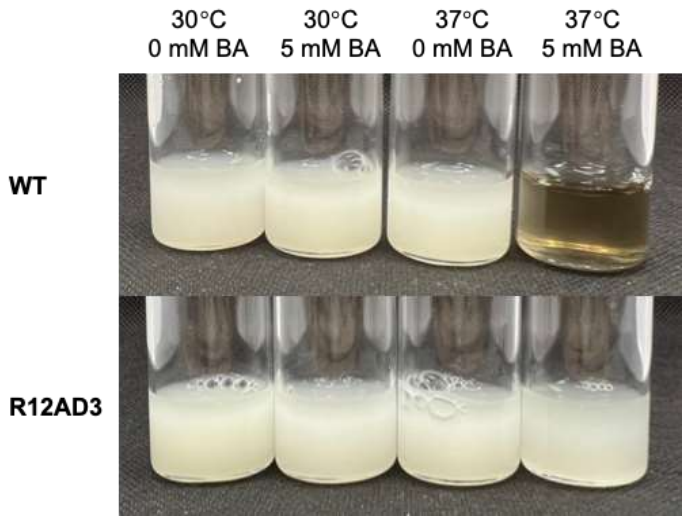

Figure 2.9 The colour of culture medium after cultivation in 5 mL MSM 1% (w/v) sodium gluconate + 5 mM (v/v) BA at 30ºC and 37ºC in an incubator shaker.

2.8.6 Mutations found in BA-tolerant variants obtained from ALE

To elucidate the nature of the mutations that enhanced the growth of the adapted variants in BA, the genomes of the WT and three of the best-performing BA-tolerant variants from round 12 (R12AE9, R12AF9, and R12AD3) of the ALE were sequenced and subsequently compared against the reference genomes (GenBank accession numbers CP039287, CP039288, and CP039289) [231]. More investigations were conducted on these genomes to determine the location, type, position, and nature of their genetic modifications.

C. necator H16 has two chromosomes and one megaplasmid [162]; the coverage of all sequenced genomes exceeded 30x. Based on the variant calling results, a list of 7 genome mutations differing from the WT was obtained (**Table 2.2**). This list includes single nucleotide polymorphisms (SNPs) and insertions/deletions (INDELs). Two mutations resulted in amino acid changes encoded at the gene loci E6A55_RS10050 and E6A55_RS14935. Except for E6A55_RS08660, E6A55_RS14935, and E6A55_RS30305, the other mutations were found in all three variants.

Based on the genome annotation (accession number NZ_CP039287, NZ_CP039288, and NZ_CP039289) for chromosome 1, chromosome 2, and megaplasmid pHG1, respectively), gene locus E6A55_RS30305 encodes GT4 family glycosyltransferase PelF, which are components of the exopolysaccharide Pel transporter. E6A55_RS32520 encodes for a nickel-dependent hydrogenase large subunit, and E6A55_RS14935 encodes a tripartite ATP-independent periplasmic transporter (TRAP). It is unknown whether or how the three genes encoded by E6A55_RS08660, E6A55_RS32520 and E6A55_RS14935 influence the tolerance to BA in *C. necator* H16. Gene locus E6A55_RS10050 encodes for the LysR family transcriptional regulator involved in benzoate catabolism ‘catR’.

Table 2.2 SNPs and INDELs detected in R12AE9, R12AF9, and R12AD3 are highlighted in yellow.

Chromosome - Locus	Position	Gene	Product	WT			R12AE9			R12AF9			R12AD3		
				TYPE	REF	ALT	TYPE	REF	ALT	TYPE	REF	ALT	TYPE	REF	ALT
NZ_CP039287	154664			ins	G	GT	ins	G	GT	ins	G	GT	ins	G	GT
NZ_CP039287	192516			SNP	G	T	SNP	G	T				SNP	G	T
NZ_CP039287	333421			SNP	G	T	SNP	G	T				SNP	G	T
NZ_CP039287	333427			SNP	G	T	SNP	G	T				SNP	G	T
NZ_CP039287 - E6A55_RS02390	500511		amino acid ABC transporter permease	SNP	G	A	SNP	G	A	SNP	G	A	SNP	G	A
NZ_CP039287 - E6A55_RS03700	791503		YgcG family protein	SNP	C	A	SNP	C	A				SNP	C	A
NZ_CP039287	1104731			SNP	G	T	SNP	G	T	SNP	G	T	SNP	G	T
NZ_CP039287	1166481			SNP	T	C	SNP	T	C	SNP	T	C	SNP	T	C
NZ_CP039287 E6A55_RS05535	1190158		hypothetical protein	SNP	C	A							SNP	C	A
NZ_CP039287E6A55_RS05630	1211314		aldehyde dehydrogenase	SNP	G	T	SNP	G	T				SNP	G	T
NZ_CP039287	1559970			SNP	G	T	SNP	G	T	SNP	G	T	SNP	G	T

NZ_CP039287 - E6A55_RS07585	1628903		glucose-6-phosphate isomerase	SNP	G	T	SNP	G	T	SNP	G	T	SNP	G	T
NZ_CP039287 - E6A55_RS09930	2108292		hypothetical protein	SNP	G	T									
NZ_CP039287 - E6A55_RS12270	2597061		adenosylcobalamin-dependent ribonucleoside-diphosphate reductase	SNP	C	A	SNP	C	A	SNP	C	A	SNP	C	A
NZ_CP039287 - E6A55_RS12270	2597067		adenosylcobalamin-dependent ribonucleoside-diphosphate reductase	SNP	C	A	SNP	C	A	SNP	C	A	SNP	C	A
NZ_CP039287 - E6A55_RS12370	2619321		ABC transporter ATP-binding protein	SNP	C	A	SNP	C	A				SNP	C	A
NZ_CP039287 - E6A55_RS13105	2768732		sugar dehydratase	SNP	G	C	SNP	G	C	SNP	G	C	SNP	G	C
NZ_CP039287 - E6A55_RS15075	3199544		translocation/assembly module TamB	SNP	G	T							SNP	G	T

NZ_CP039287 - E6A55_RS15995	3393896		glutamate-5-semialdehyde dehydrogenase	SNP	G	T	SNP	G	T				SNP	G	T
NZ_CP039287 - E6A55_RS17570	3718338		penicillin-binding protein 1A	SNP	G	T	SNP	G	T	SNP	G	T	SNP	G	T
NZ_CP039287 - E6A55_RS18085	3811856	*gspD*	type II secretion system secretin GspD	SNP	C	A	SNP	C	A				SNP	C	A
NZ_CP039287 - E6A55_RS18085	3811867	*gspD*	type II secretion system secretin GspD	SNP	C	A	SNP	C	A				SNP	C	A
NZ_CP039287 - E6A55_RS18850	3981763		response regulator	SNP	C	T	SNP	C	T	SNP	C	T	SNP	C	T
NZ_CP039288 - E6A55_RS19235	26106		polysaccharide biosynthesis tyrosine autokinase	SNP	T	C	SNP	T	C	SNP	T	C	SNP	T	C
NZ_CP039288 - E6A55_RS19830	164765		sigma-54-dependent Fis family transcriptional regulator	SNP	C	T	SNP	C	T	SNP	C	T	SNP	C	T

NZ_CP039288 - E6A55_RS20305	265365	*motA*	flagellar motor stator protein MotA	ins	G	GGGCGCCGCCTTC	ins	G	GGGCGCCGCCTTC				ins	G	GGGCGCCGCCTTC
NZ_CP039288 - E6A55_RS22125	659277		sensor histidine kinase	SNP	C	A				SNP	C	A	SNP	C	A
NZ_CP039288 - E6A55_RS22660	772834		HlyD family type I secretion periplasmic adaptor subunit	SNP	C	A	SNP	C	A				SNP	C	A
NZ_CP039288 - E6A55_RS26205	1553621	*gph*	phosphoglycolate phosphatase	SNP	G	T	SNP	G	T				SNP	G	T
NZ_CP039288 - E6A55_RS26535	1628671	*fdnG*	formate dehydrogenase-N subunit alpha	SNP	T	C	SNP	T	C	SNP	T	C	SNP	T	C
NZ_CP039288 - E6A55_RS27725	1911223		amino acid adenylation domain-containing protein	SNP	C	A	SNP	C	A				SNP	C	A
NZ_CP039288 - E6A55_RS27895	1957707		TerC family protein	SNP	C	A	SNP	C	A	SNP	C	A	SNP	C	A

NZ_CP039288 - E6A55_RS30140	2453032		hypothetical protein	SNP	G	T	SNP	G	T				SNP	G	T
NZ_CP039289 - E6A55_RS32220	682		hydrogenase small subunit	SNP	C	A	SNP	C	A	SNP	C	A	SNP	C	A
NZ_CP039289 - E6A55_RS34220	405785		MFS transporter	ins	G	GGGACGGCAGCCAGACC	ins	G	GGGACGGCAGCCAGACC	ins	G	GGGACGGCAGCCAGACC	ins	G	GGGACGGCAGCCAGACC
NZ_CP039287 - E6A55_RS08660	1862887		hypothetical protein				del	CGAGAGCTGAGAGCTGAGAGCTGAGAGCTGAGAGCTGAGAGCT	C						
NZ_CP039287 - E6A55_RS10050	2134417		LysR family transcriptional regulator				SNP	A	C	SNP	A	C	SNP	A	C

NZ_CP039287	2561945						SNP	G	A	SNP	G	A	SNP	G	A
NZ_CP039287 - E6A55_RS16335	3460447		RNA-binding protein				ins	G	GT	ins	G	GT	ins	G	GT
NZ_CP039288 - E6A55_RS30305	2491285		DUF3492 domain-containing protein				del	AGCGCTCCAC	A				del	AGCGCTCCAC	A
NZ_CP039289 - E6A55_RS32520	62278		nickel-dependent hydrogenase large subunit				SNP	C	A	SNP	C	A	SNP	C	A
NZ_CP039287 - E6A55_RS14935	3162470		TRAP transporter large permease subunit							SNP	G	T	SNP	G	T

2.8.6.1 Mutation in LysR family transcriptional regulator.

Independently best-adapted variants (R12AE9, R12AF9, R12AD3) from round 12 and WT were then characterised by whole-genome sequencing, and the relevance of the selected identified mutation was assessed. We identified that the gene locus E6A55_RS10050, which encodes the LysR family transcriptional regulator involved in benzoic acid catabolism was mutated in all best-performing adapted variants. The identified mutation was a non-synonymous mutation, where the amino acid position 151 was mutated, changing from aspartate to alanine (D151A substitution) (**Figure 2.10**). This particular mutation appeared to be the most likely candidate to contribute to BA tolerance. Based on the research of identical protein, gene locus E6A55_RS10050 showed 52.5 % identity to a positive regulator of *cat* operon (*catR*) in *Pseudomonas resinovorans* CA10 [232].

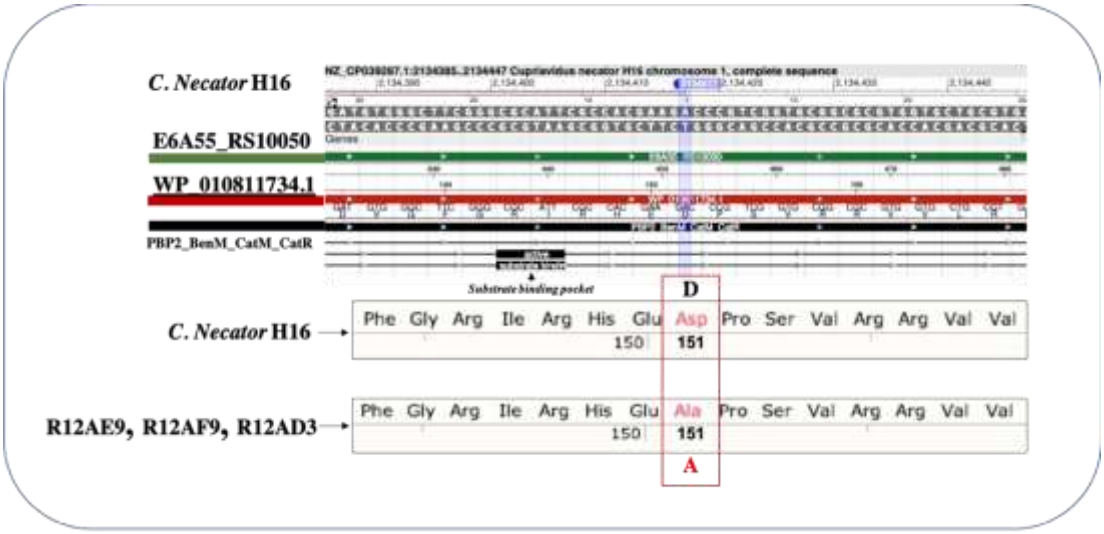

Figure 2.10 The DNA sequence of LysR family transcriptional regulator in C. necator H16 and the adapted variants. A single non-synonymous mutation was found after DNA sequencing of the LysR-type regulatory proteins of R12AE9, R12AF9, and R12AD3. The same D151A substitution was found in the three variants isolated from Round 12.

Putative *catR* genes, which are responsible for encoding LysR-type regulatory proteins, precede both the *catA1benABCD* and *catB2CXD* gene clusters in *C. necator* JMP134 [155]. BA and muconate have been reported as inducers of the BA pathway in various bacteria [187, 233, 234] , facilitated by the activity of LysR-type regulatory proteins. The CatR1 gene product may exhibit responsiveness to BA and muconate [155]. Similarly, Craven *et al.* (2009) [235] reported that BenM, a LysR-type transcriptional regulator, activates the *benABCDE* operon in

response to either BA or muconate in *Acinetobacter baylyi* ADP1. BenM is activated in a synergistic manner by two substances, benzoate and cis,cis-muconate. Craven *et al.* (2009) [235] employed site-directed mutagenesis to investigate the physiological importance of a substrate-binding pocket in BenM. The residues in BenM were modified to align with those of CatM within the hydrophobic cavity. The response to benzoate was shown to be mediated by two specific amino acid residues, R160 and Y293, in the BenM protein. Furthermore, modification of these amino acid residues resulted in the ability of BA to hinder the activation by cis,cis-muconate, which is located in a distinct primary binding site for the effector molecule of the BenM protein. The main site's position is conserved in many LysR-type regulators.

P. putida KT2440-JD1 with a point mutation in *catR*, which shares 50.2% identity with *catR* in *C. necator* H16, that blocks the induction of the *cat* operon in response to BA was described by Duuren *et al.* (2011) [236]. The enzymes in *P. putida* KT2440-JD1 that convert BA to cis, cis-muconate are encoded on the *ben* operon and are exclusively capable of accumulating cis, cis-muconate.

Residue D151 is located near R146 and 147, the C-terminal substrate binding domains of LysR-type transcriptional regulators involved in BA catabolism [237], which are fairly conserved in LysR-type transcriptional regulators from various microorganisms (**Figure 2.11**). Given the information provided, we have a strong conviction that the D151A substitution alters the interactions with the substrate. An extensive biochemical characterisation of the D151A substitution would be important to gain a comprehensive understanding of the functional consequences of this mutation.

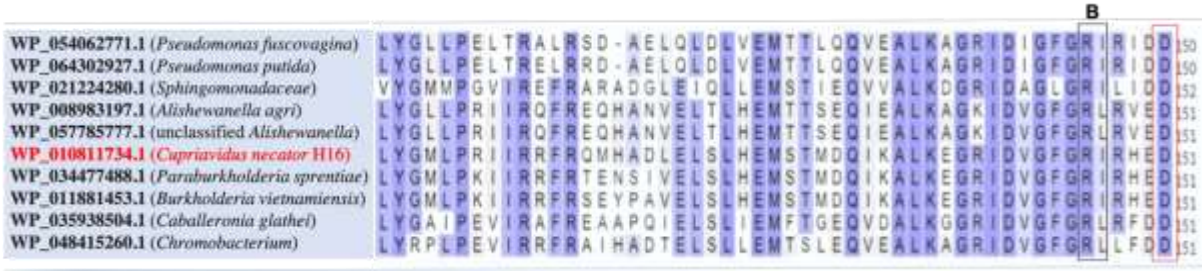

Figure 2.11 The illustration shows the multiple sequence alignments of LysR-type transcriptional regulators of various organisms. Sequence alignment is shown using multiple sequence alignment UniProt, where text is highlighted in dark purple and a red box indicates it is highly conserved. Amino acids situated within the substrate binding pocket of LysR-type transcriptional regulators are denoted using capitalised letter 'B'.

A protein model of the mutated (A151) and non-mutated (D151) LysR family transcriptional regulators is shown in **Figure 2.12**.

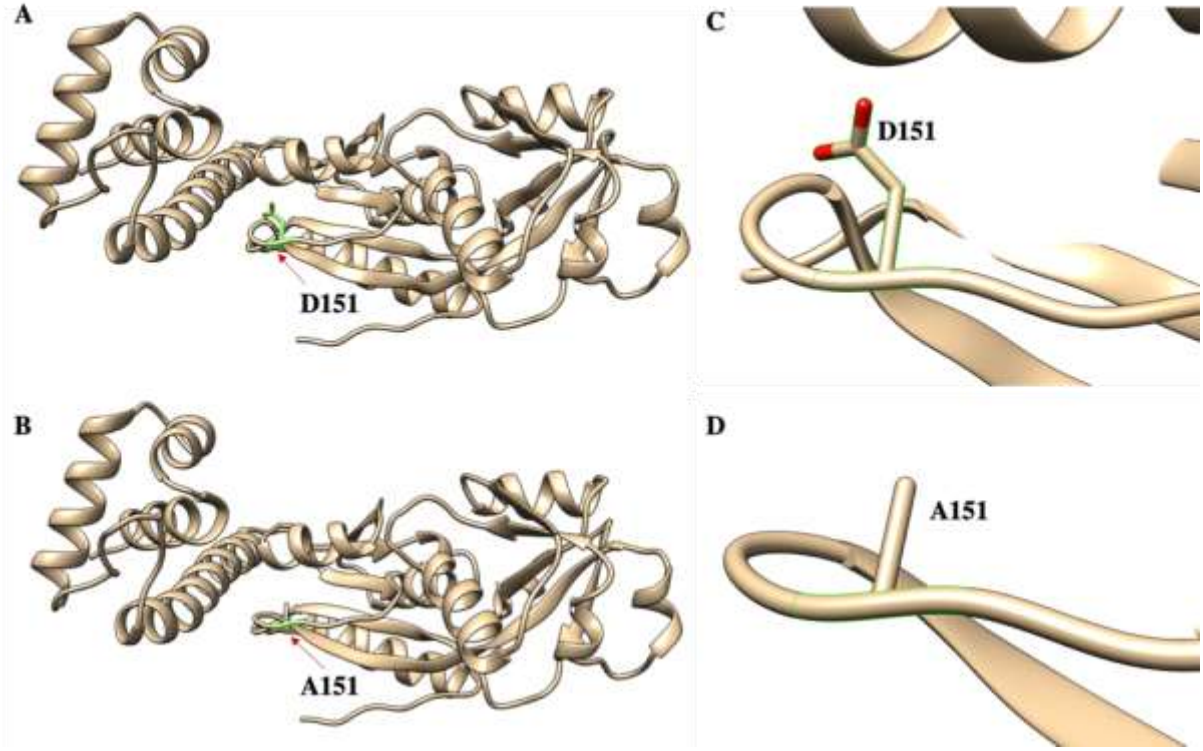

Figure 2.12 Protein models of C. necator H16 LysR family transcriptional regulator (gene locus: E6A55_RS10050) (Bottom picture). (A) and (C) show LysR family transcriptional regulator with D151. (B) and (D) show LysR family transcriptional regulator with A151. Protein prediction was created by AlphaFold [238], and A. baylyi (R156H mutant) as a template. A151 mutation was created using Chimera.

2.9 Conclusion

In summary, we have effectively identified adapted strains of *C. necator* H16 that exhibit increased tolerance to the presence of the toxic compound BA using the power of the ALE experiment. We elucidated the potential mechanisms contributing to increased tolerance to BA in the isolated adaptive variants, focusing on the mutation. A non-synonymous mutation in a gene specifically codes for a LysR-type transcriptional regulator is likely to play a crucial role in facilitating the growth of adapted variants in the presence of BA at 37ºC. The outcome of our study shows that the ALE experiment is an effective approach to enhancing the performance of wild-type *C. necator* H16 in controlled laboratory settings. This outcome may simplify reverse engineering, therefore revealing important insights into the complex dynamics

of the interaction between phenotype and genotype. Furthermore, the knowledge gained from this study is expected to be relevant for other microorganisms being developed for industrial purposes.

CHAPTER 3

Adaptive laboratory evolution (ALE) to improve the tolerance of a bioplastic producer *Cupriavidus necator* H16 to ammonium acetate found in lignocellulosic hydrolysates

Chapter 3 – Adaptive laboratory evolution (ALE) of a bioplastic producer *Cupriavidus necator* H16 for increased tolerance to ammonium acetate found in lignocellulosic hydrolysates.

Introduction

Similar to how BA-derived lignocellulosic hydrolysates are detrimental to *C. necator* H16 (as discussed in **Chapter 2**), low concentrations of ammonium acetate can potentially serve as a substrate and be converted to polyhydroxyalkanoates (PHA). Consequently, enhancing *C. necator* H16's tolerance to ammonium acetate is advantageous. However, the incomplete understanding of the genetic, physiological, and molecular mechanisms governing the conversion of ammonium acetate poses challenges for rational metabolic engineering aimed at its improvement. In such scenarios, the ALE technique emerges as a potent tool for generating desired phenotypic enhancements, even in the absence of comprehensive prior knowledge regarding the underlying mechanisms. Furthermore, the availability of affordable full-genome sequencing and advancements in bioinformatics have streamlined the identification and evaluation of potentially causative mutations, solidifying ALE as a pivotal instrument for biological discovery and strain development [26].

This study endeavours to broaden the substrate utilization capacity of *C. necator* H16, with a particular emphasis on pretreated lignocellulosic biomass, the most abundant organic compound on Earth. **Chapter 3** of this study aimed to enhance *C. necator* H16's tolerance to ammonium acetate. To achieve this goal, we employed an ALE technique involving serial batch transfers. This method aimed to naturally select for mutations that expedited cell growth. Subsequently, we conducted an extensive analysis of the adapted variants using whole-genome sequencing to elucidate the genetic changes underlying the observed improvements.

3.1 Aim

The aim of **Chapter 3** is to adapt *C. necator* H16 to a lignocellulosic hydrolysate inhibitor (ammonium acetate (AA)) and to determine the tolerance mechanism of adapted variants based on gene mutations by using whole genome sequencing.

3.2 Bacterial strain and chemical

Bacterial strain and chemicals were as described in section **2.2** (unless otherwise stated).

3.3 Cultivation of *C. necator* H16 in different mediums with AA supplementation

To investigate the impact of AA on microbial growth and identify a suitable selective condition for ALE, *C. necator* H16 cultures were cultivated at a temperature of 30°C in Personal Bioreactors RST-1 (Biosan), very similar to section **2.6**, with the following modifications: cultivations were conducted in 1% (w/v) sodium gluconate and NB medium with 100 mM of AA at a temperature of 30°C.

3.4 ALE of *C. necator* H16 for increased tolerance to AA

The ALE experiments were done according to the description provided in section **2.4**, except that this experiment used different concentrations of AA.

3.5 Isolation of the best performing AA-tolerant variants

A total of over one hundred colonies were selected from rounds 10, 14, and 16, in addition to the WT strain used for comparison and control. The adapted variants and WT were cultivated

on microplates, employing the identical procedure outlined in section **2.5**, with the exception that the experiment employed a concentration of 90 mM of AA.

3.6 Verification of improved AA-tolerant variants

The cell population obtained from the 14th and 16th rounds were subjected to a series of 5 rounds of cultivation in NB medium without AA, followed by a single round of cultivation in MSM medium with the addition of 1% (w/v) sodium gluconate (**Figure 3.1**). After every 24 hours of growth, ~ 2% (100 µL) of the culture was used to inoculate the subsequent culture. All of these cultivations were done very similar to section **2.5.** The implementation of this cultivation sequence was important in order to avoid the isolation of *C. necator* H16 strains with transient adaptation

After the last round of cultivation in MSM medium with the addition of 1% (w/v) sodium gluconate, the culture was used to inoculate the subsequent culture on MSM media supplemented with 1% (w/v) sodium gluconate, 10 µg/mL of gentamicin and 120 mM AA in Chi.Bio [68]. True variants were expected to grow better in the selective medium, in contrast to those that exhibited transient adaptation.

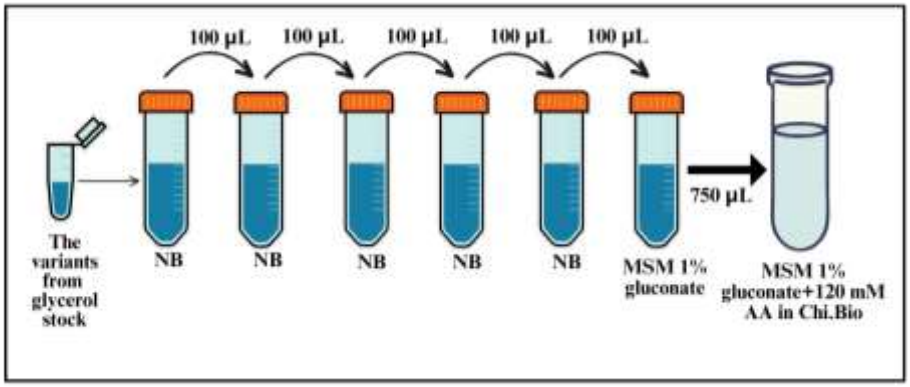

Figure 3.1 A protocol for the verification of obtained variants with permanent adaptation.

3.7 Cell growth comparison of AA-tolerant variant and unevolved WT strain

Pre-cultures of selected adapted variants and WT strains were created, similar to section **2.6**. The comparative growth investigation was performed utilising two different growing vessels: a 50-mL TPP® TubeSpin bioreactor tube with a membrane filter and a standard 30-mL container similar to section **2.3** [68] at a temperature of 30°C.

Tube cultivations were done according to the description provided in section **2.6**, except that the experiment used a different concentration of AA (200 mM).

The Chi.Bio cultivations were done according to the description provided in section **2.3,** except that the experiment used different concentrations of AA (120, 130, and 150 mM AA) at a temperature of 30°C.

3.8 Genome sequencing

The genome sequencing was done exactly as in section **2.7**.

3.9 Results

3.9.1 Selection condition scouting by cultivating *C. necator* H16 WT in different media in the presence of ammonium acetate

Before any ALE experiment can commence, the medium and initial selective pressure strength must be determined. For the population of *C. necator* H16 to evolve, the concentration of the AA must be high enough to exert selective pressure on the evolving population but not so high that growth is greatly impaired.

In this study, the selection condition for the ALE experiment was done in the NB medium and MSM 1% (w/v) sodium gluconate medium. The maximum OD of the cells in the MSM medium exhibited a better growth profile, which was five times higher than NB without AA (**Figure**

3.2). Based on this result, MSM was chosen as the medium for the ALE experiment as it will provide higher genetic diversity, which is beneficial in ALE [12].

The effect of various concentrations of AA was observed in *C. necator* H16 in the NB medium and the MSM (w/v) 1% sodium gluconate medium. The cells were grown in MSM medium with supplementation of 100 mM AA, 150 mM AA and 200 mM AA. The cells did not exhibit cell growth with the AA's supplementation above 100 mM (data not shown). Similarly, Wang *et al.* (2014) [4] reported any concentration above 116.1 mM AA exhibited growth inhibition in a glucose-utilising mutant *C. necator* H16.

In this work, when the cells were cultured with 100 mM AA, *C. necator* H16 started growing earlier in the NB medium than in the MSM medium, although in the MSM medium, the final OD was much higher. The maximum OD of the cells in MSM medium was four times higher than NB with 100 mM AA. If the growth is low and the probability of accumulating beneficial mutations is strongly limited [239]. The results indicate that the MSM medium will be more suitable for the ALE experiment.

.

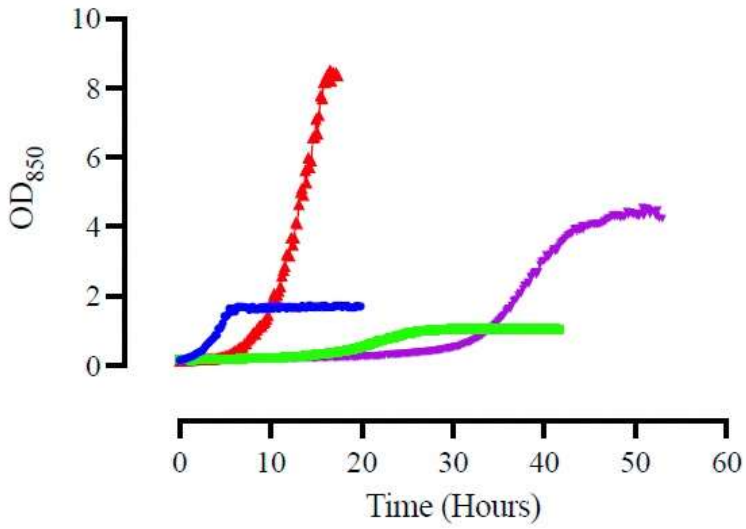

Figure 3.2 Growth curve of C. necator H16 WT in different media with different concentrations of ammonium acetate. NB – 0 mM AA (blue line), NB – 100 mM AA (green line), MSM – 0 mM AA (red line), MSM – 100 mM AA (purple line). The cultivation was carried out at 30°C using Personal Bioreactors RST-1 (Biosan) (Ghoneim, 2022) [240].

3.9.2 Growth profile of *C. necator* H16 in the sixteen-serial transfer during ALE experiments.

The technique used to increase *C. necator* H16's tolerance to AA was an ALE with serial transfer. As mentioned in the previous chapter (**Chapter 1**), adaptation is an evolutionary process that increases an organism's capacity for habitat survival. An ALE strategy has been created as a means of improving genetic traits. The ALE experiment with serial transfers maintains exponential growth by daily transferring colonies into the fresh medium under selection pressure [229]. Based on the experimental result in section **3.1**, selecting a concentration to initiate the ALE experiment, 100 mM of AA caused a long lag phase of *C. necator* H16's growth. A key characteristic of ALE experiments is that they have long timescales, on the order of months, and often require daily observation [65]. Consequently, the experimental setup should be adjusted to the desired selection pressure to reduce an extended lag phase on the initial ALE experiment.

This study employed serial transfers with 15 mL of MSM 1% (w/v) sodium gluconate supplemented with various concentrations of AA as a selective pressure. The serial transfer was monitored until 16 rounds of ALE. Very similar to section **2.8.2**, for each cultivation round, a fresh medium was inoculated with the culture from the previous round, targeting an initial OD_{600} of 0.2 (**Figure 3.3**). Cell culture continued until the early stationary phase was reached. The ALE experiment was continued until there was no further improvement in the cell growth in the presence of AA.

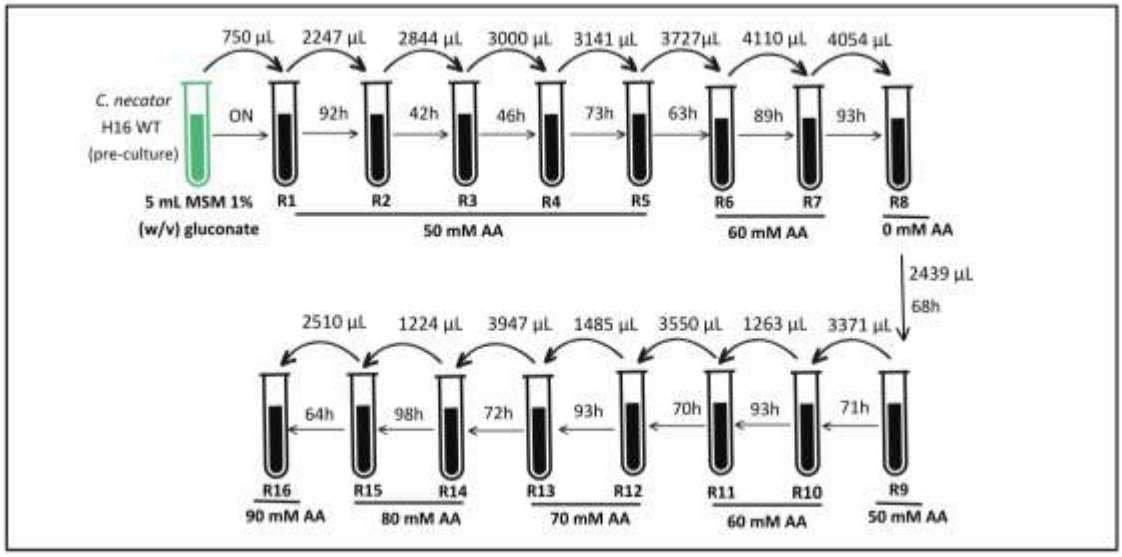

Figure 3.3 A diagram illustrating the process of sequential transfers using the ALE process. For each cultivation round, a new medium was inoculated with the previous round's culture, targeting an initial OD_{600} of 0.2. ON: overnight, R: round, h: hour.

A total of 16 rounds were performed. 50 mM AA was kept constant from round 1 to round 4. In these rounds of ALE, the maximum OD was reduced significantly after round 1. For instance, rounds 2 and 3 reached OD 650 nm of 2 in 35 hours, while round 1 surpassed OD 650 nm of 2 in 20 hours of incubation. Similarly, a prior study revealed that the growth of *G. oxydans* declined in the presence of various inhibitors at the initial serial passage (four transfers) [230]. From round 5 to round 7, the selection pressure was increased to 60 mM AA to promote more beneficial mutations (**Figure 3.4.A**).

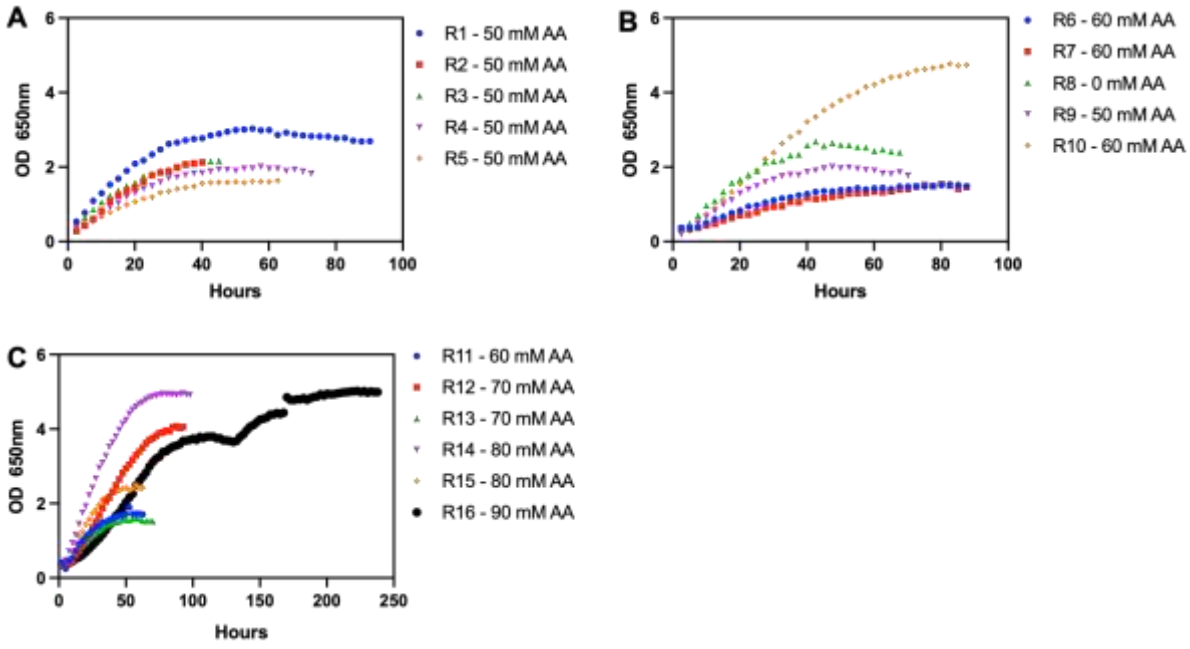

Figure 3.4 The growth of C. necator H16 through all rounds of ALE: (A) rounds 1 through 5, (B) rounds 6 through 10, and (C) rounds 11 through 16. The AA concentration ranged from 0 mM to 90 mM.

According to a review by Carpenter *et al.* (2023) [241], ALE experiments can use alternate selective conditions to enhance the performance of the resulting isolates and populations. The cell growth was, however, reduced when the AA concentration was increased to 60 mM (**Figure 3.4.B**). As a result, the cells were grown under no inhibitor conditions in round 8, allowing the cells to survive and raise population density.

The concentration of AA was brought back to its initial level of 50 mM in ALE round 9. The cells showed a growth pattern similar to that of round 4. Consequently, in the round 10, the concentration of AA was raised to 60 mM, leading to a substantial enhancement in OD growth. The cell showed a lower OD in the subsequent round with 60 mM AA than in the first round. Rounds 12 and 13 at 70 mM AA and rounds 14 and 15 at 80 mM AA displayed the same pattern, with the latter round of each concentration exhibiting lower OD.

In round 16, the AA concentration was increased to 90 mM, continuing the pattern; this round produced a higher OD than the previous round. In round 16, diauxic growth was observed, indicating that 90 mM AA stimulates growth (**Figure 3.4.C**). However, subsequent rounds of ALE did not increase the cell's OD (data not shown), so the experiment was terminated after round 17. Round 16 culture was plated to isolate individual clones for phenotype screening analysis.

3.9.3 Isolation of increased AA-tolerant variants from round 10 (A), 14 (A) and round 16 (B) populations.

We used the maximum OD of the adapted variants under a particular condition relative to the WT strain to measure tolerance. The population from rounds 10, 14, and 16 was screened using microplates to isolate the best-adapted variants. 120 single colonies (WT and variants) from the plate were transferred to microplates and screened in 150 µL of MSM with 1% (w/v) sodium gluconate and 90 mM AA. Each microplate contained control (*C. necator* H16 WT) and single colonies from round rounds 10, 14, and 16. The screening of ALE showed that the adapted variants displayed higher OD growth than WT. The growth profile of selected adapted variants and WT are depicted in **Figure 3.5**.

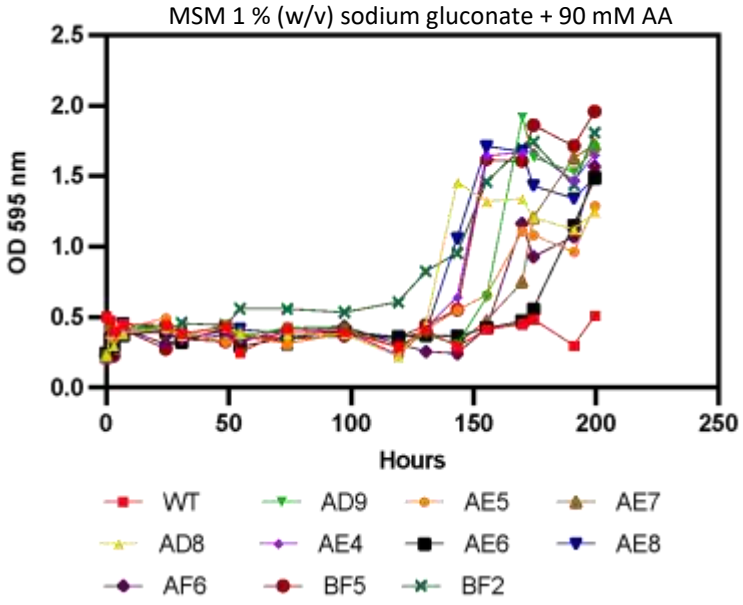

Figure 3.5 The growth of selected AA-tolerant variants from rounds 10 (A) and 16 (B). The cultivations were performed in a 96-well plate with MSM 1% (w/v) sodium gluconate + 90 mM AA at 30°C.

The ten best variants from the three microtiter plates reached various maximum OD (**Table 3.1**). All of the adapted variants showed a significant improvement of 3 to 4-fold in the maximum OD growth in the presence of 90 mM AA compared to the WT. In addition, the lag time is greater than that observed in the previous experiment. This could be due to differences in cultivation methods, including initial culture quantity, working volumes, and shaker incubator. The variant from round 16 (BF5) displayed the highest OD growth (OD 595 nm =

1.96) and was chosen to be cultivated further to confirm improved AA tolerance. This variant was indicated as BF5, “B” for round 16, followed by a letter and number related to the well of the microtiter plate where the strain was grown. The variant BF5 was confirmed to be a true variant.

Table 3.1 The maximum OD growth of *C. necator H16* WT and ten selected variants from rounds 10, 14 and 16 of ALE after 200 hours of incubation.

Variant	Round of ALE	Max OD 595 nm	Variant	Round of ALE	Max OD 595 nm
WT	-	0.5	AE7	14	1.72
AD8	14	1.46	AE8	14	1.71
AD9	10	1.92	AF6	14	1.57
AE4	14	1.67	BF2	16	1.81
AE5	14	1.29	BF5	16	1.96
AE6	14	1.49			

3.9.4 The growth profile of WT and adapted variants (AE4, BF2, and BF5) in different concentrations of AA

The growth profiles of variants from rounds 14 (AE4), 16 (BF2, BF5), and WT were determined in MSM 1% (w/v) sodium gluconate medium supplemented with AA ranging from 120-150 mM in Chi.Bio [68]. In 120 mM AA, WT grew to a maximum OD 650 nm of 2 in 50 hours of incubation, whereas the variants AE4 and BF2 reached the maximum OD 650 nm of 3, where AE4 exhibited faster growth (**Figure 3.6.A**). Interestingly, in 130 mM, the variant BF2 exhibited better growth than AE4, reaching a maximum OD of 650 nm of 2.5. AE4 and BF2 grew earlier, within 50 hours of incubation, and began to plateau. In contrast, BF5 exhibited the best growth, reaching a maximum OD of 650 nm of 4.5 in 150 hours of incubation. With 150 mM AA, BF5 grew to a maximum OD of 650 nm of 4.5 in 200 hours of incubation, higher than AE4 and BF2. WT failed to grow in 130 mM and 150 mM of AA after 100 hours of incubation (**Figure 3.6.B-C**).

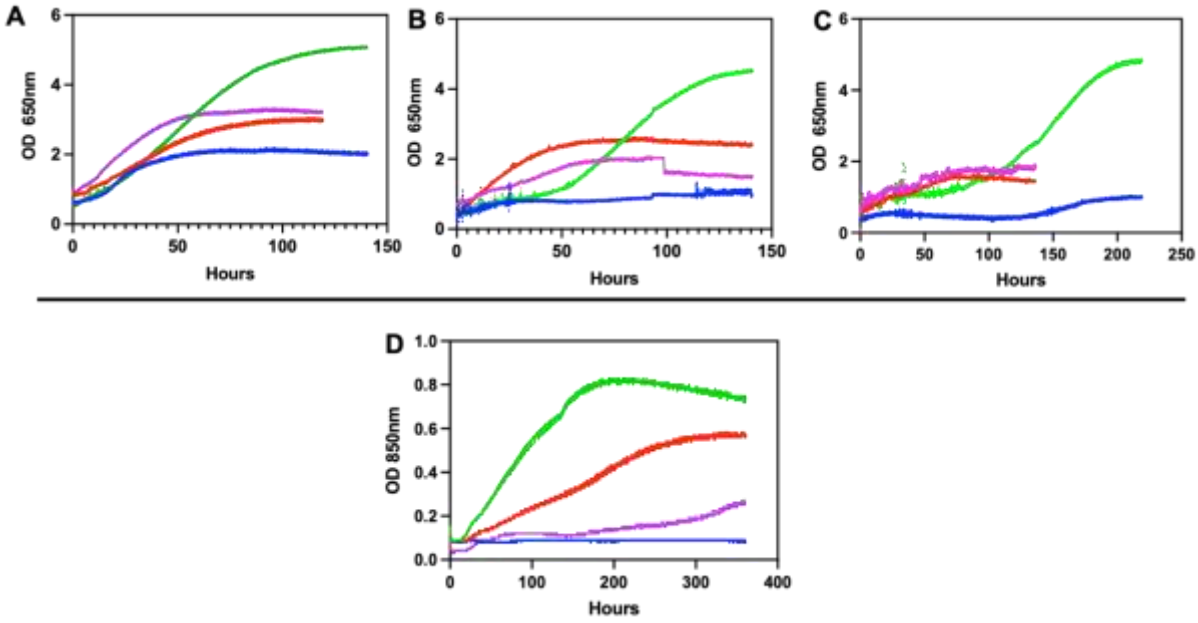

Figure 3.6 Growth profile of C. necator H16 WT (blue line) and AA-tolerant variants (AE4 (purple line), BF2 (red line), and BF5 (green line). The cultivations were performed in 15 mL MSM 1% (w/v) sodium gluconate + 120 mM AA (v/v) (A). The cultivations were performed in 15 mL MSM 1% gluconate + 130 mM AA (v/v) (B). The cultivations were performed in 15 mL MSM 1% (w/v) sodium gluconate + 150 mM AA (v/v) (C). All the cultivations were performed in Chi.Bio (A)-(C). The cultivations were performed in the Personal Bioreactors RST-1 (Biosan) (D).

Observations were made in different conditions. In this investigation, the cultivations were conducted in the Personal Bioreactors RST-1 (Biosan) using a higher concentration of AA (200 mM). WT failed to grow in 200 mM of AA. BF5 grew to a maximum OD 850 nm of 0.8 in 200 hours of incubation, higher than with AE4 and BF2 cultivated under the same conditions (**Figure 3.6.D**). BF2 exhibited the second-best growth, reaching a maximum OD 850 nm of 0.5 in 200 hours.

AE4, BF2, BF5, and WT were grown in NB agar supplemented with AA ranging from 25-50 mM (**Figure 3.7**). All adapted variants and WT exhibited growth in 25 mM AA within 72 hours of incubations. With 50 mM AA in 72 hours of incubation, BF5 showed some growth. However, only two single colonies were observed in BF2, and no colonies in AE4 and WT were observed. After 144 hours of incubation, all adapted strains exhibited some growth in 50 mM AA; consistent with the previous results, BF5 showed the best growth, followed by BF2 and AE4. No colonies were observed in WT within the time frame of the experiment. The overall result showed that all adapted variants have better tolerance to AA than WT. However, their different response to AA suggested that the improved tolerance was achieved via multiple

mechanisms depending on the evolution conditions; hence, we investigated further possible tolerance mutational mechanisms by genome sequencing of the three adapted variants.

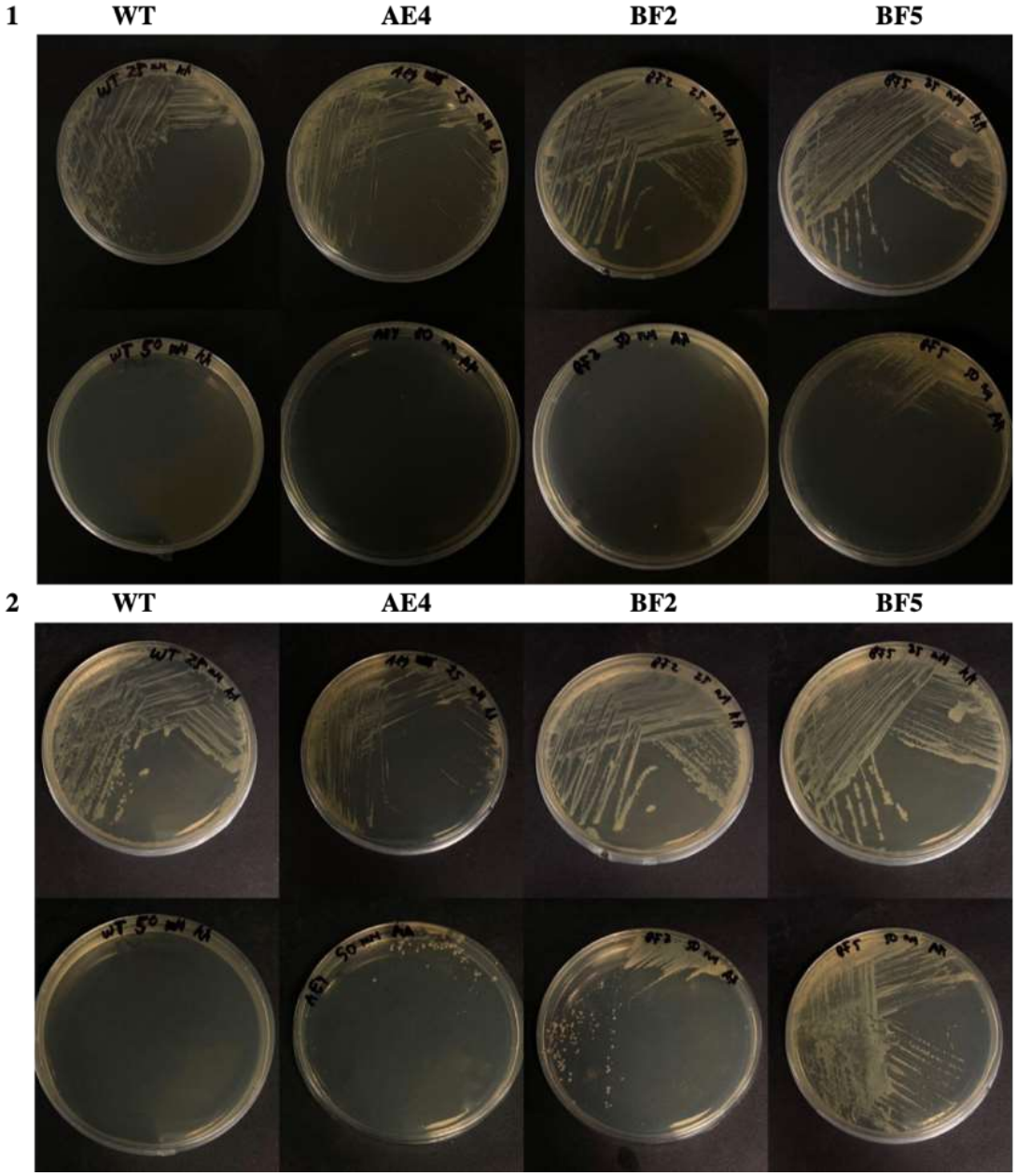

Figure 3.7 Growth of C. necator H16 WT, AA-tolerant variants (AE4, BF2, and BF5) in NB agar supplemented with 25 mM (top) and 50 mM (bottom) AA in 72 hours (1) and 144 hours (2).

3.9.5 Mutations found in sequenced variants obtained from ALE

To find the genetic mutations for adaptation to AA, the genomes of the WT and two variants from round 16 (BF2 and BF5) and one from round 14 (AE4) of the ALE were sequenced and subsequently compared against the reference genomes (GenBank accession numbers CP039287, CP039288, and CP039289) [231].

C. necator H16 contains two chromosomes and one megaplasmid [162]; the coverage of all sequenced genomes exceeded 30x. Based on the variant calling results, a list of 10 genome mutations differing from the WT was obtained (**Table 3.2**). This list includes seven non-synonymous mutations, two insertions, and one stop-gain mutation. Seven mutations resulted in amino acid changes encoded at the gene loci E6A55_RS13105, E6A55_RS22125, E6A55_RS27725, E6A55_RS05535, E6A55_RS05630, E6A55_RS15075, E6A55_RS25025. An amino acid substitution at the gene locus E6A55_RS13105 was only found in WT. A mutation at the gene locus E6A55_RS18865 was found in all three adapted variants. An amino acid substitution at the gene locus E6A55_RS22125 was found in two variants, including WT, except BF5. Mutations at the gene loci E6A55_RS05535, E6A55_RS05630, E6A55_RS08660, E6A55_RS15075, E6A55_RS25025 were specifically found in BF2 and BF5 variants. An amino acid substitution at the gene locus E6A55_RS27725 was found in WT and BF2.

Table 3.2 SNP only detected in BF5, BF2, and AE4 is highlighted in yellow, SNP only detected in WT is highlighted in brown, SNP only detected in WT, BF2, and AE4 is highlighted in blue, SNPs and INDEL detected in BF5 and BF2 are highlighted in green.

Chromosome -Locus	Location	Product	WT			BF5			BF2			AE4		
			TYPE	REF	ALT	TYPE	REF	ALT	TYPE	REF	ALT	TYPE	REF	ALT
NZ_CP039287	154664	--	ins	G	GT	ins	G	GT	ins	G	GT	ins	G	GT
NZ_CP039287	333421	--	SNP	G	T	SNP	G	T	SNP	G	T	SNP	G	T
NZ_CP039287	333427	--	SNP	G	T	SNP	G	T	SNP	G	T	SNP	G	T
NZ_CP039287-E6A55_RS02390	500511	amino acid ABC transporter permease	SNP	G	A	SNP	G	A	SNP	G	A	SNP	G	A
NZ_CP039287-E6A55_RS03700	791503	YgcG family protein	SNP	C	A	SNP	C	A	SNP	C	A	SNP	C	A
NZ_CP039287	1104731	--	SNP	G	T	SNP	G	T	SNP	G	T	SNP	G	T
NZ_CP039287	1166481	--	SNP	T	C	SNP	T	C	SNP	T	C	SNP	T	C
NZ_CP039287	1559970	--	SNP	G	T	SNP	G	T	SNP	G	T	SNP	G	T
NZ_CP039287-E6A55_RS07585	1628903	glucose-6-phosphate isomerase	SNP	G	T	SNP	G	T	SNP	G	T	SNP	G	T
NZ_CP039287-E6A55_RS12270	2597061	adenosylcobalamin-dependent ribonucleoside-diphosphate reductase	SNP	C	A	SNP	C	A	SNP	C	A			

NZ_CP039287-E6A55_RS12270	2597067	adenosylcobalamin-dependent ribonucleoside-diphosphate reductase	SNP	C	A	SNP	C	A	SNP	C	A	SNP	C	A
NZ_CP039287-E6A55_RS12370	2619321	ABC transporter ATP-binding protein	SNP	C	A	SNP	C	A	SNP	C	A			
NZ_CP039287-E6A55_RS13105	2768732	RseB	SNP	G	C									
NZ_CP039287-E6A55_RS14935	3162470	TRAP transporter large permease subunit	SNP	G	T	SNP	G	T	SNP	G	T	SNP	G	T
NZ_CP039287-E6A55_RS15995	3393896	glutamate-5-semialdehyde dehydrogenase	SNP	G	T	SNP	G	T	SNP	G	T	SNP	G	T
NZ_CP039287-E6A55_RS16335	3460447	RNA-binding protein	ins	G	GT	ins	G	GT	ins	G	GT	ins	G	GT
NZ_CP039287-E6A55_RS17570	3718338	penicillin-binding protein 1A	SNP	G	T	SNP	G	T	SNP	G	T	SNP	G	T
NZ_CP039287-E6A55_RS18085	3811856	type II secretion system secretin GspD	SNP	C	A	SNP	C	A	SNP	C	A			

NZ_CP039287-E6A55_RS18085	3811867	type II secretion system secretin GspD	SNP	C	A	SNP	C	A	SNP	C	A			
NZ_CP039287-E6A55_RS18850	3981763	response regulator	SNP	C	T	SNP	C	T	SNP	C	T	SNP	C	T
NZ_CP039288-E6A55_RS19235	26106	polysaccharide biosynthesis tyrosine autokinase	SNP	T	C	SNP	T	C	SNP	T	C	SNP	T	C
NZ_CP039288-E6A55_RS19830	164765	sigma-54-dependent Fis family transcriptional regulator	SNP	C	T	SNP	C	T	SNP	C	T	SNP	C	T
NZ_CP039288-E6A55_RS20305	265365	flagellar motor stator protein MotA	ins	G	GGGCGCCGCCTTC	ins	G	GGGCGCCGCCTTC	ins	G	GGGCGCCGCCTTC	ins	G	GGGCGCCGCCTTC
NZ_CP039288-E6A55_RS22125	659277	sensor histidine kinase	SNP	C	A				SNP	C	A	SNP	C	A
NZ_CP039288-E6A55_RS22660	772834	HlyD family type I secretion periplasmic adaptor subunit	SNP	C	A	SNP	C	A	SNP	C	A	SNP	C	A
NZ_CP039288-E6A55_RS26205	1553621	phosphoglycolate phosphatase	SNP	G	T	SNP	G	T	SNP	G	T			

NZ_CP039288-E6A55_RS26535	1628671	formate dehydrogenase-N subunit alpha	SNP	T	C	SNP	T	C	SNP	T	C	SNP	T	C
NZ_CP039288-E6A55_RS27725	1911223	amino acid adenylation domain-containing protein	SNP	C	A				SNP	C	A			
NZ_CP039288-E6A55_RS27895	1957707	TerC family protein	SNP	C	A	SNP	C	A	SNP	C	A			
NZ_CP039288-E6A55_RS30140	2453032	hypothetical protein	SNP	G	T	SNP	G	T	SNP	G	T	SNP	G	T
NZ_CP039288-E6A55_RS30310	2492779	hypothetical protein	ins	C	CT									
NZ_CP039289-E6A55_RS32220	682	hydrogenase small subunit	SNP	C	A	SNP	C	A	SNP	C	A	SNP	C	A
NZ_CP039289-E6A55_RS34220	405785	MFS transporter	ins	G	GGGACGGCAGCCAGACC	ins	G	GGGACGGCAGCCAGACC	ins	G	GGGACGGCAGCCAGACC			
NZ_CP039287-E6A55_RS05535	1190158	hypothetical protein				SNP	C	A	SNP	C	A			
NZ_CP039287-E6A55_RS05630	1211314	aldehyde dehydrogenase				SNP	G	T	SNP	G	T			

NZ_CP039287-E6A55_RS08660	1862887	hypothetical protein				ins	C	CGAGAGCT	ins	C	CGAGAGCT			
NZ_CP039287-E6A55_RS15075	3199544	translocation/assembly module TamB				SNP	G	T	SNP	G	T			
NZ_CP039287-E6A55_RS18865	3986062	16S rRNA (cytosine(967)-C(5))-methyltransferase RsmB				SNP	G	A	SNP	G	A	SNP	G	A
NZ_CP039288-E6A55_RS25025	1303261	acyl-CoA synthetase				SNP	T	G	SNP	T	G			

According to the genome annotation (accession number NZ_CP039287, NZ_CP039288, and NZ_CP039289) for chromosome 1, chromosome 2, and megaplasmid pHG1, respectively), gene locus E6A55_RS27725 encodes for non-ribosomal peptide synthetase and E6A55_RS05630 encodes for aldehydes dehydrogenase. It is unclear how the two genes encoded by E6A55_RS27725 and E6A55_RS05630 influence AA tolerance in the obtained variants. An amino acid substitution from serine to arginine (S230R) was found only in WT (gene locus E6A55_RS13105). This locus encodes MucB/RseB, responsible for a signal transduction mechanism. Bacterial cells detect environmental stresses by recognising misfolded proteins within the envelop compartment. The envelop stress signal is transmitted across the membrane to the cytoplasm by σ^E. The bacterial envelope stress response detects extracytoplasmic stress signals. It activates σ^E-dependent transcription by degrading the antisigma factor RseA, a monotopic transmembrane protein and the essential component of this signal transduction pathway (**Figure 3.8**) [242]. RseB, a binding partner of RseA, is critical for regulating this response [242-244]. Wollman & Zeth [242], based on its structure in *E. coli*, reported that RseB detects mislocalised lipoproteins and propagates the signal to activate the σ^E-response.

The periplasmic protein RseB is highly conserved among bacteria. Various bacterial species acquire orthologs of RseA and RseB, which interact and are encoded on the same operon as σ^E. In *P. aeruginosa*, for instance, MucA and MucB (the RseA and RseB orthologs) regulate both the heat-stress response and alginate production by modulating the activity of the AlgU transcription factor, a member of the stress σ^E -like family of factors [244-246]. Hence, it can be speculated that the S230R substitution in RseB of WT might contribute to AA's lower tolerance.

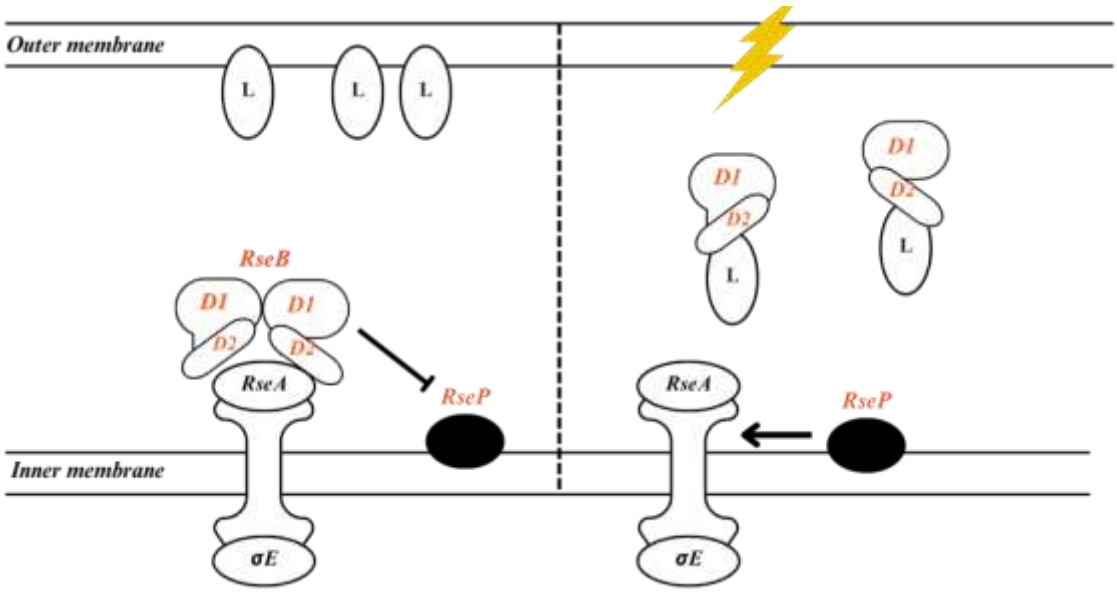

Figure 3.8 A representation of the RseB function. RseB bonds RseA through its small domains, protecting RseA from degradation by RseP, a member of the intramembrane protease family S2P. RseP catalyses the proteolytic cleavage of membrane-bound anti- σ^E protein RseA as a crucial step in transmembrane signal transduction in the σ^E extracytoplasmic stress response pathway [247]. When the integrity of the outer membrane is compromised by stress, mislocalised outer membrane lipoproteins (L) accumulate in the periplasm and are detected by the large domain of RseB. Lipoprotein binding induces a conformational change in the large domain D1 communicated to the small RseA-binding domain D2 via the interface between the two domains. This reduces the interaction between RseB and RseA, allowing RseA to be degraded by RseP. Finally, σ^E is activated to induce genes that regenerate the outer membrane's integrity and reduce the transcription of the outer membrane's most abundant proteins, thereby preventing further accumulating compounds that have already been damaged (adapted from Wollman & Zeth [242].

A stop-gain mutation (G→A) at codon 184 out of 466 codons in the 16S rRNA (cytosine (967)-C (5))-methyltransferase (*rsmB*) was common among three adapted variants derived from different selective pressures. In contrast, TamB and Acyl-CoA synthetase mutations were only found in BF2 and BF5. Therefore, RsmB appears to have been fixed until round 14 of ALE, whereas two loci (TamB, Acyl-CoA synthetase*)* were not.

RsmB catalyses the conversion of S-adenosyl-L-methionine (SAM) to S-adenosyl-L-homocysteine (SAH) (**Figure 3.9**). SAH is homocysteine's biosynthetic precursor, produced through the demethylation of SAM. SAH is converted by adenosylhomocysteinase into homocysteine and adenosine [248]. A previous study showed that the growth inhibition of *E. coli* K-12 caused by acetate in a defined medium led to the depletion of the intracellular methionine pool and the accumulation of the intermediate homocysteine, which inhibited growth [206]. Mordukhova & Pan showed that a replacement of cysteine 645 (a unique site of oxidation in the MetE protein) with alanine enhanced acetate tolerance and the introduction of the C645A mutation into the MetE-214 mutant *E. coli* enzyme produced the highest growth

rate in acetate. The *E. coli* K-12 WE variant containing acetate-tolerant MetE mutants was less inhibited by homocysteine in an l-isoleucine-rich medium [249]. However, in this study, the mutation did not occur at the first initial enzymatic steps of the methionine biosynthesis but in the latter step (**Figure 1.9**). It can be speculated that the loss-of-function mutation in RsmB is beneficial for cell growth on AA by terminating the formation of toxic intermediate homocysteine. This is supported by the fact that methionine acts as a form of negative feedback inhibition on its biosynthetic pathway, preventing the build-up of its toxic precursor, homocysteine [250].

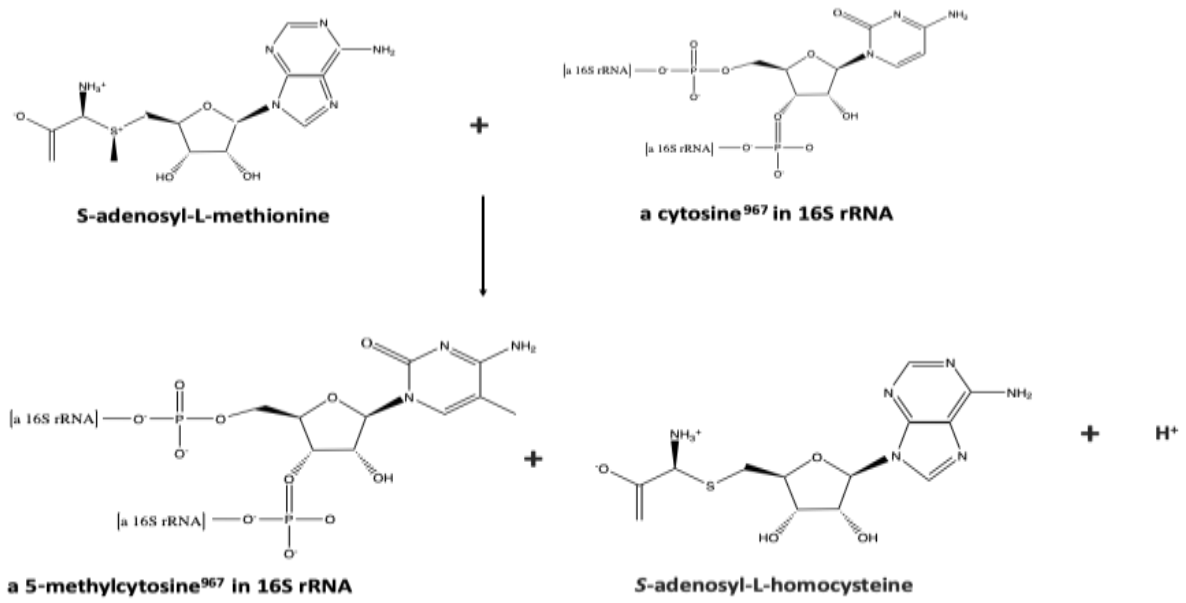

Figure 3.9 Reaction: S-adenosyl-L-methionine (SAM) + a cytosine967 in 16S rRNA → a 5-methylcytosine967 in 16S rRNA + S-adenosyl-L-homocysteine (SAH) + H^+ catalysed by rsmB.

BF2 and BF5 variants, derived from round 16, have similar mutations in chromosomes 1 and 2, in genes that encode TamB and Acyl-CoA synthetase, respectively. The translocation and assembly module TamB are important to stress resistance and are widely distributed across gram-negative bacterial variants [251, 252]. Li's group [253] also found that the survival rate of *Edwardsiella tarda* (a gram-negative bacterium) with TamB knockout was significantly lower in acidic and oxidative conditions. The internal pH of this mutant was greatly affected by the pH of its surroundings. This suggests that the mutants could not maintain pH homeostasis inside the cell [252]. BF2 and BF5 variants also obtained the Q25K substitution

(amino acid exchange from glutamine to lysine) in TamB, which may benefit cell growth on AA.

Another key mutation in improved AA tolerance is acyl-CoA synthetase found in BF2 and BF5 variants. These two variants exhibited better growth on AA than AE4 and WT. Acyl-CoA synthetase is important in intermediary metabolism by catalysing the formation of fatty acyl-CoA for β-oxidation and phospholipid biosynthesis [254]. All acetate must be converted to acetyl-CoA that can enter central metabolism, carried out by acyl-CoA short-chain synthetases (**Figure 1.10)** [255]. Lee *et al.* [170] reported that *C. necator* up-regulated fatty acid-CoA synthetase expression in the presence of acetate regardless of the ATP requirement. In addition, Lee's group also stated that *C. necator* might favour acetate as a substrate via fatty acid biosynthesis as one of the PHA-generating routes [170]. BF2 and BF5 variants obtained the M265R substitution (amino acid exchange from methionine to arginine) in acyl-CoA synthetase, which presumably benefits cell growth in AA.

Notably, the BF5 variant exhibited the best growth amongst all the adapted variants, including WT. Interestingly, the R147S substitution (amino acid exchange from arginine to serine) was found in the all sequenced strains but not in BF5. This means that the mutation was first found in the *C. necator* H16 strain, but during the ALE process, it went back to the original sequence found in the reference genome [231]. This mutation was predicted to have sensor histidine kinases in the HisKA_7TM region [237]. However, the exact function of this gene family still needs to be discovered, despite predictions of its possession of sensor histidine kinases. Notably, According to MiST (https://mistdb.com), *C. necator* H16 encodes 45 histidine kinases, including the one that has been repaired in BF5 (E6A55_RS22125). It senses a still-unknown signal, phosphorylates a still-unknown response regulator, and regulates still-unknown genes. Consequently, our comprehension of the mechanism by which this gene could impact AA tolerance is constrained.

Although variants (BF2 and BF5) derived from the same population, they did not necessarily share the same mutation. These findings imply that evolution under the same selective pressure does not necessarily result in the same genotype. This suggests that different variants in the improved AA tolerance correspond to different stress resistance mechanisms. Notably, If evolution continued, one of these variants would eventually dominate the population.

3.10 Conclusion

In conclusion, using the power of the ALE experiment, we successfully isolated adapted variants of *C. necator* H16 with enhanced growth on AA. Three adapted variants capable of increased AA tolerance were isolated using ALE with serial transfer. Adapted variants obtained from different rounds of ALE exhibited different performances on AA. Furthermore, we suggest that a layer of mutations in the adapted variants may provide an evolutionary pathway to enhanced growth in AA. These mutated genes reported in this work have not previously been implicated in improved AA tolerance.

CHAPTER 4

Chemical-assisted adaptive laboratory evolution (ALE) of a bioplastic producer *Cupriavidus necator* H16

Chapter 4 – Chemical-assisted adaptive laboratory evolution (ALE) of a bioplastic producer *Cupriavidus necator* H16

Introduction

The ALE approach is a reliable and important technique to enhance certain microbial traits vital for biotechnology [26]. These features involve maximizing the use of carbon, promoting the growth of microorganisms, and improving tolerance to substances that hinder growth, among other factors. What sets ALE apart is its straightforward technical implementation and capacity to adjust for different types of microbial strains. This method eliminates the requirement for a detailed understanding of the microbe's metabolic network and the necessity for specialist equipment or advanced genetic tools. This method not only speeds up the process of gaining important biological knowledge but also makes it easier to understand and analyse the complex relationship between an organism's physical characteristics and genetic makeup.

ALE has been shown to improve the traits of *C. necator* H16, which is known for storing up to 90% of its dry cell weight as PHA [147]. Achieving enhanced phenotypes through metabolic engineering poses challenges due to the intricate nature of microorganism metabolism. The ALE method offers a potent solution, leveraging natural evolution to yield microbial cell factories with improved traits through phenotype screening. ALE technology serves as a robust platform for constructing microbial cell factories. The employment of ALE on *C. necator* H16 has a wide range of applications, such as raising glycerol utilisation [4] and promoting growth in osmotic conditions [256].

Although the ALE process is straightforward, it can be time-consuming, typically requiring serial or continuous cultivation under selective conditions. To accelerate the process of evolution, it is essential to increase genetic variety. This involves developing a broader, more intricate range of variants for future selection. Typically, this is accomplished using physical agents such as UV radiation [6] and chemical agents [100]. Although divalent metal

ions like Co^{2+}, Mn^{2+}, and Zn^{2+} [8, 106-110] are commonly employed in random mutagenesis for protein evolution, their potential utility in ALE has not been investigated [84].

This study aimed to present a new, accelerated ALE process by integrating metal ions. In **Chapter 4**, we used metal ions to generate genetic variability and accelerate the ALE process, enabling the quick identification of *C. necator* H16 variants that can tolerate high glycerol levels. This technique represents the first use of divalent metal ions in ALE studies, indicating a significant advancement in the discipline.

4.1 Aim

The aim of the study in **Chapter 4** is to increase genetic diversity and accelerate the ALE process, enabling the rapid discovery of *C. necator* H16 variants that can tolerate elevated concentrations of glycerol. Furthermore, the objective is to determine the tolerance mechanism of the adapted variants using whole genome sequencing and analysis of gene mutations.

4.2 Bacterial strain and chemical

Bacterial strain and chemicals were as described in section **2.2**. For Genomic DNA purification, The GeneJET kit was used, containing: elution buffer (B12871F), elution buffer (B12872F), proteinase k solution (C5001), RNase A solution (C5011), digestion solution (C5021), digestion solution (C5022), lysis solution (C5031), lysis solution (C5034), wash buffer 1 (C5192), wash buffer 1 (C5194), wash buffer II (C5221), wash buffer II (C5222), and 3 M sodium acetate (pH 5.2) for DNA purification. The GeneJET kit from Thermo Fisher Scientific Baltics UAB (unless otherwise stated).

4.3 Cultivation of *C. necator* H16 and adapted variants

To investigate the impact of selected chemical mutagens ($MnCl_2$, $CoCl_2$, and $ZnCl_2$) on microbial growth and identify a suitable selective condition for ALE, *C. necator* H16 cultures were cultivated at a temperature of 30°C in Chi.Bio [68] very similar to section **2.3**, with the

following modifications: cultivations were conducted in NB medium with various concentration of $MnCl_2$ (0-25 mM), $CoCl_2$(0-20µM), or $ZnCl_2$(0-5 mM).

4.4 Chemical-assisted ALE of *C. necator* H16 for improved elevated glycerol tolerance

A schematic of chemical-assisted ALE experiments is shown in **Figure 4.1**. Each round of chemical-assisted ALE involved two stages: mutagenesis (M) and selection (S). In order to induce mutagenesis, *C. necator* H16 was cultivated in a 50-mL Falcon tube, which contained 5 mL of MSM supplemented with 1% (w/v) sodium gluconate. The medium was enriched with 10 µg/mL of gentamicin and either 10 µM $CoCl_2$, 15 mM $MnCl_2$, or 0.7 mM $ZnCl_2$. The culture was then incubated for 15 hours at 30°C. Afterwards, cells were obtained by centrifuging at 13300 rpm for 2 minutes at room temperature. The cell pellet was subjected to two washes with 1 mL of MSM with no carbon source and subsequently diluted accordingly using the same medium for selection. For the selection stage, *C. necator* H16 was grown in Chi.Bio [68], which is very similar to section **2.3**, except that this experiment used 15 mL of MSM with 10% (v/v) glycerol at 30°C. The cultivation was maintained until an initial stationary phase was reached, indicating the start of a new round of evolution.

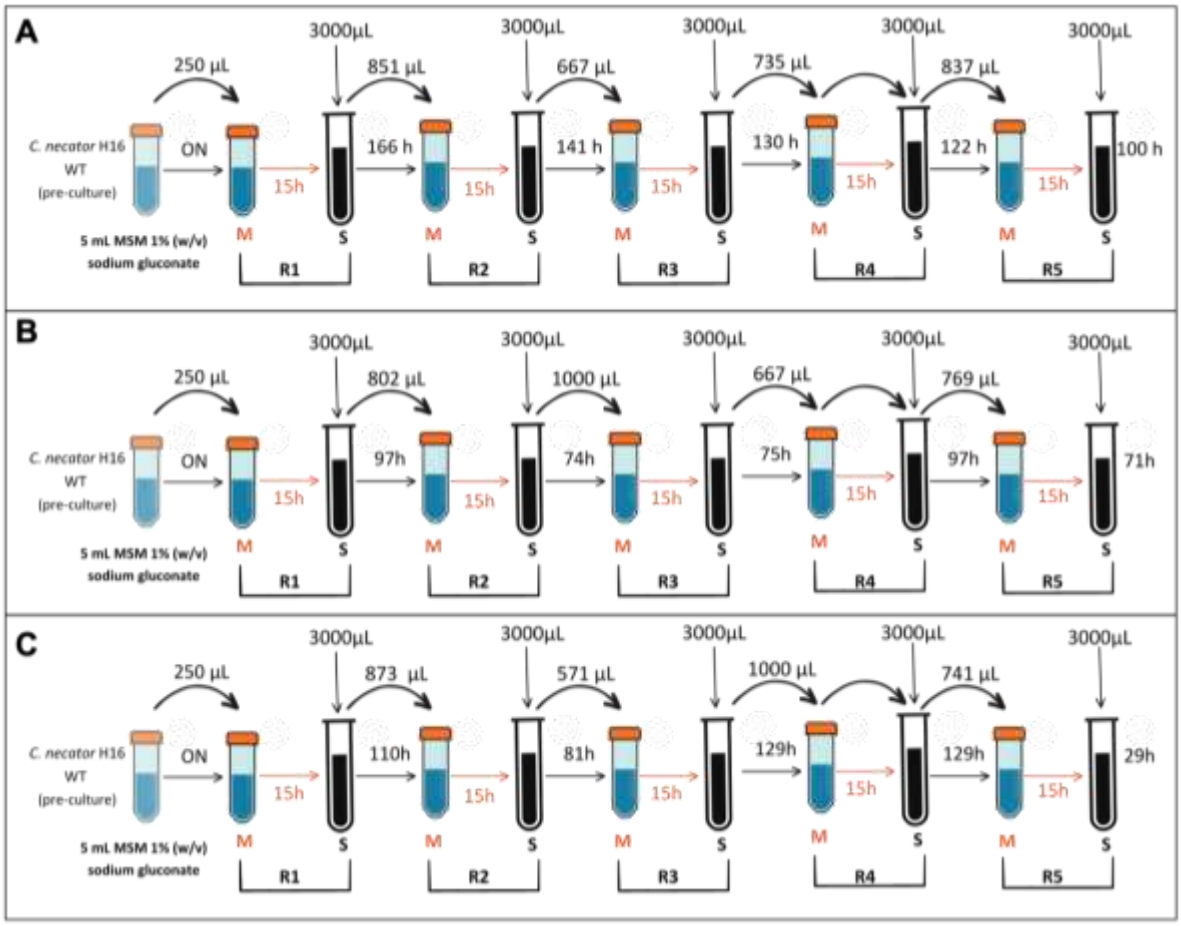

Figure 4.1 A schematic representation of a chemical-assisted laboratory evolution using $MnCl_2$ (A), $CoCl_2$ (B), or $ZnCl_2$ (C) in C. necator H16 for improved tolerance to an elevated concentration of glycerol. ON: overnight, R: round, h: hour, M: mutagenesis, and S: selection.

4.5 Genome extraction for genome sequencing

GeneJET Genomic DNA extraction, $3x10^9$ bacterial cells in a 2 mL microcentrifuge were centrifuged at 5000 x g for 10 min. The supernatant was removed, and the pellet was resuspended in 180 µL of digestion solution. The solution containing 20 µL of proteinase K was added and thoroughly mixed by vortexing. The sample was then incubated at 56 °C for 30 minutes and vortexed for 1-2 seconds for 5 minutes. The solution containing 20 µL of RNase was added to the sample and mixed by vortexing. The mixture was then incubated for 10 minutes at room temperature. A volume of 200 µL of Lysis Solution was added to the sample and thoroughly mixed by vortexing for about 15 seconds until a homogeneous mixture was

obtained. A solution containing 400 µL of 50% ethanol was added and mixed by pipetting to form a lysate solution. The prepared lysate solution was transferred into a GeneJET genomic DNA purification column and inserted in a collection tube. The solution was centrifuged for 1 min at 6000 x g. The collection tube containing the flow-through solution was discarded, and the sample in the purification column was transferred into a new 2 mL collection tube. A solution containing 500 µL of wash buffer I was added to the sample and centrifuged for 1 min at 8000 x g, and the flow-through was then discarded. The sample in the purification column was placed back in the collection tube. A solution containing 500 µL of wash buffer II was added to the sample in the column and then centrifuged for 3 minutes at 13300 rpm. The collection tube was then emptied, and the sample was re-centrifuged for 1 minute at 13300 rpm. The collection tube was discarded, and the sample in the purification column was placed in a 1.5 mL microcentrifuge tube. A solution containing 200 µL of elution buffer was added to the centre of the GeneJET genomic DNA purification column membrane to elute genomic DNA, incubated for 2 min at room temperature, and then centrifuged for 1 min at 8000 x g. The DNA concentration of the sample was measured using a Nanodrop.

Ethanol precipitation of DNA, 200 µL of DNA sample in a 1.5 mL microcentrifuge tube from the previous protocol was mixed with 20 µL sodium acetate (pH 5.2) (total volume of 220 µL). A solution containing 600 µL of ice-cold absolute ethanol was added and mixed with the DNA sample, which was incubated at -20°C overnight. The sample was centrifuged at 4°C at 13300 rpm for 30 minutes. The supernatant was discarded, and the pellet was washed with 500 µL of 75% ethanol (this washing step was repeated twice). The sample was then incubated at 37 °C for 5 minutes to remove the ethanol. The sample was air-dried at room temperature for 20 minutes. The sample was then re-suspended in 50 µL elution buffer from the GeneJET genomic DNA purification kit. The DNA concentration was measured using NanoDrop and loaded on a 1% (w/v) TAE gel to check the DNA quality.

The DNA samples were stored at -20°C. The DNA samples of Mn-R2-B11, Zn-R2-G5, and Co-R3-F3 were then prepared for genome sequencing. The genome sequencing was performed by NOVOGENE.

4.6 Results

4.6.1 Development of a chemical-assisted ALE for improved glycerol utilisation.

Traditional ALE has been demonstrated to enable the production of improved strains. However, ALE can be slow due to solely relying on natural mutations. This study tackles this concern by incorporating chemical mutagens to accelerate ALE. As stated in section **1.1.6**, various investigations have demonstrated that chemical mutagens can increase random mutations that speed up the evolution of cells [7, 85, 115].

In a previous study, Gonzalez *et al.* [1] developed a mutant strain (v6c6) of *C. necator* H16 that demonstrates a 9.5-fold acceleration in growth rate compared to the WT when cultivated in a medium containing 0.5% glycerol as the only source of carbon. Glycerol is an unfavourable carbon source that could be transformed into useful chemicals such as bioplastic. The v6c6 variant was developed after six rounds of ALE utilising batch culture. This outcome served as a stimulus for us to devise a technique to generate genetic variation to expedite the ALE procedure. This will facilitate the rapid identification of *C. necator* H16 variants that can endure higher glycerol levels. Furthermore, a v6c6 variant is employed as a standard for comparison in this inquiry.

Metal ions are crucial for supporting life, as they are necessary for the growth of bacteria. The cellular concentrations of Zn^{2+}, Mn^{2+} and Fe^{2+} typically vary from 0.4 to 1 mM under ideal conditions [257]. Metalloproteins rely on the existence of these ions to carry out essential functions, which contribute to the facilitation of catalytic processes [16]. Bacterial growth can be inhibited by metal poisoning, which can occur when enzymes crucial to important metabolic pathways are incorrectly bound to metals. Moreover, exceeding the critical levels of these metal ions can interfere with the precision of DNA synthesis [8, 108, 111]. Hence, in this work, we exposed the cells of *C. necator* H16 to three different metal ions ($MnCl_2$, ZnI_2, $CoCl_2$) to increase the mutation rate, consequently increasing the genetic diversity with beneficial mutations during the ALE experiment.

A concentration of chemical mutagens must be determined before the ALE experiment, as an excessively high concentration of chemicals can be lethal to the cell. Typically, the highest proportion of mutants per treated cell occurs at concentrations yielding 10 to 50% survival. Avoiding concentrations that destroy 95% or more of cells, in any event, is preferable [258]. The chemical-assisted ALE procedure involves determining the optimal concentration of chemical mutagens, incorporating chemical mutagens into the serial transfer ALE experiment, selecting the optimal colony in elevated concentrations of glycerol, and analysing the growth profile of the obtained adaptive variants.

4.6.1.1 Effect of chemical mutagens ($MnCl_2$, $ZnCl_2$, and $CoCl_2$) on *C. necator* H16's growth

The previous study demonstrated that substituting Mn^{2+} for Mg^{2+} modifies the accuracy of base selection by the polymerase activity and the specificity of hydrolysis by the 3′→5′ (proofreading) exonuclease activity [8, 109]. In addition, Deiry *et al.* (1984) also demonstrated when Mn^{2+} replaces $Mg^{2+,}$ there is a higher ratio of incorrect to correct dNTP insertion by the polymerase activity, accompanied by a decreased hydrolysis of a mismatched dNMP relative to a matched dNMP at the primer terminus by the 3'→5' exonuclease activity. In the presence of Mn^{2+}, the k_{cat} for inserting a complementary dNTP is decreased. In contrast, the catalytic rate for inserting a mismatched nucleotide is increased, as determined by kinetic analysis. Hence, using $MnCl_2$ as a mutagenic agent will boost the mutation rate in this work.

Based on the *in vitro* experiment by Sirover *et al.* (1979) [8], at a concentration of 3 mM Mn^{2+}, the error frequency during DNA synthesis was 15-fold higher than with Mg^{2+}, mostly resulting in single base substitutions. Additionally, based on the previous experiment [259], supplementation of 10 mM $MnCl_2$ to a cell culture of *E. coli* exhibited little growth. Since no previous research examines the effect of $MnCL_2$ on *C. necator* H16's growth, we chose the working concentration of $MnCl_2$ based on the information mentioned above. In this study, the cell *C. necator* H16 were grown in NB with different concentrations of $MnCl_2$ (0-25 mM). The result, however, showed no inhibitory effect of $MnCl_2$ on the cell at a concentration of 10 mM and below. Surprisingly, 15 mM $MnCl_2$ exhibited a 25% reduction in OD compared to 10 mM $MnCl_2$ (**Figure 4.2.A**). Hence, 15 mM $MnCl_2$ was used to generate mutants, which still allows

minimal growth for ALE and potentially generates mutants. At this particular concentration, microbial growth was possible, albeit at a diminished pace, presumably suggesting a decline in DNA synthesis. The latter impact was intended to enhance genetic diversity.

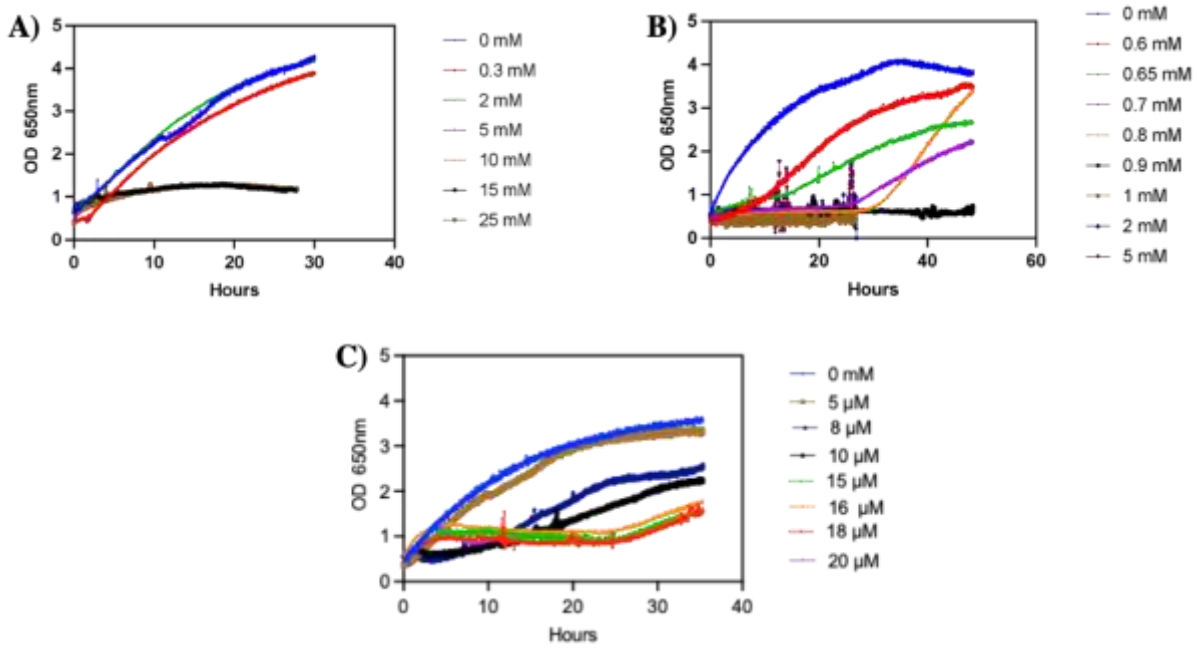

Figure 4.2 Effect of chemical mutagens at different concentrations, (A) 0-25 mM $MnCl_2$, (B) 0-5 mM $ZnCl_2$, and (C) 0-20 µM $CoCl_2$, on bacterial growth of C. necator H16.

Similarly, substituting Zn^{2+} and Co^{2+} for Mg^{2+} modifies the accuracy of base selection by the polymerase activity and the specificity of hydrolysis by the 3′→5′ (proofreading) exonuclease activity [8]. It is reported that Zn^{2+} can possibly serve as an activator for DNA polymerisation while increasing the frequency of misincorporation, similar to Mn^{2+} and Co^{2+}. Thus, using $ZnCl_2$ as a mutagenic agent will increase the rate of mutagenesis in this work.

In this study, the cell was grown in NB with different concentrations of $ZnCl_2$ (0-5 mM). The result showed that at 0.65 mM of $ZnCl_2$, the OD growth within 20 hours of incubation was reduced to 50%. At a concentration of 0.7 mM $ZnCl_2$, the cell showed nearly 25% of obtained OD growth compared to no mutagen supplementation (**Figure 4.2.B**); hence, this concentration was chosen for mutagenesis in ALE, which still allows minimal growth and potentially generates mutants for the ALE experiment.

Previous *in vitro* work [8] reported that a concentration of 4 mM Co^{2+} in 3′→5′ exonuclease assay promoted the misincorporation of poly(d(A-T) or poly(dA).oligo(dT). Hence, the supplementation of $CoCl_2$ in this work might increase the mutation rate. In this study, the cell was grown in NB with different concentrations of $CoCl_2$ (0-20 μM). The 8 μM and 10 μM $CoCl_2$ concentrations exhibited nearly identical growth curves within 20 hours of incubation. This study chose a concentration of 10 μM $CoCl_2$ for mutagenesis in ALE.

4.6.2 Growth curve of *C. necator* H16 in five rounds of chemical-assisted adaptive evolution in 10% glycerol as sole carbon source.

To demonstrate the practical implementation of the chemical-assisted ALE technique, we chose to adapt *C. necator* H16 to utilise a 10% (v/v) concentration of glycerol, higher than the previous work [47]. The cells were subjected to chemical mutagens for 15 hours before being transferred to the serial transfer of ALE. This work used 15 mM $MnCl_2$, 0.7 mM $ZnCl_2$, and 10 μM $CoCl_2$ to induce mutations. The previous report showed the growth of *C. necator* H16 in glycerol, characterised by an extended log phase of up to 110 hours in a 0.5% glycerol [47]. Surprisingly, during chemical-assisted ALE in this study, unlike previously reported *C. necator* H16's growth on glycerol, the cells pre-exposed to all three chemical mutagens did not experience a lengthy log phase but reached the stationary phase after 50 hours of incubation (**Figure 4.3.A-C**). It could be due to differing growing conditions.

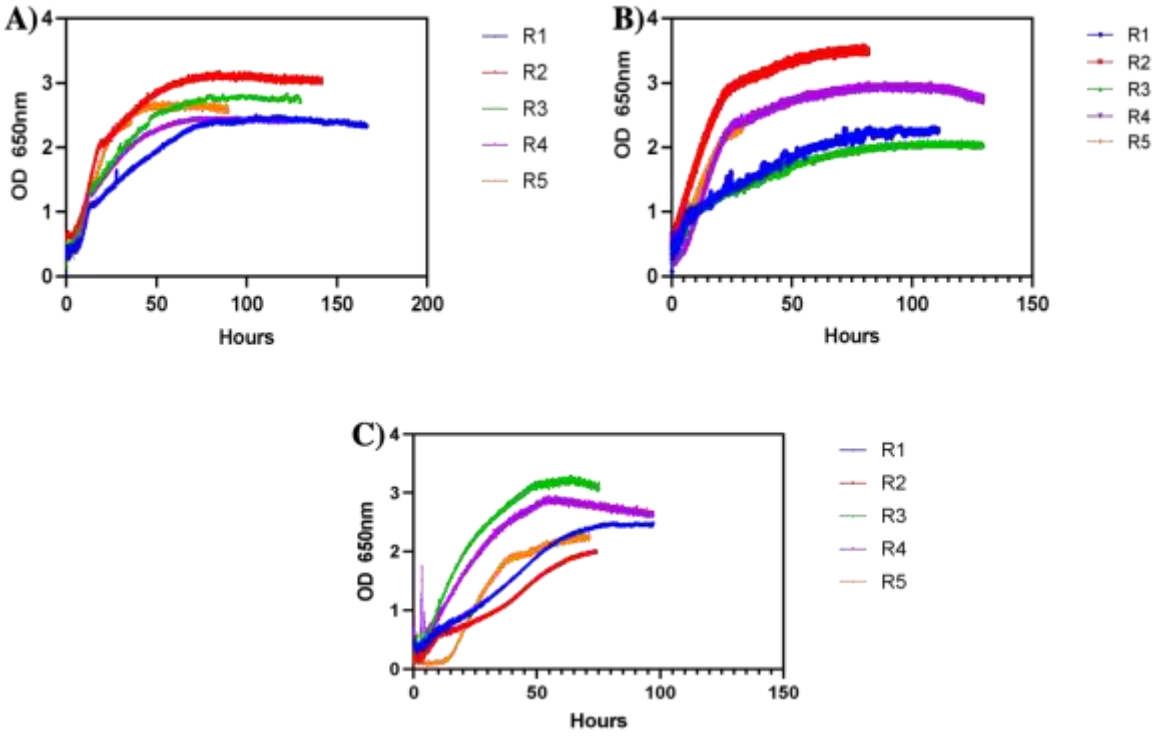

Figure 4.3 Growth profile of C. necator H16 in five serial transfers of ALE in 10% (v/v) glycerol in Chi.Bio, following treatment with 15 mM $MnCl_2$ (A), 0.7 mM $ZnCl_2$(B), and (C) 10 μM $CoCl_2$.

The cell population exhibited nearly similar growth profiles across all ALE conditions, with the highest achieved optical density (OD_{650}) being 3. $MnCl_2$-Assisted ALE and $ZnCl_2$-Assisted ALE displayed the best cell populations at round 2 (**Figure 4.3.A&B**), requiring time to reach the maximum OD of 50 hours of incubation. The maximum OD that was achieved did not improve after round 2. Meanwhile, $CoCl_2$-Assisted ALE displayed the best cell population at round 3, and no improvement in OD was achieved after round 3 (**Figure 4.3.C**). The population of round 2 from $MnCl_2$-Assisted ALE and $ZnCl_2$-Assisted ALE and round 3 from $CoCl_2$-Assisted ALE were used to isolate the single colony of the improved glycerol growth variant. In addition, we grew *C. necator* H16 in a 10% (v/v) glycerol without any pre-treatment involving a chemical mutagen. It is noteworthy that *C. necator* H16 can thrive at this concentration. Nevertheless, we noticed a progressive decline in growth over sequential cultivation rounds, particularly evident in the fall of the final OD_{650} measurement (data not shown). This suggests that to have a population with enhanced performance, it would be necessary to continue cultivating 10% (v/v) glycerol for longer. By using chemical mutagens to increase genetic variety, we were able to catch advantageous mutations, thereby reducing the time needed for improvement.

4.6.3 Isolation of best variants from the population of chemical-assisted ALE

159 single colonies were screened for improved glycerol growth in microplates from the cell population in rounds 1 and 2 of $MnCl_2$-assisted ALE, round 2 of $ZnCl_2$-assisted ALE, and round 3 of $CoCl_2$-assisted ALE. The cell growth profile was observed and compared to that of WT and v6c6.

The lag phase of the adapted variants in a 5% (v/v) glycerol medium exhibited a more pronounced duration than cultivations in a 1% (w/v) sodium gluconate medium (**Figure 4.4.A**). All adapted variants from $MnCl_2$-assisted ALE and v6c6 exhibited substantially greater growth than the WT, reaching a maximum OD of 2 at 595 nm after 150 hours of incubation in a 5% (v/v) glycerol solution (**Figure 4.4.B**). The adapted variants took about 50 hours to attain an OD of 595 nm of 1 and an additional 100 hours to reach the maximum OD_{595} of 2.5. Surprisingly, the performance of the Mn-R1-D3 variant was found to be comparable to that of v6c6, highlighting the benefit of chemical-assisted ALE in accelerating the identification of improved variants.

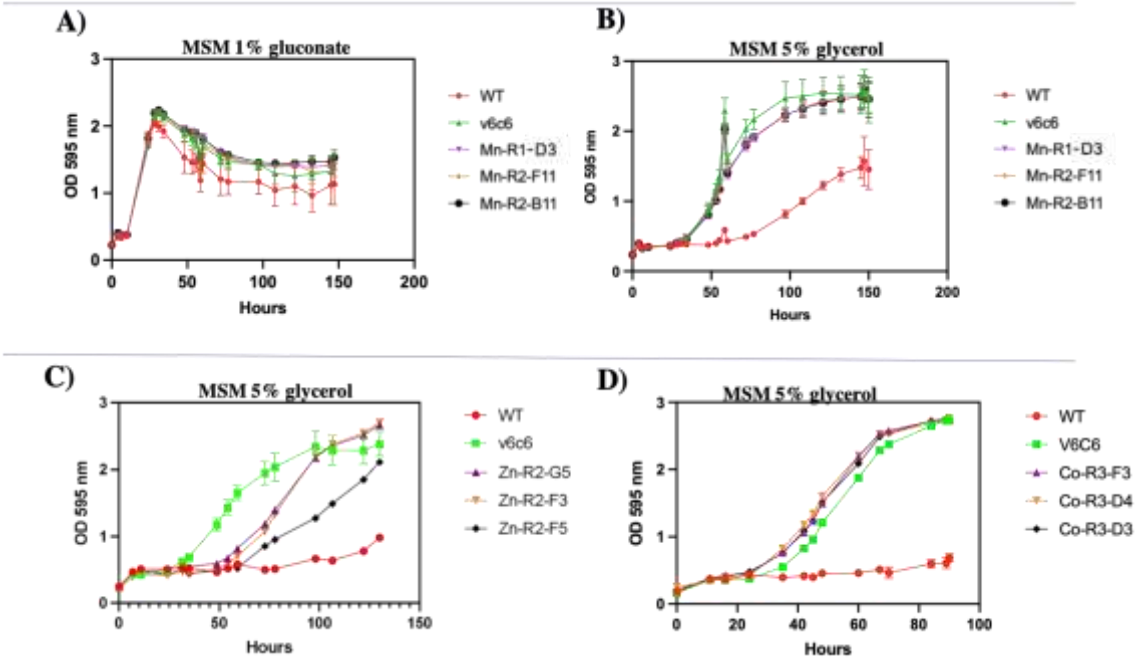

Figure 4.4 Growth profile of adapted variants in glycerol, in comparison to the WT and v6c6. (A) The best $MnCl_2$ variants from rounds 1 and 2 were grown in 1% (w/v) gluconate. (B) The best $MnCl_2$ variants from rounds 1 and 2. (C) The best $ZnCl_2$ variants from round 2. (D) The best $CoCl_2$ variants from round 3.

The growth profile of the selected adapted variants from round 2 of $ZnCl_2$-assisted ALE is shown in **Figure 4.4.C**. The top three mutants (Zn-R2-G5, Zn-R2-F3, and Zn-R2-F5) had slower growth than the v6v6 variant, but OD was found to be comparatively higher than the WT in 5% (v/v) glycerol. The highest OD was achieved by Zn-R2-G5 and Zn-R2-F3 variants, reaching an OD of 595 nm of 2.6 and 2.7, respectively, in 130 hours of incubation, with Zn-R2-G5 having slightly faster growth.

A similar result was also found in the $CoCl_2$-assisted ALE. The growth profile of the selected adapted variants from round 3 of $CoCl_2$-assisted ALE is shown in **Figure 4.4.D**. The top three mutants (Co-R3-F3, Zn-R3-D4, and Zn-R3-D3) had a comparatively higher OD than the WT in 5% (v/v) glycerol. The highest OD was achieved by all three adapted variants, reaching an OD of 595 nm of 2.7 in 90 hours of incubation.

4.6.4 Cell growth studies of selected adapted variants in different concentrations of glycerol.

Cultivations were performed using selected adapted variants in higher concentrations of glycerol. Notably, the Co-R3-F3 variant (**Figure 4.5.A**) exhibited accelerated growth compared to other cells during a 12-hour incubation period when cultured in a 5% (v/v) glycerol medium. Accelerated growth of the Co-R3-F3 variant was seen in a 96-well plate cultivation. Nevertheless, the cellular growth reached a saturation point after an incubation period of 50 hours, reaching a maximum OD of 850 nm of 5. The v6c6 variant had the highest OD growth (OD of 850 nm of 15). In contrast to the growth seen on a 96-well plate, the variant Zn-R2-G5 exhibits comparable growth to the WT in a 5% (v/v) glycerol medium. (**Figure 4.5.A**).

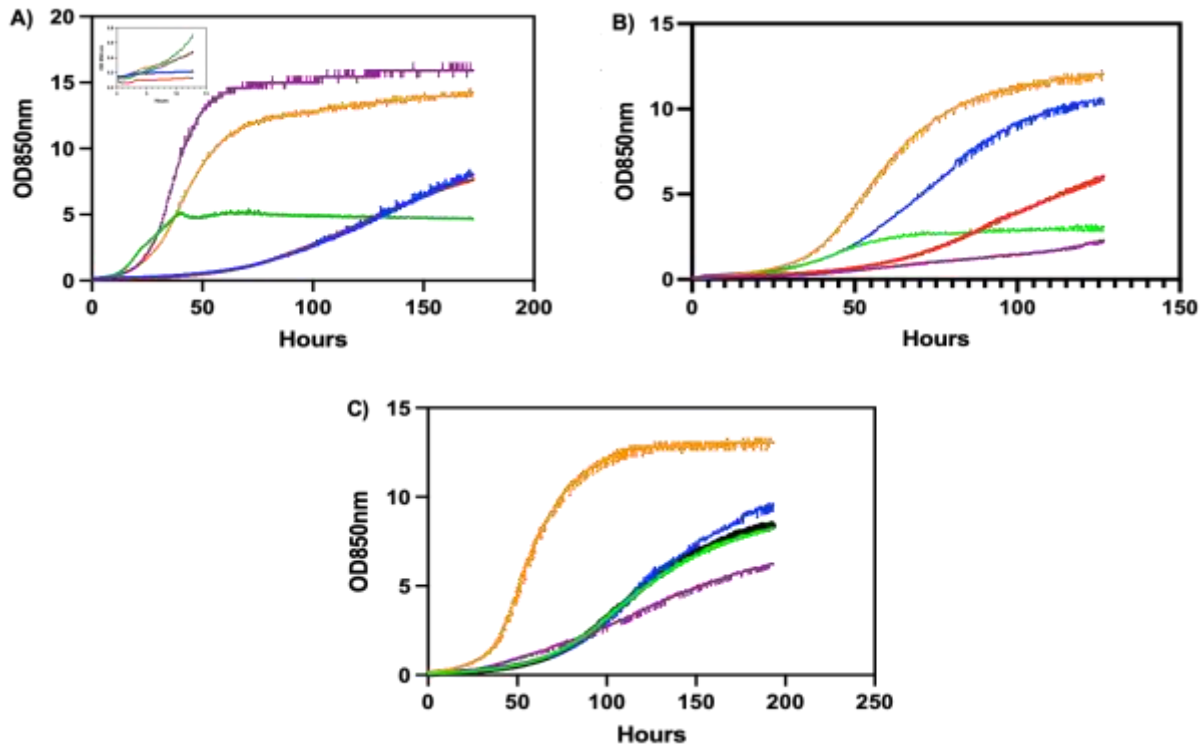

Figure 4.5 The growth performance of C. necator H16 WT (red line), v6c6 (dark purple line), and the selected variants (Mn-R2-B11 (orange line), Zn-R2-G5 (blue line), Co-R3-F3 (green line)) in different glycerol concentrations. A, B, C. The cultivations were performed in a Personal Bioreactor RST-1 (Biosan) with 20 mL of MSM + 5% (v/v) (A), 10% (v/v (B), and 15% (v/v) (C) glycerol.

When cultivated in 10% glycerol (**Figure 4.5.B**). Variant Mn-R2-B11 exhibited superior growth (OD maximum of 850 nm = 12), outcompeting the improved glycerol-utilising v6c6 (OD maximum of 850 nm = 2). The v6c6 variant did not show significant growth within an incubation period of 100 hours. Notably, the Zn-R2-G5 variant had better growth (OD maximum of 850 nm = 10) than WT (OD maximum of 850 nm = 2) and v6c6. Consistently, superior growth in 15% glycerol was demonstrated by variant Mn-R2-B11 (OD maximum of 850 nm = 13). Interestingly, the variant v6c6 exhibited the lowest growth compared to the other variants.

Since mutation occurs randomly during ALE, the cause of the different growth profiles of adapted variants in different concentrations of glycerol suggested that the improved glycerol growth was achieved via multiple mechanisms depending on the evolution conditions.

4.6.5 Mutations were found in adapted variants obtained from chemical-assisted ALE.

We found both transition and transversion mutations in the obtained chemical-assisted ALE variants. Additionally, the number of mutations found was greater compared to the previous variants obtained from serial cultivation, such as v6c6 [84].

$MnCl_2$ and $CoCl_2$ showed markedly greater mutagenic effects than $ZnCl_2$, as seen in **Table 4.1**, consistent with prior research by Sirover *et al*. [8].

Table 4.1 Analysis of mutational spectra adapted from Sitompul *et al.* [84]

Nucleotide substitution	Co-C3-F3	Mn-C2-B11	Zn-C2-G5
Transition, A→G, T→C	5	6	0
Transition, G→A, C→T	4	6	0
Transversion, A→T, T→A	3	2	0
Transversion, A→C, T→G	7	5	2
Transversion, G→C, C→G	4	5	1
Transversion, G→T, C→A	1	1	1
Transition/ Transversion	0.6	0.9	0
InDel	11	10	1

4.6.6 Interesting mutations were found in adapted variants obtained from chemical-assisted ALE.

Mn-R2-B11, Zn-R2-G5, and Co-R3-F3 variants were sequenced to uncover underlying genetic changes. With a genomic size of 7,416,678 bp, *C. necator* H16 has one megaplasmid and two chromosomes [1]. In this work, every adapted variant that has been sequenced had a mean sequencing coverage of greater than 30× and was subsequently compared against the reference genomes (GenBank accession numbers CP039287, CP039288, and CP039289) [231].

Based on the sequenced genome's variant calling results, we identified six interesting mutations that might contribute to increased tolerance to higher glycerol concentrations. These six mutations resulted in amino acid changes in the five proteins encoded at the gene loci E6A55_RS12840, E6A55_RS13105, E6A55_RS19830, E6A55_RS03700 and

E6A55_RS18850 (**Table 4.2**). Additionally, other mutations were seen in adapted variants (Mn-R2-B11, Zn-R2-G5, and Co-R3-F3) that had undergone adaptation. Nevertheless, the specific mechanisms by which these mutations led to the increased glycerol growth remain uncertain.

Based on the genome annotation (accession number NZ_CP039287, NZ_CP039288, and NZ_CP039289) for chromosome 1, chromosome 2, and megaplasmid pHG1, respectively), gene locus E6A55_RS12840 is predicted to encode a glycerol kinase (GlpK). GlpK gene plays a role in glycerol metabolism by phosphorylating glycerol to generate glycerol-3-phosphate. Gene loci E6A55_RS13105, E6A55_RS19830, E6A55_RS03700, and E6A55_RS18850 encode RseB (a negative regulator of σ^E activity), transcriptional regulator DhaR (a regulator for acetoin/glycerol metabolism), YgcG family protein and DNA-binding transcriptional response regulator, respectively.

Table 4.2.A SNPs detected in Co-R3-F3, Mn-R2-B11 and Zn-R2-G5 are highlighted in green (US: upstream, DS: downstream) adapted from Sitompul *et al.* [84]

Chromosome	Location	Position	Locus tag	Gene	WT		Co-R3-F3		Mn-R2-B11		Zn-R2-G5	
					REF	ALT	REF	ALT	REF	ALT	REF	ALT
NZ_CP039287.1	US/DS	192516	gene-E6A55_RS00915;gene-E6A55_RS00905,gene-E6A55_RS00910		G	T	G	T			G	T
NZ_CP039287.1	US/DS	333421	gene-E6A55_RS01595;gene-E6A55_RS01590		G	T			G	T	G	T
NZ_CP039287.1	US/DS	333427	gene-E6A55_RS01595;gene-E6A55_RS01590		G	T			G	T	G	T
NZ_CP039287.1	Exonic	500511	gene-E6A55_RS02390	amino acid ABC transporter permease	G	A					G	A
NZ_CP039287.1	Exonic	572008	gene-E6A55_RS02750	recombinase RecA			C	T	C	T		
NZ_CP039287.1	Exonic	578522	gene-E6A55_RS02785	ligase			A	G	A	G		
NZ_CP039287.1	Exonic	738904	gene-E6A55_RS03485	ornithine cyclodeaminase			T	A	T	A		
NZ_CP039287.1	Exonic	791503	gene-E6A55_RS03700	YgcG family protein			C	A	C	A		
NZ_CP039287.1	US/DS	1166481	gene-E6A55_RS05420;gene-E6A55_RS05410,gene-E6A55_RS05415		T	C					T	C
NZ_CP039287.1	Exonic	1485292	gene-E6A55_RS06940	PAS domain-containing sensor histidine kinase			G	C	G	C		
NZ_CP039287.1	ncRNA-exonic	1807929	rna-E6A55_RS08390				A	T				
NZ_CP039287.1	ncRNA-exonic	1807930	rna-E6A55_RS08390				T	A				
NZ_CP039287.1	Exonic	2101221	gene-E6A55_RS09900	D-galactonate dehydratase family protein			A	C				
NZ_CP039287.1	Exonic	2597061	gene-E6A55_RS12270	adenosylcobalamin-dependent ribonucleoside-diphosphate reductase	C	A	C	A	C	A		
NZ_CP039287.1	US/DS	2612983	rna-E6A55_RS12325,rna-E6A55_RS12330;gene-E6A55_RS12320,rna-E6A55_RS12335,rna-						T	C		

			E6A55_RS12340,rna-E6A55_RS12345,rna-E6A55_RS12350										
NZ_CP039287.1	US/DS	2612986	rna-E6A55_RS12325,rna-E6A55_RS12330;gene-E6A55_RS12320,gene-E6A55_RS12355,rna-E6A55_RS12335,rna-E6A55_RS12340,rna-E6A55_RS12345,rna-E6A55_RS12350							A	T		
NZ_CP039287.1	US/DS	2612991	rna-E6A55_RS12325,rna-E6A55_RS12330;gene-E6A55_RS12320,gene-E6A55_RS12355,rna-E6A55_RS12335,rna-E6A55_RS12340,rna-E6A55_RS12345,rna-E6A55_RS12350							G	A		
NZ_CP039287.1	US/DS	2626787	gene-E6A55_RS12395,gene-E6A55_RS34550,gene-E6A55_RS35235;gene-E6A55_RS12400,gene-E6A55_RS12405,gene-E6A55_RS12410							C	G		
NZ_CP039287.1	US/DS	2626790	gene-E6A55_RS12395,gene-E6A55_RS34550,gene-E6A55_RS35235;gene-E6A55_RS12400,gene-E6A55_RS12405,gene-E6A55_RS12410							T	G		
NZ_CP039287.1	US/DS	2626815	gene-E6A55_RS12395,gene-E6A55_RS34550,gene-E6A55_RS35235;gene-E6A55_RS12400,gene-E6A55_RS12405,gene-E6A55_RS12410							A	C		
NZ_CP039287.1	Exonic	2721992	gene-E6A55_RS12840	glycerol kinase						C	T		
NZ_CP039287.1	Exonic	2722640	gene-E6A55_RS12840	glycerol kinase			G	C	G	C			
NZ_CP039287.1	Exonic	2768732	gene-E6A55_RS13105	RseB							G	C	
NZ_CP039287.1	Exonic	3718338	gene-E6A55_RS17570	penicillin-binding protein 1A	G	T					G	T	
NZ_CP039287.1	Exonic	3981763	gene-E6A55_RS18850	response regulator	C	T					C	T	

NZ_CP039288.1	Exonic	56691	gene-E6A55_RS19345,gene-E6A55_RS19350	MFS transporter			A	C				
NZ_CP039288.1	Exonic	56695	gene-E6A55_RS19345,gene-E6A55_RS19350	MFS transporter							A	C
NZ_CP039288.1	Exonic	164765	gene-E6A55_RS19830	sigma-54-dependent Fis family transcriptional regulator	C	T					C	T
NZ_CP039288.1	ncRNA-exonic	177502	rna-E6A55_RS19890				T	G				
NZ_CP039288.1	Exonic	649721	gene-E6A55_RS22090	hypothetical protein			G	C	G	C		
NZ_CP039288.1	Exonic	1205170	gene-E6A55_RS24600	MurR/RpiR family transcriptional regulator			C	T	C	T		
NZ_CP039288.1	Exonic	1628671	gene-E6A55_RS26535	formate dehydrogenase-N subunit alpha	T	C					T	C
NZ_CP039288.1	Exonic	1820152	gene-E6A55_RS27345	VWA domain-containing protein			G	C	G	C		
NZ_CP039288.1	Exonic	2496322	gene-E6A55_RS30325	tetratricopeptide repeat protein							G	T
NZ_CP039289.1	Exonic	682	gene-E6A55_RS32220	twin-arginine translocation signal domain-containing protein	C	A					C	A
NZ_CP039289.1	Exonic	202180	gene-E6A55_RS33140	nucleotidyl transferase AbiEii/AbiGii toxin family protein			T	C	T	C		

Table 4.3.B InDels detected in Co-R3-F3, Mn-R2-B11 and Zn-R2-G5 are highlighted in green (**US**: upstream, **DS**: downstream) adapted from Sitompul *et al.* [84]

Chromosome	Location	Position 1	Position 2	Locus tag	Function	WT		Co-R3-F3		Mn-R2-B11		Zn-R2-G5	
						REF	ALT	REF	ALT	REF	ALT	REF	ALT
NZ_CP039287.1	Exonic	1309779	1309779	gene-E6A55_RS34760	Hypothetical protein	-	CAGCAG CCGGAG CAG						
NZ_CP039287.1	Exonic	1712937	1712984	gene-E6A55_RS07985	DNA segregation ATPase FtsK/SpoIIIE or related protein	AGCCGA AGCCGA AGCCGA AGCCGA AGCCGA AGCCGA AGCCGA AGCCGA	-					AGCCGA AGCCGA AGCCGA AGCCGA AGCCGA AGCCGA AGCCGA AGCCGA	-
NZ_CP039287.1	ncRNA_exonic	1807932	1807932	rna-E6A55_RS08390	23S rRNA			-	GCAC				
NZ_CP039287.1	US/DS	2626802	2626805	gene-E6A55_RS12395,gene-E6A55_RS34550,gene-E6A55_RS35235;gene-E6A55_RS12400,gene-	Predicted arabinose efflux permease AraJ, MFS family					TGTG	-		

				E6A55_RS12405,gene-E6A55_RS12410									
NZ_CP039287.1	US/DS	2626808	2626810	gene-E6A55_RS12395,gene-E6A55_RS34550,gene-E6A55_RS35235;gene-E6A55_RS12400,gene-E6A55_RS12405,gene-E6A55_RS12410	Predicted arabinose efflux permease AraJ, MFS family					TGG	-		
NZ_CP039287.1	Exonic	3720874	3720877	gene-E6A55_RS34910	Hypothetical protein			GCCA	-				
NZ_CP039287.1	Exonic	3720882	3720883	gene-E6A55_RS34910	Hypothetical protein			TG	-				
NZ_CP039287.1	Exonic	3800472	3800472	gene-E6A55_RS18020	DNA-binding transcriptional regulator, Lrp family			G	-	G	-		
NZ_CP039287.1	Exonic	3943689	3943700	gene-E6A55_RS18695	Choline dehydrogenase or related flavoprotein			CAGGCGGTTGGC	-	CAGGCGGTTGGC	-		
NZ_CP039288.1	ncRNA_exonic	177504	177504	rna-E6A55_RS19890	23S rRNA			-	G				
NZ_CP039288.1	Exonic	265365	265365	gene-E6A55_RS20305	Flagellar motor component MotA	-	GGCGCCGCCTTC					-	GGCGCCGCCTTC
NZ_CP039288.1	Exonic	649714	649714	gene-E6A55_RS22090	Hypothetical protein					-	CCCCCC		
NZ_CP039288.1	Exonic	2219351	2219372	gene-E6A55_RS29140	Membrane carboxypeptidase/penicillin-binding protein			GCGCCGGCGTGC	-	GCGCCGGCGTGC	-		

								GCCGCT ACCT		GCCGCT ACCT			
NZ_CP039288.1	Exonic	2459882	2459882	gene-E6A55_RS30165	Glycosyltransferase, catalytic subunit of cellulose synthase and poly-beta-1,6-N-acetylglucosamine synthase					-	CGCCCCC		
NZ_CP039289.1	Exonic	204769	204769	gene-E6A55_RS33155	HAMP domain-containing histidine kinase			-	CGGGCT				

Mutations in the g*lpK* gene have been seen in the ALE experiments conducted on a minimum glycerol medium [1, 128, 260, 261]. According to Kim *et al*. (2022) [128], *glpK* mutations found in *E. coli* may be classified as specialist mutations because these can provide fitness benefits under culture conditions when glycerol is the sole accessible carbon source. In *C. necator* H16, glycerol metabolism requires the genes encoding a putative FAD-dependent glycerol 3-phosphate dehydrogenase (GlpD) and a putative glycerol kinase (GlpK) [262] (**Figure 4.6**). In this study, the best adaptive variant, Mn-R2-B11, and the Co-R3-F3 variant, have a non-synonymous mutation at GlpK (the W480S substitution; an amino acid change from tryptophan to serine). The W480S substitution was also found in previous work in *C. necator* H16 [1]. According to Gonzalez *et al.* [1], based on the GlpK protein in *C. necator* H16, W480 resides in a coiled region distant from the catalytic core. As W480 is not located on any known activation loop or glycerol-binding and ATP-binding site in the GlpK [263], it can be difficult to predict whether or not the mutation altered the enzyme's catalytic function. The mutation may improve protein expression due to a codon change, protein folding, or solubility within the cellular environment. Cheng *et al.* (2014) stated that a point mutation in the *glpK* gene allows growth by improving glycerol utilisation [260]. Notably, a search for conserved domains revealed that W480 is highly conserved in multiple sequence alignments of GlpK in *C. necator* H16 with related proteins from a wide range of organisms (**Figure 4.6.A**). A protein model of the mutated (S480) and non-mutated GlpK (W480) is shown in **Figure 4.6.B**.

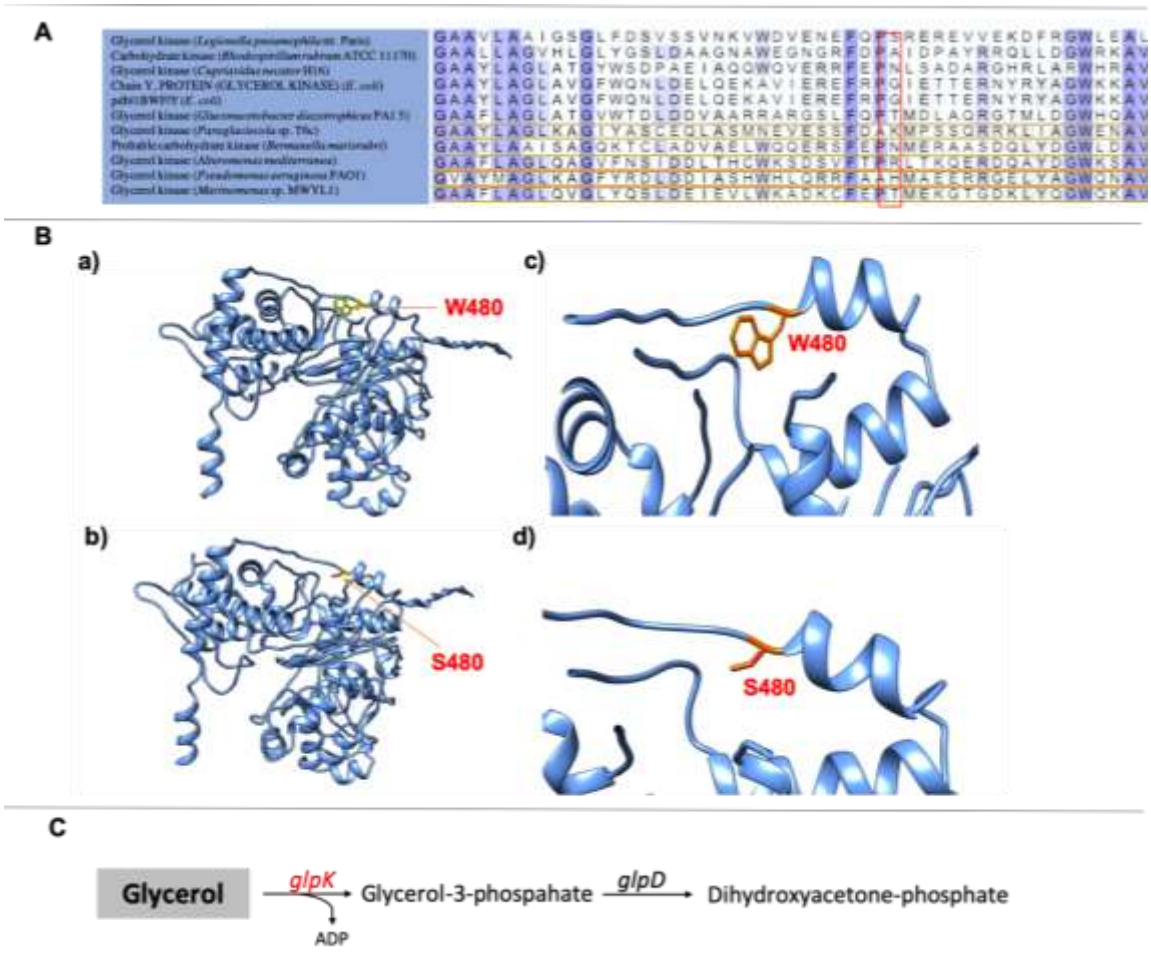

Figure 4.6 The illustration shows the multiple sequence alignments of GlpK of various organisms. Sequence alignment is shown using multiple sequence alignment UniProt, where text highlighted in the dark purple and red box indicates highly conserved (A). Protein models of GlpK in C. necator H16 (B). (B.a) and (B.c) show GlpK with Try480. (B.b) and (B.d) show GlpK with Ser480. Protein prediction was created using the Swiss Model and Staphylococcus aureus as a template, and S480 mutation was created using Chimera. The metabolic pathway for glycerol in C. necator H16 (C).

In this study, the Mn-R2-B11 variant demonstrated superior growth in 10% and 15% glycerol compared to the WT, v6c6, and other adapted variants (Zn-R2-G5 and Co-R3-F3). Surprisingly, the nonsynonymous mutation (A264V) was also identified in the GlpK gene of Mn-R2-B11. This mutation was discovered close to the active site [222]. The codon substitution in *glpK* could enhance the growth of the Mn-R2-B11 variant at increased glycerol concentrations. It is plausible to hypothesise that the combined occurrence of the two-point mutations in *glpK*, particularly in Mn-R2-B11, facilitates enhanced growth at a glycerol concentration of 15%. Notably, a search for conserved domains uncovered that A264 is fairly conserved in multiple sequence alignments of GlpK in *C. necator* H16 with proteins from other organisms (**Figure 4.7.A**). A protein model of the mutated (V264) and non-mutated GlpK (A264) is shown in **Figure 4.7.B**.

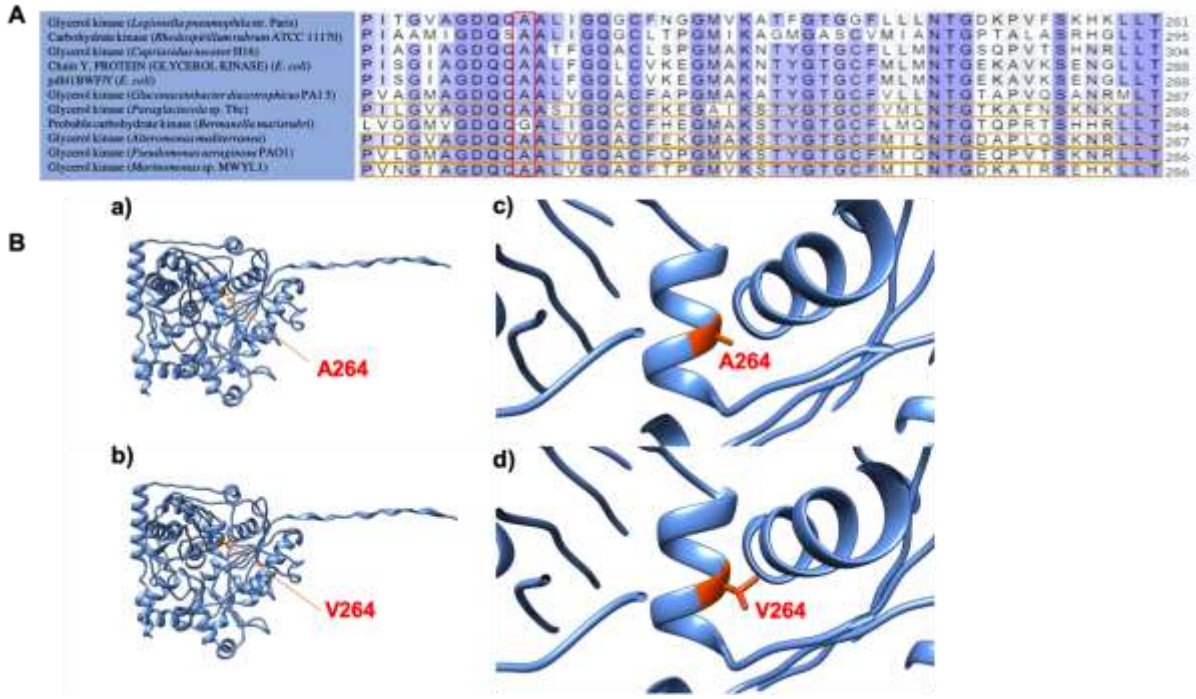

Figure 4.7 The illustration shows the multiple sequence alignments of GlpK of various organisms. Sequence alignment is shown using multiple sequence alignment UniProt, where text in the red box indicates moderately conserved (A). Protein models of GlpK in C. necator H16 (B). (B.a) and (B.c) show GlpK with Ala264. (B.b) and (B.d) show GlpK with Val264. Protein prediction was created using the Swiss Model and S. aureus as a template, and S480 mutation was created using Chimera.

The S230R substitution was only identified in the Zn-R2-G5 variant encoded by the gene locus E6A55_RS13105. This gene is responsible for encoding RseB, which plays a crucial role in the signal transduction pathway. Bacterial cells possess the ability to sense environmental stressors via the recognition of misfolded proteins inside the envelope compartment. The transmission of the envelope stress signal from the membrane to the cytoplasm is facilitated by the sigma factor E (σ^E). The bacterial envelope stress response is responsible for detecting extracytoplasmic stress signals. The activation of σ^E-dependent transcription is achieved by degrading the antisigma factor RseA. RseA is a monotopic transmembrane protein crucial in this signal transduction pathway (**Figure 3.7**) [242]. The regulatory response in question [226-228] depends on the presence of RseB, which acts as a binding partner for RseA. According to Wollman and Zeth [242], detecting mislocalised lipoproteins by RseB in *E. coli* is responsible for initiating the signal that activates the σ^E-response. In *P. aeruginosa*, the regulatory proteins MucA and MucB, which are orthologs of RseA and RseB, regulate the response to heat stress and the synthesis of alginate. They achieve this regulation by modifying the activity of the AlgU transcription factor, which belongs to the stress family of σ^E-like transcription factors

[244-246]. Therefore, it is possible to hypothesise that the S230R substitution in RseB may improve glycerol growth in the Zn-R2-G5 variant.

Zn-R2-G5 variant and WT have similar mutations in chromosomes 2 and 1, which encode AcoR (a Transcriptional regulator of acetoin/glycerol metabolism) and AtoC (a DNA-binding transcriptional response regulator), respectively. The A15V substitution may be associated with reduced growth in glycerol. The AcoR gene is located in the downstream region of the *acoABCL* operon and is responsible for encoding a positive regulator that enhances the transcription of the operon. The characteristics of the AcoR product resemble transcriptional activators that operate on sigma 54-dependent promoters [264], which are also involved in various stress responses [265]. In *C. necator H16*, the acetoin catabolic pathway is regulated by the AcoR [266]. It has been previously reported that acetoin can be produced from glycerol. DhaR also features sequence similarity (<30% identity) to AcoR [267]. In the glycerol degradation pathway, excess glycerol is removed by oxidation to dihydroxyacetone (DHA), catalysed by glycerol dehydrogenase (also known as DHA reductase), and DHA is converted to DHAP by DHA kinase (DhaK) [268]. It is believed that a positive regulator encoded by DhaR transcriptionally activates the genes in the DHA system [269]. We can only assume that proteins/reactions are involved directly or indirectly in the glycerol metabolic pathway.

A nonsynonymous mutation (D23N) was found in the Zn-R2-G5 variant and WT. Based on protein homology, the D23N substitution was predicted to be a response regulator. A response regulator is a protein that facilitates cellular response to changes in its surroundings, functioning as an integral component within a two-component regulatory system [270]. In yeast, a response regulator plays a crucial role in regulating the activity of a mitogen-activated protein kinase (MAPK) pathway, which governs cellular growth in the response to osmotic stress [271]. Hence, it can be speculated that the amino acid exchange D23N in response regulator of the Zn-R2-G5 variant and WT may also be associated with reduced growth in the presence of glycerol against Mn-R2-B1.

Variants Mn-R2-B11 and Co-R3-F3 both contain the G253W substitution in the YgcG family protein, which is predicted to possess a transmembrane domain and is classified as a potential phosphatase. This substitution may lead to improved glycerol growth.

4.7 Conclusion

The experimental results from **Chapters 2** and **3** prove that the traditional ALE strategy effectively generates improved variants with desired characteristics. Furthermore, a prior study [1], produced a variant (v6c6) using six rounds of the traditional ALE method. This variant has shown a 9.5-fold increase in growth rate in glycerol and has effectively activated the glycerol utilisation capability of *C. necator* H16. To accelerate the traditional ALE procedure, we have developed a method known as assisted-chemical ALE. In **Chapter 4**, we incorporated three chemicals ($MnCl_2$, Znl_2, and $CoCl_2$) with ALE using serial transfers. Incorporating $MnCl_2$, Znl_2, and $CoCl_2$ in the ALE procedure enhances the efficiency of the process by facilitating the rapid generation of superior variants. The best variant (Mn-R2-B11) was obtained from $MnCl_2$-assited ALE, exhibiting significant improvements in OD cell growth and outperforming the growth of the v6c6 variant under increased glycerol concentrations. The use of whole-genome sequencing on the WT and three variants revealed notable non-synonymous modifications within the genome.

CHAPTER 5

Concluding remarks and future work

Chapter 5 – Concluding remarks and conclusion

5.1 Concluding remarks

The work presented within this thesis was divided into three major workflows: the use of the ALE experiment to increase the tolerance to two major inhibitors found in lignocellulosic hydrolysate (BA & AA) and the development of chemical-assisted ALE to improve industrial phenotypes of *C. necator* H16. In this study, our aim is to delve deep into the intricate metabolic pathways of this microbe, seeking to unveil pivotal insights that can enrich our understanding on a broader scale.

The selection of ALE as the primary methodology in this study was supported by a comprehensive evaluation of the literature, which demonstrated the successful results of ALE in generating improved variants. Several techniques for the ALE experiment have been developed. To effectively use ALE in the fields of bioproduction and basic studies, it is essential to determine the most suitable method(s) that should be employed to accomplish the desired goals. Therefore, **Chapter 1** discussed the current techniques, methodologies, and tools used in ALE studies for producing improved variants. Additionally, it explores novel methods to reduce the time required for conducting ALE experiments. In addition, ALE experiments, including environmental conditions and microbial strains, must be meticulously designed with the research objective(s) in mind before ALE experimentation. Considering the ultimate objective of this research, bioplastic production from lignocellulosic hydrolysate, the strain *C. necator* H16, known for its natural ability to make bioplastic, was selected as the focal point for phenotype improvement. Furthermore, this chapter discussed the natural metabolism of *C. necator* H16, including the ability of this strain to accumulate PHB. In addition, a study was conducted on the two most common toxic compounds found in the lignocellulosic hydrolysate. BA and AA were chosen as selective pressures. Besides being toxic, both compounds can potentially serve as a carbon source for producing PHB [4, 219].

In **Chapter 2**, the ALE experiment with serial transfer was chosen to improve the tolerance of *C. necator* H16 to BA, one of the most abundant toxic compounds found in lignocellulosic

hydrolysate. Furthermore, Wang *et al.* (2014) [4] discovered that among the breakdown products of lignin, BA had the highest level of toxicity. While BA may exhibit toxicity, it may serve as a suitable carbon source for *C. necator*, converting it into PHB. In total, 12 rounds of ALE in the presence of 5mM BA (selective pressure was kept constant) were performed. The ALE experiment stopped when no significant improvement was observed. This ALE strategy successfully adapted a starting strain of *C. necator* H16 to 5 mM BA, surpassing the growth of its parent strain. An adapted variant (R12AD3) was selected to study its growth performance against WT in various concentrations of BA. The experimental results indicate that the growth of the R12AD3 variant was superior to the WT when exposed to BA. Notably, we discovered that the toxicity of BA increased with temperature. At 5 mM of BA at 37°C, *C. necator* H16 WT did not grow. On the contrary, the R12AD3 strain exhibited a maximum OD of 850 nm of 6. In addition, when cultivated under 5 mM BA at 37°C, the WT strain exhibited a noticeable dark brown colouration in the growth medium. This observation suggests the presence of toxic intermediate catechol accumulated throughout the cultivation period [4].

Whole-genome sequencing of the WT and three adapted variants identified two non-synonymous mutations, one synonymous mutation, one insertion, and two deletions in the genome. They provided insights into the genetic changes that led to the improved growth in the presence of BA. The three variants (R12AE9, R12AF9, R12AD3) had the D151A substitution in the gene locus E6A55_RS10050. It is predicted that this gene, which codes for the transcriptional regulator of the LysR family involved in benzoate catabolism, is crucial for growth in the presence of BA. Therefore, we propose that the D151A substitution modifies the interactions with the substrate, resulting in enhanced growth when BA is present. Despite not conducting the PHB production test with the acquired adapted strain, the findings of this study have the potential to enhance the utilisation of cost-effective substrate (BA) for the synthesis of valuable bioplastics. The widespread implementation of this approach would significantly contribute to a more sustainable utilisation of natural resources.

In brief, the findings presented in **Chapter 2** have successfully unlocked the enhanced BA tolerance mechanism of *C. necator* H16 via ALE. The whole-genome sequencing of both the parental strain and the adapted variants yielded a comprehensive dataset that revealed the presence of mutations within the genome. The thorough examination identified these genetic modifications and provided insight into the complex processes that underlie the observed improvement in the BA phenotype. By unravelling these mutations, we've unlocked a deeper

understanding of the genetic landscape governing BA metabolism. For instance, this study's identification of the D151A substitution at the gene locus E6A55_RS10050 represents a previously undocumented mutation in the BA tolerance mechanism. This observation is a critical indicator in unravelling the evolutionary pathway that resulted in the variants' refined phenotypic characteristics. Acquiring this knowledge not only strengthens our understanding of fundamental genetic principles but also offers substantial potential for the progression of biotechnological applications, specifically in industrial bioprocessing and metabolic engineering. For instance, Pereira *et al.* (2020) [137] increased tolerance to two aromatic acids via ALE and performed reverse engineering using the resulting mutations.

Similarly, in **Chapter 3**, the ALE experiments were performed to evolve *C. necator* H16 to grow in AA. Although AA has the potential to display harmful properties, it may be used as a viable carbon source for *C. necator*, facilitating the conversion of AA into PHB [222]. Sixteen rounds of ALE experiments were performed by applying stress conditions in the serial transfer with gradually increasing concentrations of AA (50, 60, 70, 80, and 90 mM of AA). At round 8 of ALE, the culture was grown under no-stress conditions to revive the cell. After sixteen rounds of ALE, the obtained adapted variants (AE4, BF2, BF5) showed greater AA tolerance than their parents. Interestingly, every obtained adapted variant from different rounds displayed a different growth performance in the presence of AA. For instance, BF5 and BF2 variants were isolated from round 16, exhibiting different growth in AA. Notably, BF5 showed greater growth than BF2 and AE4. We sequenced the three best variants from rounds 14 (AE4) and 16 (BF2 and BF5) to identify beneficial or key mutations of the observed adapted variants in AA. The search for genetic alterations might facilitate the identification of possibly causal genetic factors, considering the diverse phenotypic profiles of the adapted variants. Through whole genome sequencing, unique mutations were identified against the WT genome. Seven mutations resulted in alterations to the amino acids encoded at gene loci E6A55_RS13105, E6A55_RS22125, E6A55_RS27725, E6A55_RS05535, E6A55_RS05630, E6A55_RS15075, and E6A55_RS25025. Five mutations were predicted to impact growth in AA, including mutations in genes encoding TamB, acyl-CoA synthetase, RseB, RsmB, and a sensor histidine kinase.

According to its phenotypic profile, the Q25K substitution in TamB and the M265R substitution in acyl-CoA synthetase likely contribute to a greater AA tolerance in BF2 and BF5 than in AE4 and WT variants. Important for stress resistance, the translocation and assembly

module TamB can be found widely among gram-negative bacterial variants [251, 252]. Acyl-CoA synthetase is essential for intermediary metabolism as the enzyme catalyses the formation of fatty acyl-CoA from acetate for oxidation and phospholipid biosynthesis [254]. M265R in acyl-CoA synthetase in BF2 and BF5 possibly lead to better expression due to codon change or better protein solubility.

It is hypothesised that the S230R substitution in RseB in WT contributes to reduced growth on AA. This locus encodes MucB/RseB, the protein responsible for signal transduction. Bacterial organisms recognise misfolded proteins within the envelope compartment [242] to detect environmental stresses. A stop-gain mutation (G→A) in the *rsmB* gene, positively affects growth in the presence of AA. This mutation arose in three adapted variants derived from different selective pressures, indicating that it confers a fitness benefit. The loss-of-function of RsmB may be advantageous for cell growth on AA by preventing the formation of a toxic intermediate homocysteine [250].

The absence of the R147S substitution in a histidine kinase in the best AA-tolerance variant (BF5) suggests that this mutation may result in enhanced growth in the presence of AA. Nevertheless, the precise role of this gene family has to be elucidated, notwithstanding the hypotheses regarding its possession of sensor histidine kinases. It is worth mentioning that *C. necator* H16 possesses 45 histidine kinases, one of which has undergone repair in BF5 (E6A55_RS22125). The system detects an unidentified signal, phosphorylates an unidentified response regulator, and controls genes that are still unidentified. As a result, our understanding of the mechanism by which this gene may influence AA tolerance is limited.

In summary, in **Chapter 3**, our research has effectively generated AA-tolerant variants of *C. necator* H16 through ALE employing serial transfer techniques. These variants demonstrated enhanced growth rates in AA in comparison to the parental strain. Notably, they displayed remarkable tolerance to AA concentrations of up to 50 mM, surpassing the limitations observed in the parental strain. This investigation underscores the efficacy of ALE with serial transfer in isolating improved variants. A similar study with *E. coli*, on the other hand, used error-prone PCR to induce mutations in CRP, resulting in a fivefold increase in growth on acetate [209].

Previously, we showed the ALE experiments have greatly improved the tolerance of *C. necator* H16 to two of the most toxic and abundant compounds in lignocellulosic hydrolysate. Nevertheless, the ALE experiment may still proceed at a slow rate. To overcome this limitation, in **Chapter 4**, we developed a chemical-assisted ALE to accelerate traditional ALE. Chemical mutagenesis is an effective method for rapidly creating mutant libraries. Several metal ions, including Mn^{2+}, Zn^{2+}, and Co^{2+}, have been shown to have mutagenic potential in *in vitro* studies [8]. These three metal ions have not been reported to be used in *C. necator* using an *in vivo* approach, which subsequently provides a novelty work. ALE with serial transfer was used in a previous work to increase the glycerol growth in *C. necator* H16. This work has successfully produced a variant (v6v6) capable of utilising glycerol 9.5 times faster than WT after six rounds of ALE [1]. Hence, this study aims to produce variants with improved glycerol utilisation more rapidly than traditional ALE experiments.

$MnCl_2$-Assisted ALE and $ZnCl_2$-Assisted ALE produced the best cell populations at round 2. Meanwhile, $CoCl_2$-Assisted ALE produced the best cell population at round 3. Thus, the population of round 2 from $MnCl_2$-Assisted ALE and $ZnCl_2$-Assisted ALE and round 3 from $CoCl_2$-Assisted ALE were used to isolate the single colony of improved glycerol growth variant. The concentration of glycerol used in this study is significantly higher than in the previous work [1]. One best variant from each chemical-assisted ALE was selected to study their phenotype performance in different concentrations of glycerol, namely Mn-R2-B11, Co-R3-F5, and Zn-R2-G5. When cultivated in 10% glycerol, Mn-R2-B11 exhibited superior growth, surpassing the improved glycerol-utilising v6c6 [1]. Notably, the Zn-R2-G5 variant had better growth than WT and v6c6. Consistently, superior growth in 15% glycerol was demonstrated by the Mn-R2-B11 variant. Interestingly, the v6c6 variant exhibited the lowest growth compared to the other cells. The v6c6 variant only displayed a greater final OD in 5% glycerol. Meanwhile, Co-R3-F5 showed more rapid growth within 24 hours in 5% glycerol than all variants, including WT.

Chapter 4 included genome sequencing on three adapted variants (Mn-R2-B11, Zn-R2-G5, and Co-R3-F3) obtained from chemical-assisted ALE. The purpose was to analyse the genetic variations to identify potential causative mutations. Based on the results of variant calling from the sequenced genome, six mutations that might have a role in glycerol growth were found. A total of six mutations were observed, leading to alterations in the amino acid sequences of the

five proteins encoded at the gene loci E6A55_RS12840, E6A55_RS13105, E6A55_RS19830, E6A55_RS03700, and E6A55_RS18850.

The gene locus E6A55_RS12840 is predicted to be responsible for encoding glycerol kinase (GlpK). The enzymatic function of glycerol kinase is to catalyse the phosphorylation of glycerol, producing glycerol-3-phosphate participating in the metabolic pathway of glycerol. This work presents a non-synonymous mutation at GlpK (W480S; an amino acid shift from tryptophan to serine) in the Co-R3-F3 variant and the best adaptive variant, Mn-R2-B11. The W480S substitution was also identified in a prior study on *C. necator* H16 [1]. Gonzales *et al*. [1] suggested that the W480S substation enhanced glycerol utilisation via increased protein expression. A search for conserved domains showed that W480 is highly conserved in GlpK in *C. necator* H16 sequence alignments with comparable proteins from various other organisms. Compared to the WT, v6c6, and other adapted variants (Zn-R2-G5 and Co-R3-F3), the Mn-R2-B11 variant showed higher growth in 10% and 15% glycerol. The *glpK* gene of Mn-R2-B11 also exhibited the A264V substitution. The presence of this mutation was identified in proximity to the active site [222]. The co-occurrence of the two-point mutations in GlpK, namely in Mn-R2-B11, may contribute to increased growth when the glycerol concentration is 15%. Notably, a search for conserved domains revealed that A264 is highly conserved in multiple sequence alignments of GlpK from *C. necator* H16 and proteins from other organisms.

We also hypothesised that S230R and D23N substitution s might contribute to the lower growth in glycerol as these mutations were only detected in WT and Zn-R2-G5. Overall, the chemical-assisted ALE method for generating random mutations resulted in a successful mutagenesis strategy for enhancing glycerol utilisation of *C. necator* H16 strains.

In summary, we have successfully constructed an accelerated ALE approach, demonstrating its effectiveness in evolving *C. necator* H16 for increased tolerance to high glycerol concentrations. This approach possesses numerous benefits. Firstly, increasing genetic diversity drastically reduces the time required to attain a desired phenotype. Notably, we identified an improved variant in this analysis after only one cycle of ALE, demonstrating our method's efficacy. By comparison, prior research on the ALE of *E. coli* MG1655 in M9 minimal medium supplemented with 0.2% glycerol required log-phase serial transfers spanning over 800 generations to increase growth rates by more than 2-fold [84, 261].

Furthermore, our ALE workflow does not necessitate the initiation of a genetically modified strain, such as a genome-reduced strain [272]. Our approach eliminates the need for DNA-modifying agents, frequently categorized as carcinogens. Lastly, we can easily modify this approach to accommodate additional microbial strains, thereby enhancing its adaptability and practicality.

5.2 Future works

This section provides future works to get a comprehensive understanding of the findings of this study. This section also examines the prospects and potential extension of this work to the industrial sector.

The following bullet points list some potential future work that may be done:

Chapter 2. Adaptive laboratory evolution (ALE) to improve the tolerance of a bioplastic producer *Cupriavidus necator* H16 to benzoic acid found in lignocellulosic hydrolysates

- All three variants that exhibited enhanced tolerance to benzoic acid had a common mutation: substituting amino acid residue D151 with A in a transcriptional regulator belonging to the LysR family. Proteomic analysis of WT and adapted variants (R12AE9, R12AF9, R12AD3) may identify important proteins related to benzoic acid tolerance mechanisms in several pathways. For instance, proteomic analysis enables the identification and characterisation of the expression profiles of many proteins that play a role in the β-ketoadipate path.
- The transcriptome analysis may be conducted by examining the gene expression patterns in response to diverse environmental factors, such as variable concentrations of BA and temperature, during the growth of *C. necator* H16.
- Cross-tolerance and antagonistic pleiotropy phenomena were often discovered in microbial systems characterised by diverse and intricate phenotypes [273]. Therefore, it is possible to investigate cross-tolerance to other compounds found in lignocellulosic hydrolysate, such as acetic acid, sulfuric acid, ammonium sulphate, furfural, and HMF. This test has the potential to unveil if the mutation facilitates improved growth in other toxic compounds or causes a trade-off for the adapted variants.

- The quantification of PHB production will be of utmost significance in this study. For example, the synthesis of PHB in *C. necator* H16 (WT) and adapted variants (R12AE9, R12AF9, R12AD3) may be compared. This outcome may provide valuable insights into the impact of the identified mutation on PHB accumulation in adapted variants. The quantification of PHB production may be achieved by using HPLC or Nile red test, as shown by Gonzalez *et al.* in their study [1].
- The examination of benzoic acid consumption may be performed to assess the ability of the obtained adapted variants to use gluconate and benzoic acid as carbon sources simultaneously. Moreover, this research may provide significant insights into the potential of the variants to enhance PHB production from gluconate-benzoic acid medium or gluconate alone. This outcome may also be extended to the industrial sector since there is a preference for more affordable feedstock for the production of bioplastics.

Chapter 3. Adaptive laboratory evolution (ALE) to improve the tolerance of a bioplastic producer *Cupriavidus necator* H16 to ammonium acetate found in lignocellulosic hydrolysates

- To further understand the two distinct mutations in the best performance adapted variant (BF5) revealed by genome sequencing, two genes encoding TamB and Acyl-CoA synthetase could be used for an allelic replacement in *C. necator* H16 WT.
- This study hypothesised that a stop gain mutation in the RsmB gene is associated with increased growth of adaptive variants in AA. This hypothesis might be verified by performing a knockout of *rsmB* in *C. necator* H16.
- Cross-tolerance and antagonistic pleiotropy phenomena were often discovered in microbial systems characterised by diverse and complex phenotypes [273]. Therefore, it is possible to investigate cross-tolerance to other compounds found in lignocellulosic hydrolysate, such as benzoic acid, acetic acid, sulfuric acid, ammonium sulphate, furfural, and HMF. This test has the potential to unveil if the mutation facilitates improved growth in other toxic compounds or causes a trade-off for the adapted variants.
- The quantification of PHB production will be of utmost significance in this study. For example, the synthesis of PHB in *C. necator* H16 (WT) and adapted variants (AE4, BF2, BF5) may be compared. This outcome may provide valuable insights into

the impact of the identified mutation on PHB accumulation in adapted variants. The quantification of PHB production may be achieved by using HPLC or Nile Red test, as shown by Gonzalez *et al.* in their study [1].

- Ammonium acetate consumption may be examined to assess the ability of the obtained variants to use ammonium acetate and gluconate simultaneously as carbon sources. Moreover, this research may provide significant insights into the potential of the variants to enhance PHB production from gluconate-AA medium or gluconate alone. This outcome may also be extended to the industrial sector since there is a preference for cheaper feedstock for the production of bioplastics.

Chapter 4. Chemical-assisted adaptive laboratory evolution (ALE) of a bioplastic producer *Cupriavidus necator* H16

- To further understand the two distinct mutations in GlpK, the best performance-adapted variant (Mn-R2-B11) revealed by genome sequencing, two mutations (W480S and A264V) could be amplified and cloned to enable their constitutive expression from the variants to *C. necator* H16 (WT).
- The quantification of PHB production will be of utmost significance in this study. For example, the synthesis of PHB in *C. necator* H16 (WT) and adapted variants (Mn-R2-B11, Zn-R2-G5, Co-R3-F3) may be compared. This outcome may provide valuable insights into the impact of the identified mutation on PHB accumulation in adapted variants. The quantification of PHB production may be achieved by using HPLC or Nile Red test, as shown by Gonzalez *et al.* in their study [1].
- Glycerol consumption may be examined to assess the ability of the obtained variants to use high glycerol concentrations. This outcome may also be extended to the industrial sector since there is a preference for cheaper feedstock for the production of bioplastics.

References

1. Gonzalez-Villanueva, M., et al., *Adaptive Laboratory Evolution of Cupriavidus necator H16 for Carbon Co-Utilization with Glycerol.* Int J Mol Sci, 2019. **20**(22).
2. Wickham-Smith, C., N. Malys, and K. Winzer, *Improving carbon monoxide tolerance of Cupriavidus necator H16 through adaptive laboratory evolution.* Frontiers in Bioengineering and Biotechnology, 2023. **11**.
3. Dolpatcha, S., et al., *Adaptive laboratory evolution under acetic acid stress enhances the multistress tolerance and ethanol production efficiency of Pichia kudriavzevii from lignocellulosic biomass.* Scientific Reports, 2023. **13**(1): p. 21000.
4. Wang, W., et al., *Connecting lignin-degradation pathway with pre-treatment inhibitor sensitivity of Cupriavidus necator.* Frontiers in microbiology, 2014. **5**: p. 247-247.
5. Pinhal, S., et al., *Acetate Metabolism and the Inhibition of Bacterial Growth by Acetate.* J Bacteriol, 2019. **201**(13).
6. Lim, D.K.Y., et al., *Isolation of High-Lipid Tetraselmis suecica Strains Following Repeated UV-C Mutagenesis, FACS, and High-Throughput Growth Selection.* BioEnergy Research, 2015. **8**(2): p. 750-759.
7. Mobini-Dehkordi, M., et al., *Isolation of a novel mutant strain of Saccharomyces cerevisiae by an ethyl methane sulfonate-induced mutagenesis approach as a high producer of bioethanol.* Journal of Bioscience and Bioengineering, 2008. **105**(4): p. 403-408.
8. Sirover, M.A., D.K. Dube, and L.A. Loeb, *On the fidelity of DNA replication. Metal activation of Escherichia coli DNA polymerase I.* J Biol Chem, 1979. **254**(1): p. 107-11.
9. Clomburg, J.M. and R. Gonzalez, *Biofuel production in Escherichia coli: the role of metabolic engineering and synthetic biology.* Applied microbiology and biotechnology, 2010. **86**: p. 419-434.
10. Falch, E.A., *Industrial enzymes—developments in production and application.* Biotechnology advances, 1991. **9**(4): p. 643-658.
11. Ferrer-Miralles, N., et al., *Microbial factories for recombinant pharmaceuticals.* Microbial cell factories, 2009. **8**: p. 1-8.
12. Dragosits, M. and D. Mattanovich, *Adaptive laboratory evolution -- principles and applications for biotechnology.* Microb Cell Fact, 2013. **12**: p. 64.
13. Kim, T.Y., et al., *Strategies for systems-level metabolic engineering.* Biotechnology Journal: Healthcare Nutrition Technology, 2008. **3**(5): p. 612-623.
14. Sandberg, T.E., et al., *The emergence of adaptive laboratory evolution as an efficient tool for biological discovery and industrial biotechnology.* Metabolic Engineering, 2019. **56**: p. 1-16.
15. LaCroix, R.A., et al., *Use of adaptive laboratory evolution to discover key mutations enabling rapid growth of Escherichia coli K-12 MG1655 on glucose minimal medium.* Applied and environmental microbiology, 2015. **81**(1): p. 17-30.
16. Pfeifer, E., et al., *Adaptive laboratory evolution of Corynebacterium glutamicum towards higher growth rates on glucose minimal medium.* Scientific Reports, 2017. **7**(1): p. 16780.
17. Fletcher, E., et al., *Evolutionary engineering reveals divergent paths when yeast is adapted to different acidic environments.* Metabolic Engineering, 2017. **39**: p. 19-28.

18. Rajaraman, E., et al., *Transcriptional analysis and adaptive evolution of Escherichia coli strains growing on acetate.* Applied Microbiology and Biotechnology, 2016. **100**(17): p. 7777-7785.
19. Charusanti, P., et al., *Exploiting Adaptive Laboratory Evolution of Streptomyces clavuligerus for Antibiotic Discovery and Overproduction.* PLOS ONE, 2012. **7**(3): p. e33727.
20. Fu, W., et al., *Enhancement of carotenoid biosynthesis in the green microalga Dunaliella salina with light-emitting diodes and adaptive laboratory evolution.* Applied Microbiology and Biotechnology, 2013. **97**(6): p. 2395-2403.
21. Lee, S.H., et al., *Adaptive engineering of a hyperthermophilic archaeon on CO and discovering the underlying mechanism by multi-omics analysis.* Scientific Reports, 2016. **6**(1): p. 22896.
22. Lauer, S., et al., *Single-cell copy number variant detection reveals the dynamics and diversity of adaptation.* PLOS Biology, 2018. **16**(12): p. e3000069.
23. Kao, K.C. and G. Sherlock, *Molecular characterization of clonal interference during adaptive evolution in asexual populations of Saccharomyces cerevisiae.* Nature Genetics, 2008. **40**(12): p. 1499-1504.
24. Maddamsetti, R., R.E. Lenski, and J.E. Barrick, *Adaptation, Clonal Interference, and Frequency-Dependent Interactions in a Long-Term Evolution Experiment with <em>Escherichia coli</em&gt.* Genetics, 2015. **200**(2): p. 619.
25. Mavrommati, M., et al., *Adaptive laboratory evolution principles and applications in industrial biotechnology.* Biotechnology Advances, 2022. **54**: p. 107795.
26. Sandberg, T.E., et al., *The emergence of adaptive laboratory evolution as an efficient tool for biological discovery and industrial biotechnology.* Metab Eng, 2019. **56**: p. 1-16.
27. Bennett, A.F. and B.S. Hughes, *Microbial experimental evolution.* American Journal of Physiology-Regulatory, Integrative and Comparative Physiology, 2009. **297**(1): p. R17-R25.
28. Hirasawa, T. and T. Maeda *Adaptive Laboratory Evolution of Microorganisms: Methodology and Application for Bioproduction*. Microorganisms, 2023. **11**, DOI: 10.3390/microorganisms11010092.
29. Gresham, D. and M.J. Dunham, *The enduring utility of continuous culturing in experimental evolution.* Genomics, 2014. **104**(6 Pt A): p. 399-405.
30. Wallace-Salinas, V. and M.F. Gorwa-Grauslund, *Adaptive evolution of an industrial strain of Saccharomyces cerevisiae for combined tolerance to inhibitors and temperature.* Biotechnology for Biofuels, 2013. **6**(1): p. 151.
31. Winkler, J.D., et al., *Evolved osmotolerant Escherichia coli mutants frequently exhibit defective N-acetylglucosamine catabolism and point mutations in cell shape-regulating protein MreB.* Applied and environmental microbiology, 2014. **80**(12): p. 3729-3740.
32. Harris, D.R., et al., *Directed Evolution of Ionizing Radiation Resistance in <em>Escherichia coli</em&gt.* Journal of Bacteriology, 2009. **191**(16): p. 5240.
33. Goldman, R.P. and M. Travisano, *EXPERIMENTAL EVOLUTION OF ULTRAVIOLET RADIATION RESISTANCE IN ESCHERICHIA COLI.* Evolution, 2011. **65**(12): p. 3486-3498.
34. Hansen, A.S.L., et al., *Systems biology solutions for biochemical production challenges.* Current Opinion in Biotechnology, 2017. **45**: p. 85-91.
35. Hindré, T., et al., *New insights into bacterial adaptation through in vivo and in silico experimental evolution.* Nature Reviews Microbiology, 2012. **10**(5): p. 352-365.

36. Conrad, T.M., N.E. Lewis, and B.Ø. Palsson, *Microbial laboratory evolution in the era of genome-scale science.* Molecular Systems Biology, 2011. **7**(1): p. 509.
37. Lenski, R.E., et al., *Long-Term Experimental Evolution in Escherichia coli. I. Adaptation and Divergence During 2,000 Generations.* The American Naturalist, 1991. **138**(6): p. 1315-1341.
38. Barrick, J.E. and R.E. Lenski, *Genome dynamics during experimental evolution.* Nature Reviews Genetics, 2013. **14**(12): p. 827-839.
39. Fernandes, T., et al. *Contributions of Adaptive Laboratory Evolution towards the Enhancement of the Biotechnological Potential of Non-Conventional Yeast Species*. Journal of Fungi, 2023. **9**, DOI: 10.3390/jof9020186.
40. Westphal, L.L., et al., *Adaptation of Escherichia coli to long-term batch culture in various rich media.* Research in Microbiology, 2018. **169**(3): p. 145-156.
41. Zambrano, M.M., et al., *Microbial Competition: Escherichia coli Mutants That Take Over Stationary Phase Cultures.* Science, 1993. **259**(5102): p. 1757-1760.
42. Flynn, K.M., et al., *The environment affects epistatic interactions to alter the topology of an empirical fitness landscape.* PLoS genetics, 2013. **9**(4): p. e1003426-e1003426.
43. Gresham, D. and J. Hong, *The functional basis of adaptive evolution in chemostats.* FEMS Microbiology Reviews, 2014. **39**(1): p. 2-16.
44. Lorz, A., B. Perthame, and C. Taing, *Dirac concentrations in a chemostat model of adaptive evolution.* Chinese Annals of Mathematics, Series B, 2017. **38**(2): p. 513-538.
45. Jeong, H., S.J. Lee, and P. Kim, *Procedure for Adaptive Laboratory Evolution of Microorganisms Using a Chemostat.* Journal of Visualized Experiments, 2016. **2016**(115).
46. Lee, L.J., *The response of chemostat-cultured Escherichia coli to zinc stress*. 2006, 2006.
47. Ferenci, T., *Bacterial Physiology, Regulation and Mutational Adaptation in a Chemostat Environment*, in *Advances in Microbial Physiology*, R.K. Poole, Editor. 2007, Academic Press. p. 169-315.
48. Novick, A. and L. Szilard, *Description of the Chemostat.* Science, 1950. **112**(2920): p. 715.
49. Rao, V.S.H. and P.R.S. Rao, *Global stability in chemostat models involving time delays and wall growth.* Nonlinear Analysis: Real World Applications, 2004. **5**(1): p. 141-158.
50. Dunham, M.J., *Chapter 19 - Experimental Evolution in Yeast: A Practical Guide*, in *Methods in Enzymology*. 2010, Academic Press. p. 487-507.
51. Blaby, I.K., et al., *Experimental evolution of a facultative thermophile from a mesophilic ancestor.* Applied and environmental microbiology, 2012. **78**(1): p. 144-155.
52. Rudolph, B., et al., *Evolution of Escherichia coli for growth at high temperatures.* Journal of Biological Chemistry, 2010. **285**(25): p. 19029-19034.
53. Lenski, R.E. and M. Travisano, *Dynamics of adaptation and diversification: a 10,000-generation experiment with bacterial populations.* Proceedings of the National Academy of Sciences of the United States of America, 1994. **91**(15): p. 6808-6814.
54. Hong, K.-K., et al., *Unravelling evolutionary strategies of yeast for improving galactose utilization through integrated systems level analysis.* Proceedings of the National Academy of Sciences, 2011. **108**(29): p. 12179-12184.
55. Jiang, L.-Y., et al., *Metabolic evolution of Corynebacterium glutamicum for increased production of L-ornithine.* BMC Biotechnology, 2013. **13**(1): p. 47.

56. Lu, L., et al., *Combining metabolic engineering and adaptive evolution to enhance the production of dihydroxyacetone from glycerol by Gluconobacter oxydans in a low-cost way.* Bioresource Technology, 2012. **117**: p. 317-324.
57. Kildegaard, K.R., et al., *Evolution reveals a glutathione-dependent mechanism of 3-hydroxypropionic acid tolerance.* Metabolic Engineering, 2014. **26**: p. 57-66.
58. Dhar, R., et al., *Adaptation of Saccharomyces cerevisiae to saline stress through laboratory evolution.* Journal of Evolutionary Biology, 2011. **24**(5): p. 1135-1153.
59. Antonovsky, N., et al., *Sugar Synthesis from CO2 in Escherichia coli.* Cell, 2016. **166**(1): p. 115-125.
60. Basso, T.O., et al., *Engineering topology and kinetics of sucrose metabolism in Saccharomyces cerevisiae for improved ethanol yield.* Metabolic Engineering, 2011. **13**(6): p. 694-703.
61. Koppram, R., E. Albers, and L. Olsson, *Evolutionary engineering strategies to enhance tolerance of xylose utilizing recombinant yeast to inhibitors derived from spruce biomass.* Biotechnol Biofuels, 2012. **5**(1): p. 32.
62. Voordeckers, K., et al., *Adaptation to High Ethanol Reveals Complex Evolutionary Pathways.* PLOS Genetics, 2015. **11**(11): p. e1005635.
63. Bromig, L. and D. Weuster-Botz *Accelerated Adaptive Laboratory Evolution by Automated Repeated Batch Processes in Parallelized Bioreactors*. Microorganisms, 2023. **11**, DOI: 10.3390/microorganisms11020275.
64. Toprak, E., et al., *Building a morbidostat: an automated continuous-culture device for studying bacterial drug resistance under dynamically sustained drug inhibition.* Nature Protocols, 2013. **8**(3): p. 555-567.
65. LaCroix, R.A., B.O. Palsson, and A.M. Feist, *A Model for Designing Adaptive Laboratory Evolution Experiments.* Applied and Environmental Microbiology, 2017. **83**(8): p. e03115-16.
66. Siepert, E.-M., et al., *Short-chain fluorescent tryptophan tags for on-line detection of functional recombinant proteins.* BMC Biotechnology, 2012. **12**(1): p. 65.
67. Back, A., et al., *High-throughput fermentation screening for the yeast Yarrowia lipolytica with real-time monitoring of biomass and lipid production.* Microbial Cell Factories, 2016. **15**(1): p. 147.
68. Steel, H., et al., *Chi.Bio: An open-source automated experimental platform for biological science research.* bioRxiv, 2019: p. 796516.
69. Au - Heins, Z.J., et al., *Designing Automated, High-throughput, Continuous Cell Growth Experiments Using eVOLVER.* JoVE, 2019(147): p. e59652.
70. Leder, E.H., et al., *The evolution and adaptive potential of transcriptional variation in sticklebacks--signatures of selection and widespread heritability.* Molecular biology and evolution, 2015. **32**(3): p. 674-689.
71. Wong, B.G., et al., *Precise, automated control of conditions for high-throughput growth of yeast and bacteria with eVOLVER.* Nature Biotechnology, 2018. **36**(7): p. 614-623.
72. Horinouchi, T., et al., *Development of an Automated Culture System for Laboratory Evolution.* SLAS Technology, 2014. **19**(5): p. 478-482.
73. Horinouchi, T., et al., *Development of an Automated Culture System for Laboratory Evolution.* Journal of Laboratory Automation, 2014. **19**(5): p. 478-482.
74. Huber, R., et al., *Robo-Lector - a novel platform for automated high-throughput cultivations in microtiter plates with high information content.* Microbial cell factories, 2009. **8**: p. 42-42.

75. Mühlmann, M., et al., *Cellulolytic RoboLector – towards an automated high-throughput screening platform for recombinant cellulase expression.* Journal of Biological Engineering, 2017. **11**(1): p. 1.
76. Liu, P., et al., *Design and Use of a Low Cost, Automated Morbidostat for Adaptive Evolution of Bacteria Under Antibiotic Drug Selection.* Journal of Visualized Experiments, 2016. **2016**.
77. Jian, X., et al., *Microbial microdroplet culture system (MMC): an integrated platform for automated, high–throughput microbial cultivation and adaptive evolution.* bioRxiv, 2019: p. 2019.12.19.883561.
78. Balagaddé, F.K., et al., *Long-Term Monitoring of Bacteria Undergoing Programmed Population Control in a Microchemostat.* Science, 2005. **309**(5731): p. 137.
79. Miller, A.W., et al., *Design and use of multiplexed chemostat arrays.* Journal of visualized experiments : JoVE, 2013(72): p. e50262-e50262.
80. Kensy, F. and J. Hemmerich, *Automation of Microbioreactors - Operating 48 Parallel Fed-Batch Fermentations at Microscale.* BPI, 2013. **11**: p. 68-76.
81. Unthan, S., et al., *Bioprocess automation on a Mini Pilot Plant enables fast quantitative microbial phenotyping.* Microbial Cell Factories, 2015. **14**(1): p. 32.
82. de Crécy, E., et al., *Development of a novel continuous culture device for experimental evolution of bacterial populations.* Applied Microbiology and Biotechnology, 2007. **77**(2): p. 489-496.
83. de Crecy, E., et al., *Directed evolution of a filamentous fungus for thermotolerance.* BMC Biotechnology, 2009. **9**(1): p. 74.
84. Sitompul, S.N., et al., *Fast-track adaptive laboratory evolution of Cupriavidus necator H16 with divalent metal cations.* bioRxiv, 2023: p. 2023.10.24.563758.
85. Hu, M.-R., et al., *Molecular evolution of Fome lignosus laccase by ethyl methane sulfonate-based random mutagenesis in vitro.* Biomolecular Engineering, 2007. **24**(6): p. 619-624.
86. Echols, H., C. Lu, and P.M. Burgers, *Mutator strains of Escherichia coli, mutD and dnaQ, with defective exonucleolytic editing by DNA polymerase III holoenzyme.* Proceedings of the National Academy of Sciences, 1983. **80**(8): p. 2189-2192.
87. Eom, G.-e., H. Lee, and S. Kim, *Development of a genome-targeting mutator for the adaptive evolution of microbial cells.* Nucleic Acids Research, 2022. **50**(7): p. e38-e38.
88. Zheng, Y., et al., *Genetic Diversity for Accelerating Microbial Adaptive Laboratory Evolution.* ACS Synthetic Biology, 2021. **10**(7): p. 1574-1586.
89. Wang, H.H., et al., *Programming cells by multiplex genome engineering and accelerated evolution.* Nature, 2009. **460**(7257): p. 894-898.
90. Garst, A.D., et al., *Genome-wide mapping of mutations at single-nucleotide resolution for protein, metabolic and genome engineering.* Nature Biotechnology, 2017. **35**(1): p. 48-55.
91. Lotfy, W.A., K.M. Ghanem, and E.R. El-Helow, *Citric acid production by a novel Aspergillus niger isolate: I. Mutagenesis and cost reduction studies.* Bioresource Technology, 2007. **98**(18): p. 3464-3469.
92. Hida, H., T. Yamada, and Y. Yamada, *Genome shuffling of Streptomyces sp. U121 for improved production of hydroxycitric acid.* Applied Microbiology and Biotechnology, 2007. **73**(6): p. 1387-1393.
93. Luan, G., et al., *Genome replication engineering assisted continuous evolution (GREACE) to improve microbial tolerance for biofuels production.* Biotechnology for Biofuels, 2013. **6**(1): p. 137.

94. Overbeck Tom, J., et al., *Transient MutS-Based Hypermutation System for Adaptive Evolution of Lactobacillus casei to Low pH.* Applied and Environmental Microbiology, 2017. **83**(20): p. e01120-17.
95. Asakura, Y., H. Kojima, and I. Kobayashi, *Evolutionary genome engineering using a restriction–modification system.* Nucleic Acids Research, 2011. **39**(20): p. 9034-9046.
96. Zheng, Y., et al., *Improving Furfural Tolerance of Escherichia coli by Integrating Adaptive Laboratory Evolution with CRISPR-Enabled Trackable Genome Engineering (CREATE).* ACS Sustainable Chemistry & Engineering, 2022. **10**(7): p. 2318-2330.
97. Zhou, S. and H.S. Alper, *Strategies for directed and adapted evolution as part of microbial strain engineering.* Journal of Chemical Technology & Biotechnology, 2019. **94**(2): p. 366-376.
98. Wang, G., et al., *Recent progress in adaptive laboratory evolution of industrial microorganisms.* Journal of Industrial Microbiology and Biotechnology, 2023. **50**(1): p. kuac023.
99. Snow, E.T., R.S. Foote, and S. Mitra, *Base-pairing properties of O6-methylguanine in template DNA during in vitro DNA replication.* J Biol Chem, 1984. **259**(13): p. 8095-100.
100. Amini, M., *Ethyl Methanesulfonate*, in *Encyclopedia of Toxicology (Third Edition)*, P. Wexler, Editor. 2014, Academic Press: Oxford. p. 522-524.
101. Nadeem, M., J. Qazi, and S. Baig, *Enhanced Production of Alkaline Protease by a Mutant of Bacillus licheniformis N-2 for Dehairing.* Brazilian Archives of Biology and Technology, 2010. **53**: p. 1015-1025.
102. Ribeiro, O., et al., *Random and direct mutagenesis to enhance protein secretion in Ashbya gossypii.* Bioengineered, 2013. **4**(5): p. 322-31.
103. Perera, L., et al., *Requirement for transient metal ions revealed through computational analysis for DNA polymerase going in reverse.* Proceedings of the National Academy of Sciences, 2015. **112**(38): p. E5228-E5236.
104. Harris, V.H., et al., *The Effect of Tautomeric Constant on the Specificity of Nucleotide Incorporation during DNA Replication: Support for the Rare Tautomer Hypothesis of Substitution Mutagenesis.* Journal of Molecular Biology, 2003. **326**(5): p. 1389-1401.
105. Vashishtha, A.K., J. Wang, and W.H. Konigsberg, *Different Divalent Cations Alter the Kinetics and Fidelity of DNA Polymerases.* J Biol Chem, 2016. **291**(40): p. 20869-20875.
106. Vaisman, A., et al., *Fidelity of Dpo4: effect of metal ions, nucleotide selection and pyrophosphorolysis.* Embo j, 2005. **24**(17): p. 2957-67.
107. Villani, G., et al., *Effect of manganese on in vitro replication of damaged DNA catalyzed by the herpes simplex virus type-1 DNA polymerase.* Nucleic Acids Research, 2002. **30**(15): p. 3323-3332.
108. Miyaki, M., et al., *Effect of metal cations on misincorporation by E. coli DNA polymerases.* Biochemical and Biophysical Research Communications, 1977. **77**(3): p. 854-860.
109. Goodman, M.F., et al., *On the enzymatic basis for mutagenesis by manganese.* J Biol Chem, 1983. **258**(6): p. 3469-75.
110. Beckman, R.A., A.S. Mildvan, and L.A. Loeb, *On the fidelity of DNA replication: manganese mutagenesis in vitro.* Biochemistry, 1985. **24**(21): p. 5810-7.
111. Chin, Y.E., et al., *The Effect of Divalent Nickel (Ni2+) on in Vitro DNA Replication by DNA Polymerase α1.* Cancer Research, 1994. **54**(9): p. 2337-2341.

112. Khattab, A.A. and W.A. Bazaraa, *Screening, mutagenesis and protoplast fusion of Aspergillus niger for the enhancement of extracellular glucose oxidase production.* Journal of Industrial Microbiology and Biotechnology, 2005. **32**(7): p. 289-294.
113. Hapala, I., et al., *Two mutants selectively resistant to polyenes reveal distinct mechanisms of antifungal activity by nystatin and amphotericin B.* Biochemical Society Transactions, 2005. **33**(5): p. 1206-1209.
114. Arshad, R., S. Farooq, and S.S. Ali, *Effect of mutations induced by N-methyl-N'-nitro-N-nitrosoguanidine on expression of penicillin G acylase and β-lactamase in wild-type Escherichia coli strains.* Annals of Microbiology, 2010. **60**(4): p. 645-652.
115. Gao, H., et al., *Assessing the Potential of an Induced-Mutation Strategy for Avermectin Overproducers.* Applied and Environmental Microbiology, 2010. **76**(13): p. 4583-4586.
116. Nestmann, E.R., *Mutagenesis by nitrosoguanidine, ethyl methanesulfonate, and mutator gene mutH in continuous cultures of Escherichia coli.* Mutat Res, 1975. **28**(3): p. 323-30.
117. Ohnishi, J., et al., *Characterization of mutations induced by N-methyl-N'-nitro-N-nitrosoguanidine in an industrial Corynebacterium glutamicum strain.* Mutation Research/Genetic Toxicology and Environmental Mutagenesis, 2008. **649**(1): p. 239-244.
118. Adelberg, E.A., M. Mandel, and G.C. Ching Chen, *Optimal conditions for mutagenesis by N-methyl-N'-nitro-N-nitrosoguanidine in escherichia coli K12.* Biochemical and Biophysical Research Communications, 1965. **18**(5): p. 788-795.
119. Morita, H. and T. Iwata, *Penicillin Acylase Activity in Mutants of Escherichia coli Highly Sensitive to Penicillin G.* Journal of fermentation technology, 1984. **62**(2): p. 217-220.
120. Silverman, J.A., et al., *Resistance Studies with Daptomycin.* Antimicrobial Agents and Chemotherapy, 2001. **45**(6): p. 1799-1802.
121. Matthews, P.R., K.C. Reed, and P.R. Stewart, *The Cloning of Chromosomal DNA Associated with Methicillin and Other Resistances in Staphylococcus aureus.* Microbiology, 1987. **133**(7): p. 1919-1929.
122. Dornbusch, K., H.O. Hallander, and F. Löfquist, *Extrachromosomal Control of Methicillin Resistance and Toxin Production in Staphylococcus aureus.* Journal of Bacteriology, 1969. **98**(2): p. 351-358.
123. Barnes, I.J., A. Bondi, and A.G. Moat, *Biochemical Characterization of Lysine Auxotrophs of Staphylococcus aureus.* Journal of Bacteriology, 1969. **99**(1): p. 169-174.
124. Maeda, T., et al., *Mutational property of newly identified mutagen l-glutamic acid γ-hydrazide in Escherichia coli.* Mutation Research/Fundamental and Molecular Mechanisms of Mutagenesis, 2021. **823**: p. 111759.
125. Drake, J.W., *A constant rate of spontaneous mutation in DNA-based microbes.* Proceedings of the National Academy of Sciences, 1991. **88**(16): p. 7160-7164.
126. Large, C.R.L., et al., *Genomic stability and adaptation of beer brewing yeasts during serial repitching in the brewery.* bioRxiv, 2020: p. 2020.06.26.166157.
127. Sarkar, P., et al., *Adaptive laboratory evolution induced novel mutations in Zymomonas mobilis ATCC ZW658: a potential platform for co-utilization of glucose and xylose.* Journal of Industrial Microbiology and Biotechnology, 2020. **47**(3): p. 329-341.
128. Kim, K., et al., *Adaptive laboratory evolution of Escherichia coli W enhances gamma-aminobutyric acid production using glycerol as the carbon source.* Metabolic Engineering, 2022. **69**: p. 59-72.

129. Krebs, H.A., et al., *Studies on the mechanism of the antifungal action of benzoate.* Biochem J, 1983. **214**(3): p. 657-63.
130. Chen, S.-F., et al., *High-performance liquid chromatography method for simultaneous determination of aliphatic acid, aromatic acid and neutral degradation products in biomass pretreatment hydrolysates.* Journal of Chromatography A, 2006. **1104**(1): p. 54-61.
131. Caspeta, L., et al., *Biofuels. Altered sterol composition renders yeast thermotolerant.* Science, 2014. **346**(6205): p. 75-8.
132. Kusumawardhani, H., et al., *Adaptive Laboratory Evolution Restores Solvent Tolerance in Plasmid-Cured Pseudomonas putida S12: a Molecular Analysis.* Appl Environ Microbiol, 2021. **87**(9).
133. Jönsson, L.J., B. Alriksson, and N.-O. Nilvebrant, *Bioconversion of lignocellulose: inhibitors and detoxification.* Biotechnology for Biofuels, 2013. **6**(1): p. 16.
134. Parawira, W. and M. Tekere, *Biotechnological strategies to overcome inhibitors in lignocellulose hydrolysates for ethanol production: review.* Critical Reviews in Biotechnology, 2011. **31**(1): p. 20-31.
135. Menegon, Y.A., J. Gross, and A.P. Jacobus, *How adaptive laboratory evolution can boost yeast tolerance to lignocellulosic hydrolyses.* Curr Genet, 2022. **68**(3-4): p. 319-342.
136. Royce, L.A., et al., *Evolution for exogenous octanoic acid tolerance improves carboxylic acid production and membrane integrity.* Metabolic Engineering, 2015. **29**: p. 180-188.
137. Pereira, R., et al., *Adaptive laboratory evolution of tolerance to dicarboxylic acids in Saccharomyces cerevisiae.* Metab Eng, 2019. **56**: p. 130-141.
138. Lee, D.-H. and Ø. Palsson Bernhard, *Adaptive Evolution of Escherichia coli K-12 MG1655 during Growth on a Nonnative Carbon Source, l-1,2-Propanediol.* Applied and Environmental Microbiology, 2010. **76**(13): p. 4158-4168.
139. Mahr, R., et al., *Biosensor-driven adaptive laboratory evolution of l-valine production in Corynebacterium glutamicum.* Metabolic Engineering, 2015. **32**: p. 184-194.
140. Smith, K.M. and J.C. Liao, *An evolutionary strategy for isobutanol production strain development in Escherichia coli.* Metab Eng, 2011. **13**(6): p. 674-81.
141. Yu, S., et al., *Enhancement of lipid production in low-starch mutants Chlamydomonas reinhardtii by adaptive laboratory evolution.* Bioresour Technol, 2013. **147**: p. 499-507.
142. Reyes, L.H., J.M. Gomez, and K.C. Kao, *Improving carotenoids production in yeast via adaptive laboratory evolution.* Metab Eng, 2014. **21**: p. 26-33.
143. Tuyishime, P., et al., *Engineering Corynebacterium glutamicum for methanol-dependent growth and glutamate production.* Metabolic Engineering, 2018. **49**: p. 220-231.
144. Wang, X., et al., *GREACE-assisted adaptive laboratory evolution in endpoint fermentation broth enhances lysine production by Escherichia coli.* Microbial Cell Factories, 2019. **18**(1): p. 106.
145. Fong, S.S., et al., *In silico design and adaptive evolution of Escherichia coli for production of lactic acid.* Biotechnology and Bioengineering, 2005. **91**(5): p. 643-648.
146. Jugder, B.-E., et al., *Construction and use of a Cupriavidus necator H16 soluble hydrogenase promoter (PSH) fusion to gfp (green fluorescent protein).* PeerJ, 2016. **4**: p. e2269-e2269.

147. Volodina, E., M. Raberg, and A. Steinbüchel, *Engineering the heterotrophic carbon sources utilization range of Ralstonia eutropha H16 for applications in biotechnology.* Critical Reviews in Biotechnology, 2016. **36**(6): p. 978-991.
148. Cramm, R., *Genomic view of energy metabolism in Ralstonia eutropha H16.* J Mol Microbiol Biotechnol, 2009. **16**(1-2): p. 38-52.
149. Pohlmann, A., et al., *Genome sequence of the bioplastic-producing "Knallgas" bacterium Ralstonia eutropha H16.* Nature Biotechnology, 2006. **24**(10): p. 1257-1262.
150. Wong, T.S. and H. Omar Ali, *Carbon Dioxide Capture and Utilization using Biological Systems: Opportunities and Challenges.* Journal of Bioprocessing & Biotechniques, 2014. **04**.
151. Pohlmann, A., et al., *Genome sequence of the bioplastic-producing "Knallgas" bacterium Ralstonia eutropha H16.* Nat Biotechnol, 2006. **24**(10): p. 1257-62.
152. Bowien, B. and B. Kusian, *Genetics and control of CO2 assimilation in the chemoautotroph Ralstonia eutropha.* Archives of Microbiology, 2002. **178**(2): p. 85-93.
153. Krieg, T., et al., *CO2 to Terpenes: Autotrophic and Electroautotrophic alpha-Humulene Production with Cupriavidus necator.* Angew Chem Int Ed Engl, 2018. **57**(7): p. 1879-1882.
154. Chae, T.U., et al., *Metabolic engineering for the production of dicarboxylic acids and diamines.* Metab Eng, 2019.
155. Pérez-Pantoja, D., et al., *Metabolic reconstruction of aromatic compounds degradation from the genome of the amazing pollutant-degrading bacterium Cupriavidus necator JMP134.* FEMS Microbiol Rev, 2008. **32**(5): p. 736-94.
156. Humphreys, C.M. and N.P. Minton, *Advances in metabolic engineering in the microbial production of fuels and chemicals from C1 gas.* Curr Opin Biotechnol, 2018. **50**: p. 174-181.
157. Hitoshi, M., et al., *Polyhydroxyalkanoate (PHA) Production from Carbon Dioxide by Recombinant Cyanobacteria.* 2013.
158. Sudesh, K., H. Abe, and Y. Doi, *Synthesis, structure and properties of polyhydroxyalkanoates: biological polyesters.* Progress in Polymer Science, 2000. **25**(10): p. 1503-1555.
159. Tomizawa, S., et al., *Understanding the Limitations in the Biosynthesis of Polyhydroxyalkanoate (PHA) from Lignin Derivatives.* ACS Sustainable Chemistry & Engineering, 2014. **2**(5): p. 1106-1113.
160. Kim, H.-Y. and H.-D. Shin, *Isolation of Glucose Utilizing Mutant of Alcaligenes eutrophus, its Substrate Selectivity, Accumulation of Poly b -hydroxybutyrate.* J. Microbiol., 1995. **33**.
161. Calvey, C.H., et al., *Improving growth of Cupriavidus necator H16 on formate using adaptive laboratory evolution-informed engineering.* Metabolic Engineering, 2023. **75**: p. 78-90.
162. Schwartz, E., et al., *Complete nucleotide sequence of pHG1: a Ralstonia eutropha H16 megaplasmid encoding key enzymes of H(2)-based ithoautotrophy and anaerobiosis.* J Mol Biol, 2003. **332**(2): p. 369-83.
163. Reshmy, R., et al., *Bioplastic production from renewable lignocellulosic feedstocks: a review.* Reviews in Environmental Science and Bio/Technology, 2021. **20**(1): p. 167-187.
164. Yang, Y., et al., *Progress and perspective on lignocellulosic hydrolysate inhibitor tolerance improvement in Zymomonas mobilis.* Bioresources and Bioprocessing, 2018. **5**(1): p. 6.

165. Mussatto, S.I. and J.A.C. Teixeira. *Lignocellulose as raw material in fermentation processes*. 2010.
166. Olsson, L. and B. Hahn-Hägerdal, *Fermentation of lignocellulosic hydrolysates for ethanol production.* Enzyme and Microbial Technology, 1996. **18**(5): p. 312-331.
167. Marriott, P.E., L.D. Gómez, and S.J. McQueen-Mason, *Unlocking the potential of lignocellulosic biomass through plant science.* New Phytologist, 2016. **209**(4): p. 1366-1381.
168. Zha, Y., et al., *Identifying inhibitory compounds in lignocellulosic biomass hydrolysates using an exometabolomics approach.* BMC Biotechnology, 2014. **14**(1): p. 22.
169. Chen, R., et al., *Hydrolysates of lignocellulosic materials for biohydrogen production.* BMB reports, 2013. **46**(5): p. 244-251.
170. Lee, S.E., Q.X. Li, and J. Yu, *Diverse protein regulations on PHA formation in Ralstonia eutropha on short chain organic acids.* Int J Biol Sci, 2009. **5**(3): p. 215-25.
171. Jönsson, L.J., B. Alriksson, and N.-O. Nilvebrant, *Bioconversion of lignocellulose: inhibitors and detoxification.* Biotechnology for biofuels, 2013. **6**(1): p. 16-16.
172. Jung, Y.H. and K.H. Kim, *Chapter 3 - Acidic Pretreatment*, in *Pretreatment of Biomass*, A. Pandey, et al., Editors. 2015, Elsevier: Amsterdam. p. 27-50.
173. Cesário, M.T.F. and M.C.M.D. de Almeida, *Lignocellulosic Hydrolysates for the Production of Polyhydroxyalkanoates*, in *Microorganisms in Biorefineries*, B. Kamm, Editor. 2015, Springer Berlin Heidelberg: Berlin, Heidelberg. p. 79-104.
174. Palmqvist, E. and B. Hahn-Hägerdal, *Fermentation of lignocellulosic hydrolysates. II: inhibitors and mechanisms of inhibition.* Bioresource Technology, 2000. **74**(1): p. 25-33.
175. Pan, W., C.T. Nomura, and J.P. Nakas, *Estimation of inhibitory effects of hemicellulosic wood hydrolysate inhibitors on PHA production by Burkholderia cepacia ATCC 17759 using response surface methodology.* Bioresource Technology, 2012. **125**: p. 275-282.
176. Jönsson, L.J., et al., *Detoxification of wood hydrolysates with laccase and peroxidase from the white-rot fungus Trametes versicolor.* Applied Microbiology and Biotechnology, 1998. **49**(6): p. 691-697.
177. Palmqvist, E., et al., *Main and interaction effects of acetic acid, furfural, and p-hydroxybenzoic acid on growth and ethanol productivity of yeasts.* Biotechnology and Bioengineering, 1999. **63**(1): p. 46-55.
178. Warth, A.D., *Mechanism of action of benzoic acid on Zygosaccharomyces bailii: effects on glycolytic metabolite levels, energy production, and intracellular pH.* Applied and environmental microbiology, 1991. **57**(12): p. 3410-3414.
179. Verduyn, C., et al., *Effect of benzoic acid on metabolic fluxes in yeasts: A continuous-culture study on the regulation of respiration and alcoholic fermentation.* Yeast, 1992. **8**(7): p. 501-517.
180. Klinke, H., A. Thomsen, and B. Ahring, *Potential inhibitors from wet oxidation of wheat straw and their effect on growth and ethanol production by Thermoanaerobacter mathranii.* Applied Microbiology and Biotechnology, 2001. **57**(5): p. 631-638.
181. Zaldivar, J. and L.O. Ingram, *Effect of organic acids on the growth and fermentation of ethanologenic Escherichia coli LY01.* Biotechnology and Bioengineering, 1999. **66**(4): p. 203-210.
182. Nishikawa, N.K., R. Sutcliffe, and J.N. Saddler, *The effect of wood-derived inhibitors on 2, 3-butanediol production by Klebsiella pneumoniae.* Biotechnol Bioeng, 1988. **31**(6): p. 624-7.

183. Ando, S., et al., *Identification of aromatic monomers in steam-exploded poplar and their influences on ethanol fermentation by Saccharomyces cerevisiae.* Journal of Fermentation Technology, 1986. **64**(6): p. 567-570.
184. Berezina, N., B. Yada, and R. Lefebvre, *From organic pollutants to bioplastics: insights into the bioremediation of aromatic compounds by Cupriavidus necator.* New Biotechnology, 2015. **32**(1): p. 47-53.
185. Li, D., et al., *Genome-wide investigation and functional characterization of the beta-ketoadipate pathway in the nitrogen-fixing and root-associated bacterium Pseudomonas stutzeri A1501.* BMC Microbiol, 2010. **10**(1): p. 36-36.
186. Corti Monzón, G., et al., *New Findings on Aromatic Compounds' Degradation and Their Metabolic Pathways, the Biosurfactant Production and Motility of the Halophilic Bacterium Halomonas sp. KHS3.* Curr Microbiol, 2018. **75**(8): p. 1108-1118.
187. Harwood, C.S. and R.E. Parales, *The β-ketoadipate pathway and the biology of self-identity.* Annual review of microbiology, 1996. **50**(1): p. 553-590.
188. Shi, Y., et al., *Characterization and genomic analysis of kraft lignin biodegradation by the beta-proteobacterium Cupriavidus basilensis B-8.* Biotechnology for Biofuels, 2013. **6**(1): p. 1.
189. Cserháti, M., et al., *De Novo Genome Project of Cupriavidus basilensis OR16.* Journal of Bacteriology, 2012. **194**(8): p. 2109.
190. Cowles, C.E., N.N. Nichols, and C.S. Harwood, *BenR, a XylS homologue, regulates three different pathways of aromatic acid degradation in Pseudomonas putida.* J Bacteriol, 2000. **182**(22): p. 6339-46.
191. Brzostowicz, P.C., et al., *Transcriptional Cross-Regulation of the Catechol and Protocatechuate Branches of the β-Ketoadipate Pathway Contributes to Carbon Source-Dependent Expression of the Acinetobacter sp. Strain ADP1 pobA Gene.* Applied and Environmental Microbiology, 2003. **69**(3): p. 1598.
192. Donoso, R.A., D. Pérez-Pantoja, and B. González, *Strict and direct transcriptional repression of the pobA gene by benzoate avoids 4-hydroxybenzoate degradation in the pollutant degrader bacterium Cupriavidus necator JMP134.* Environ Microbiol, 2011. **13**(6): p. 1590-600.
193. Jimenez, J.I., et al., *Genomic analysis of the aromatic catabolic pathways from Pseudomonas putida KT2440.* Environ Microbiol, 2002. **4**(12): p. 824-841.
194. MacLean, A.M., et al., *Characterization of the β-Ketoadipate Pathway in <em>Sinorhizobium meliloti</em&gt.* Applied and Environmental Microbiology, 2006. **72**(8): p. 5403.
195. Matsumura, E., et al., *Constitutive expression of catABC genes in the aniline-assimilating bacterium Rhodococcus species AN-22: production, purification, characterization and gene analysis of CatA, CatB and CatC.* The Biochemical journal, 2006. **393**(Pt 1): p. 219-226.
196. Zídková, L., et al., *Biodegradation of phenol using recombinant plasmid-carrying Rhodococcus erythropolis strains.* International Biodeterioration & Biodegradation, 2013. **84**: p. 179-184.
197. Silva-Rocha, R. and V. de Lorenzo, *The pWW0 plasmid imposes a stochastic expression regime to the chromosomal ortho pathway for benzoate metabolism in Pseudomonas putida.* FEMS Microbiol Lett, 2014. **356**(2): p. 176-183.

198. Moreno, R. and F. Rojo, *The Target for the Pseudomonas putida Crc Global Regulator in the Benzoate Degradation Pathway Is the BenR Transcriptional Regulator.* J Bacteriol, 2007. **190**(5): p. 1539-1545.
199. Moreno, M.d.L., et al., *Cloning, Characterization and Analysis of cat and ben Genes from the Phenol Degrading Halophilic Bacterium Halomonas organivorans.* PLoS One, 2011. **6**(6): p. e21049-e21049.
200. Becker, J., et al., *Metabolic engineering of Corynebacterium glutamicum for the production of cis, cis-muconic acid from lignin.* Microb Cell Fact, 2018. **17**(1): p. 115-14.
201. Jung, H.-M., M.-Y. Jung, and M.-K. Oh, *Metabolic engineering of Klebsiella pneumoniae for the production of cis,cis-muconic acid.* Appl Microbiol Biotechnol, 2015. **99**(12): p. 5217-5225.
202. Kim, D., et al., *Molecular cloning and functional characterization of the genes encoding benzoate and p-hydroxybenzoate degradation by the halophilic Chromohalobacter sp. strain HS-2.* FEMS Microbiol Lett, 2008. **280**(2): p. 235-241.
203. Parulekar, C. and S. Mavinkurve, *Formation of ortho-benzoquinone from sodium benzoate by Pseudomonas mendocina P2d.* Indian J Exp Biol, 2006. **44**(2): p. 157-62.
204. Franden, M.A., P.T. Pienkos, and M. Zhang, *Development of a high-throughput method to evaluate the impact of inhibitory compounds from lignocellulosic hydrolysates on the growth of Zymomonas mobilis.* Journal of Biotechnology, 2009. **144**(4): p. 259-267.
205. Smirnova, G.V. and O.N. Oktiabr'skiĭ, *[Effect of the activity of primary proton pumps on the growth of Escherichia coli in the presence of acetate].* Mikrobiologiia, 1988. **57**(4): p. 554-559.
206. Roe, A.J., et al., *Inhibition of Escherichia coli growth by acetic acid: a problem with methionine biosynthesis and homocysteine toxicity.* Microbiology (Reading), 2002. **148**(Pt 7): p. 2215-2222.
207. Yang, X., et al., *Microbial protein production from CO2, H2, and recycled nitrogen: Focusing on ammonia toxicity and nitrogen sources.* Journal of Cleaner Production, 2021. **291**: p. 125921.
208. Wittmann, C., A.P. Zeng, and W.D. Deckwer, *Growth inhibition by ammonia and use of a pH-controlled feeding strategy for the effective cultivation of Mycobacterium chlorophenolicum.* Appl Microbiol Biotechnol, 1995. **44**(3-4): p. 519-25.
209. Chong, H., et al., *Improving Acetate Tolerance of Escherichia coli by Rewiring Its Global Regulator cAMP Receptor Protein (CRP).* PLOS ONE, 2013. **8**(10): p. e77422.
210. Jawed, K., et al. *Establishing Mixotrophic Growth of Cupriavidus necator H16 on CO2 and Volatile Fatty Acids*. Fermentation, 2022. **8**, DOI: 10.3390/fermentation8030125.
211. Mordukhova, E.A., H.-S. Lee, and J.-G. Pan, *Improved Thermostability and Acetic Acid Tolerance of Escherichia coli via Directed Evolution of Homoserine o-Succinyltransferase.* Applied and Environmental Microbiology, 2008. **74**(24): p. 7660-7668.
212. Castaño-Cerezo, S., et al., *An insight into the role of phosphotransacetylase (pta) and the acetate/acetyl-CoA node in Escherichia coli.* Microbial Cell Factories, 2009. **8**(1): p. 54.
213. Enjalbert, B., et al., *Acetate fluxes in Escherichia coli are determined by the thermodynamic control of the Pta-AckA pathway.* Scientific Reports, 2017. **7**(1): p. 42135.

214. Reitzer, L., *Nitrogen Assimilation and Global Regulation in Escherichia coli.* Annual Review of Microbiology, 2003. **57**(1): p. 155-176.
215. Yuan, J., et al., *Metabolomics-driven quantitative analysis of ammonia assimilation in E. coli.* Molecular Systems Biology, 2009. **5**(1): p. 302.
216. Lykidis, A., et al., *The complete multipartite genome sequence of Cupriavidus necator JMP134, a versatile pollutant degrader.* PLoS One, 2010. **5**(3): p. e9729.
217. Shi, H., M. Shiraishi, and K. Shimizu, *Metabolic flux analysis for biosynthesis of poly(β-hydroxybutyric acid) in Alcaligenes eutrophus from various carbon sources.* Journal of Fermentation and Bioengineering, 1997. **84**(6): p. 579-587.
218. Third, K.A., M. Newland, and R. Cord-Ruwisch, *The effect of dissolved oxygen on PHB accumulation in activated sludge cultures.* Biotechnology and Bioengineering, 2003. **82**(2): p. 238-250.
219. Reddy, C.S.K., et al., *Polyhydroxyalkanoates: an overview.* Bioresource Technology, 2003. **87**(2): p. 137-146.
220. Dias, J.M.L., et al., *Metabolic modelling of polyhydroxyalkanoate copolymers production by mixed microbial cultures.* BMC systems biology, 2008. **2**: p. 59-59.
221. Lemos, P.C., L.S. Serafim, and M.A.M. Reis, *Synthesis of polyhydroxyalkanoates from different short-chain fatty acids by mixed cultures submitted to aerobic dynamic feeding.* Journal of Biotechnology, 2006. **122**(2): p. 226-238.
222. Van Aalst-Van Leeuwen, M.A., et al., *Kinetic modeling of poly(β-hydroxybutyrate) production and consumption by Paracoccus pantotrophus under dynamic substrate supply.* Biotechnology and Bioengineering, 1997. **55**(5): p. 773-782.
223. Higuchi-Takeuchi, M. and K. Numata, *Acetate-Inducing Metabolic States Enhance Polyhydroxyalkanoate Production in Marine Purple Non-sulfur Bacteria Under Aerobic Conditions.* Frontiers in bioengineering and biotechnology, 2019. **7**: p. 118-118.
224. Salinas, A., et al., *Metabolic engineering of Cupriavidus necator H16 for heterotrophic and autotrophic production of 3-hydroxypropionic acid.* Metab Eng, 2022. **74**: p. 178-190.
225. Collas, F., et al., *Engineering the biological conversion of formate into crotonate in Cupriavidus necator.* Metabolic Engineering, 2023. **79**: p. 49-65.
226. Schlegel, H., H. Kaltwasser, and G. Gottschalk, *Ein submersverfahren zur kultur wasserstoffoxydierender bakterien: wachstumsphysiologische untersuchungen.* Archiv für Mikrobiologie, 1961. **38**: p. 209-222.
227. Trüper, H.G. and N. Pfennig, *Characterization and identification of the anoxygenic phototrophic bacteria*, in *The prokaryotes: a handbook on habitats, isolation, and identification of bacteria*. 1981, Springer. p. 299-312.
228. Sheu, D.S., et al., *Mutations derived from the thermophilic polyhydroxyalkanoate synthase PhaC enhance the thermostability and activity of PhaC from Cupriavidus necator H16.* J Bacteriol, 2012. **194**(10): p. 2620-9.
229. Porcar, M., *Beyond directed evolution: Darwinian selection as a tool for synthetic biology.* Syst Synth Biol, 2010. **4**(1): p. 1-6.
230. Jin, C., et al., *Adaptive evolution of Gluconobacter oxydans accelerates the conversion rate of non-glucose sugars derived from lignocellulose biomass.* Bioresource Technology, 2019. **289**: p. 121623.
231. Little, G.T., et al., *Complete Genome Sequence of Cupriavidus necator H16 (DSM 428).* Microbiology Resource Announcements, 2019. **8**(37): p. 10.1128/mra.00814-19.

232. Nojiri, H., et al., *Organization and transcriptional characterization of catechol degradation genes involved in carbazole degradation by Pseudomonas resinovorans strain CA10.* Bioscience, biotechnology, and biochemistry, 2002. **66**(4): p. 897-901.
233. McFall, S.M., S.A. Chugani, and A. Chakrabarty, *Transcriptional activation of the catechol and chlorocatechol operons: variations on a theme.* Gene, 1998. **223**(1-2): p. 257-267.
234. Bundy, B.M., et al., *Synergistic transcriptional activation by one regulatory protein in response to two metabolites.* Proceedings of the National Academy of Sciences, 2002. **99**(11): p. 7693-7698.
235. Craven, S.H., et al., *Inducer responses of BenM, a LysR-type transcriptional regulator from Acinetobacter baylyi ADP1.* Mol Microbiol, 2009. **72**(4): p. 881-94.
236. van Duuren, J.B.J.H., et al., *Generation of a catR deficient mutant of P. putida KT2440 that produces cis, cis-muconate from benzoate at high rate and yield.* Journal of Biotechnology, 2011. **156**(3): p. 163-172.
237. Wang, J., et al., *The conserved domain database in 2023.* Nucleic Acids Research, 2023. **51**(D1): p. D384-D388.
238. Jumper, J., et al., *Highly accurate protein structure prediction with AlphaFold.* Nature, 2021. **596**(7873): p. 583-589.
239. Swings, T., et al., *Adaptive tuning of mutation rates allows fast response to lethal stress in Escherichia coli.* eLife, 2017. **6**: p. e22939.
240. Ghoneim, Y., *Using adaptive laboratory evolution to increase Cupriavidus necator H16's tolerance to ammonium acetate to facilitate economic polyhydroxybutyrate production from lignocellulose.* Final Project 2022(University of Sheffield).
241. Carpenter, A.C., et al., *Have you tried turning it off and on again? Oscillating selection to enhance fitness-landscape traversal in adaptive laboratory evolution experiments.* Metab Eng Commun, 2023. **17**: p. e00227.
242. Wollmann, P. and K. Zeth, *The Structure of RseB: A Sensor in Periplasmic Stress Response of E. coli.* Journal of Molecular Biology, 2007. **372**(4): p. 927-941.
243. Kim, D.Y., et al., *Crystal structure of RseB and a model of its binding mode to RseA.* Proceedings of the National Academy of Sciences, 2007. **104**(21): p. 8779-8784.
244. Missiakas, D., et al., *Modulation of the Escherichia coliσE (RpoE) heat-shock transcription-factor activity by the RseA, RseB and RseC proteins.* Molecular Microbiology, 1997. **24**(2): p. 355-371.
245. Cezairliyan, B.O. and R.T. Sauer, *Inhibition of regulated proteolysis by RseB.* Proceedings of the National Academy of Sciences, 2007. **104**(10): p. 3771-3776.
246. Martin, D.W., et al., *Differentiation of Pseudomonas aeruginosa into the alginate-producing form: inactivation of mucB causes conversion to mucoidy.* Molecular Microbiology, 1993. **9**(3): p. 497-506.
247. Koide, K., K. Ito, and Y. Akiyama, *Substrate Recognition and Binding by RseP, an Escherichia coli Intramembrane Protease*.* Journal of Biological Chemistry, 2008. **283**(15): p. 9562-9570.
248. James, S.J., et al., *Elevation in S-Adenosylhomocysteine and DNA Hypomethylation: Potential Epigenetic Mechanism for Homocysteine-Related Pathology.* The Journal of Nutrition, 2002. **132**(8): p. 2361S-2366S.
249. Mordukhova Elena, A. and J.-G. Pan, *Evolved Cobalamin-Independent Methionine Synthase (MetE) Improves the Acetate and Thermal Tolerance of Escherichia coli.* Applied and Environmental Microbiology, 2013. **79**(24): p. 7905-7915.

250. Tuite, N.L., K.R. Fraser, and C.P. O'Byrne, *Homocysteine Toxicity in Escherichia coli Is Caused by a Perturbation of Branched-Chain Amino Acid Biosynthesis.* Journal of Bacteriology, 2005. **187**(13): p. 4362-4371.
251. Heinz, E., et al., *Evolution of the Translocation and Assembly Module (TAM).* Genome Biol Evol, 2015. **7**(6): p. 1628-43.
252. Ruiz, N., R.M. Davis, and S. Kumar, *YhdP, TamB, and YdbH Are Redundant but Essential for Growth and Lipid Homeostasis of the Gram-Negative Outer Membrane.* mBio, 2021. **12**(6): p. e02714-21.
253. Li, M.-f., et al., *The Translocation and Assembly Module (TAM) of Edwardsiella tarda Is Essential for Stress Resistance and Host Infection.* Frontiers in Microbiology, 2020. **11**.
254. Weimar, J.D., et al., *Functional Role of Fatty Acyl-Coenzyme A Synthetase in the Transmembrane Movement and Activation of Exogenous Long-chain Fatty Acids: AMINO ACID RESIDUES WITHIN THE ATP/AMP SIGNATURE MOTIF OFESCHERICHIA COLI FadD ARE REQUIRED FOR ENZYME ACTIVITY AND FATTY ACID TRANSPORT**. Journal of Biological Chemistry, 2002. **277**(33): p. 29369-29376.
255. Moffett, J.R., et al., *Acetate Revisited: A Key Biomolecule at the Nexus of Metabolism, Epigenetics and Oncogenesis—Part 1: Acetyl-CoA, Acetogenesis and Acyl-CoA Short-Chain Synthetases.* Frontiers in Physiology, 2020. **11**.
256. Adams, J.D., et al., *Engineering osmolysis susceptibility in Cupriavidus necator and Escherichia coli for recovery of intracellular products.* Microb Cell Fact, 2023. **22**(1): p. 69.
257. Chandrangsu, P., C. Rensing, and J.D. Helmann, *Metal homeostasis and resistance in bacteria.* Nature Reviews Microbiology, 2017. **15**(6): p. 338-350.
258. Lawrence, C.W., *Classical mutagenesis techniques.* Methods Enzymol, 2002. **350**: p. 189-99.
259. Silver, S., et al., *Manganese-resistant mutants of Escherichia coli: physiological and genetic studies.* J Bacteriol, 1972. **110**(1): p. 186-95.
260. Cheng, K.-K., et al., *Global metabolic network reorganization by adaptive mutations allows fast growth of Escherichia coli on glycerol.* Nature Communications, 2014. **5**(1): p. 3233.
261. Kang, M., et al., *Inactivation of a Mismatch-Repair System Diversifies Genotypic Landscape of Escherichia coli During Adaptive Laboratory Evolution.* Frontiers in Microbiology, 2019. **10**.
262. Sharma, P.K., et al., *Global changes in the proteome of Cupriavidus necator H16 during poly-(3-hydroxybutyrate) synthesis from various biodiesel by-product substrates.* AMB Express, 2016. **6**(1): p. 36.
263. Yeh, J.I., et al., *Structures of enterococcal glycerol kinase in the absence and presence of glycerol: correlation of conformation to substrate binding and a mechanism of activation by phosphorylation.* Biochemistry, 2004. **43**(2): p. 362-373.
264. Ali, N.O., et al., *Regulation of the acetoin catabolic pathway is controlled by sigma L in Bacillus subtilis.* J Bacteriol, 2001. **183**(8): p. 2497-504.
265. Danson, A.E., et al., *Mechanisms of σ54-Dependent Transcription Initiation and Regulation.* Journal of Molecular Biology, 2019. **431**(20): p. 3960-3974.
266. Krüger, N. and A. Steinbüchel, *Identification of acoR, a regulatory gene for the expression of genes essential for acetoin catabolism in Alcaligenes eutrophus H16.* Journal of Bacteriology, 1992. **174**(13): p. 4391-4400.
267. Bächler, C., et al., *Escherichia coli dihydroxyacetone kinase controls gene expression by binding to transcription factor DhaR.* Embo j, 2005. **24**(2): p. 283-93.

268. Chen, H., Y. Lu, and J.G. Jiang, *Comparative analysis on the key enzymes of the glycerol cycle metabolic pathway in Dunaliella salina under osmotic stresses.* PLoS One, 2012. **7**(6): p. e37578.
269. Wang, Y., et al., *Switch of metabolic status: redirecting metabolic flux for acetoin production from glycerol by activating a silent glycerol catabolism pathway.* Metabolic Engineering, 2017. **39**: p. 90-101.
270. Zschiedrich, C.P., V. Keidel, and H. Szurmant, *Molecular mechanisms of two-component signal transduction.* Journal of molecular biology, 2016. **428**(19): p. 3752-3775.
271. Posas, F., M. Takekawa, and H. Saito, *Signal transduction by MAP kinase cascades in budding yeast.* Current opinion in microbiology, 1998. **1**(2): p. 175-182.
272. Park, M.K., et al., *Enhancing recombinant protein production with an Escherichia coli host strain lacking insertion sequences.* Appl Microbiol Biotechnol, 2014. **98**(15): p. 6701-13.
273. Reyes, L.H., A.S. Abdelaal, and K.C. Kao, *Genetic Determinants for n-Butanol Tolerance in Evolved Escherichia coli Mutants: Cross Adaptation and Antagonistic Pleiotropy between n-Butanol and Other Stressors.* Applied and Environmental Microbiology, 2013. **79**(17): p. 5313-5320.